Charles University

Faculty of Science

Novel conjugated polymers of the metallo-supramolecular and polyelectrolyte class

PhD Thesis

Mgr. Sviatoslav Hladysh

Supervisor: Prof. RNDr. Jiří Vohlídal, CSc.

Prague, 2017

Statement

I proclaim that this doctoral thesis is my personal work and it has been done under guidance of my supervisor Prof. RNDr. Jiří Vohlídal, CSc. The results of this dissertation have not been presented at any other institution in order to obtain any other academic degrees. I declare that I have properly cited all previously published results which are listed in the references.

Prague, ...

Acknowledgments

First of all, I would like to thank my supervisor, Prof. Jiří Vohlídal for giving me a good opportunity to work and perform PhD thesis in his group at Charles University, Department Physical and Macromolecular Chemistry. I want sincerely gratitude him for supporting me throughout my thesis and allowing me work in my own way.

My deep gratitude is directed to Dr. Jiří Zedník and Dr. Jan Svoboda for their help in different spectroscopic measurements and discussions. I want to express my gratitude to all above mentioned people for knowledge and experience obtained during PhD study.

I want to thank my friends and colleagues from Department of Physical and Macromolecular Chemistry (Tereza Vitvarová, Pavla Štenclová, Radoslava Sivkova, Kristýna Šichová, Tomáš Faukner, David Vrbata), and I apologize if I have not mentioned someone into this list. I owe you a debt of gratitude for all you have done for me personally. It was a big pleasure to work with all of you. My friends, your suggestions, hints and our discussion or communication has encouraged and supported me. I would also like to thank my colleague Dr. Dmitrij Bondarev, who was interested in helping me, especially during the first year of my PhD program.

My research would not have been possible without financial support. The Grant Agency of Charles University (project number 876213) and the Czech Science Foundation (project number P108/12/1143 and 15-22305S) are sincerely acknowledged.

In the end, I would like to thank my family especially my wife for their loving support and encouragement in my PhD process. I saw their feelings and emotions all the time and it helped me to successfully complete this PhD thesis.

Sviatoslav Hladysh, Prague, July 2017

Abstract

This thesis targets the development of conjugated polymers with improved processability from solutions. Two types of ionic polymers are addressed: *(i)* conjugated metallo-supramolecular polymers (MSPs) composed of conjugated heteroaromatic unimers (building blocks) linked to chains by various metal ions giving charged main chains, and *(ii)* polythiophene polyelectrolytes containing ionic pendants. Processing advantages of conjugated polyelectrolytes consist in the possibility of their processing from solutions in green solvents such as alcohols or even water. The advantages of MSPs consist in the thermodynamic control of the degree of polymerization (length) of their chains in solutions by the choice of solvent and temperature. As a result, MSPs reversibly provide systems of low viscosity that can be processed from solutions more easily than high-molar-mass polymers giving highly viscous solutions.

Synthesis of appropriately designed unimer(s) is the key step of preparation of an MSP. Within this thesis, a series of novel unimers composed of linear oligothiophene type (mono-, bi-, ter- a thieno-thiophene –diyl) central blocks capped with 2,6-bis(2-oxazolinyl)pyridine (*pybox*) or 2,6-bis(2-imidazolyl)pyridine (*bzimpy*) end-groups have been successfully prepared, characterized and assembled with various metal ions into MSPs. It is worth noting that the cheap and commercially easy available chelidamic acid was the starting compound for the syntheses of both the above chelating end-groups (ion selectors).

The bis(*pybox*) unimers were assembled with metal ions such as Fe^{2+}, Zn^{2+}, Ni^{2+}, Cu^{2+} and lanthanide ions Eu^{3+} or Tb^{3+} to give corresponding MSPs. On the other hand, MSPs derived from bis(*bzimpy*) unimers were found to show significantly lower solubility thus they were studied less in detailed using only Fe^{2+} and Zn^{2+} ion couplers. The detailed study of the MSP assembly revealed three stages of this process, same as observed for bis(*tpy*) unimers: formation of "butterfly" dimers U-Mt^{z+}-U (U stands for a unimer species) at the Mt^{z+}/U mole ratios *r* up to ca 0.5, formation of longer MSP chains for *r* from above 0.5 to ca 1, and end-capping of MSP chains and their equilibrium depolymerization at *r* values above 1. The latter proves the constitutional-dynamic nature of the novel MSPs, which is the fastest for Zn-dynamers and the slowest for Fe-dynamers that exhibit the presence of the metal-to-ligand charge transfer transitions. Photoluminescence properties of new *pybox*- and *bzimpy*-MSPs are also similar to those of the *tpy*-MSPs; only Zn^{2+}-MSPs show high photoluminescence

while the other ones exhibit quenching the luminescence with increasing content of metal ions.

Novel cationic conjugated polyelectrolytes have been prepared by modification of the parent poly[3-(6-bromohexyl)thiophene-2,5-diyl bromide]s of the low to high regioregularity, consisting in replacing the bromine side-chain-capping atoms with triethyl- or triphenyl-phosphonium bromide groups. The parent polymers were prepared by means of the Grignard metathesis polymerization and their regioregularity has been tuned by temperature regime of the polymerization process. Studies on the optical properties of these polyelectrolytes revealed their solvatochromism and possibility of tuning their luminescence through the solvent polarity. The luminescence quenching by $K_4[Fe(CN)_6]$ and $K_3[Fe(CN)_6]$ has been also studied. All experiments performed point to the principle influence of the main-chain regioregularity on the polymer properties except for its solubility in polar solvents.

Abstrakt

Tato disertace se zabývá vývojem nových iontových konjugovaných polymerů se zlepšenou zpracovatelností z roztoků: *(i)* metalo-supramolekulárních polymerů (MSP) vzniklých samoseskupením konjugovaných unimerů (U, stavebních bloků) s ionty kovů Mt^{z+} do lineárních řetězců s alternačním uspořádáním stavebních jednotek $[-Mt^{z+}-U-]_n$ a *(ii)* polythiofenových polyelektrolytů s triethyl- a trifenyl- fosfoniovými bočními skupinami. Předností polyelektrolytů je jejich rozpustnost v ekologicky akceptovatelných rozpouštědlech, zejména alkoholech, optimálně ve vodě. Oproti tomu výhody MSP spočívají v termodynamické kontrole polymerizačního stupně jejich molekul díky reverzibilitě samoseskupovací reakce (polymerizace), kterou lze ovlivnit zejména výběrem rozpouštědla a teplotou. MSP tak obecně tvoří podstatně méně viskózní a tím I lépe zpracovatelné roztoky než kovalentní polymery.

Klíčovým krokem přípravy MSP je syntéza odpovídajícího(ch) unimeru(ů). V rámci této studie byla připravena serie nových unimerů s lineárními centrálními bloky oligothiofenového typu (mono-, bi-, ter- a thieno- thiofene –diyl bloky) a koncovými skupinami 6-bis(2-oxazolinyl)pyridine (*pybox*) a 2,6-bis(2-imidazolyl)pyridine (*bzimpy*). Unimery byly charakterizovány a použity k přípravě MSP. Je dobré zde zdůraznit, že výchozí surovinou pro přípravu chelátových koncových skupin unimerů byla levná, snadno dostupná chelidamová (4-hydroxypyridin-2,6-dikarboxylová kyselina).

Z bis(*pybox*) unimerů byly připraveny MSP s ionty Fe^{2+}, Zn^{2+}, Ni^{2+}, Cu^{2+}, Eu^{3+} a Tb^{3+}. Protože bis(*bzimpy*) unimery vykazovaly značně nižší rozpustnost, byla jim věnována menší pozornost; studovány byly pouze jejich Fe^{2+} a Zn^{2+} MSP. Podrobné studium odhalilo tři faze samoseskupování iontů s unimery do MSP, což odpovídá zjištěním pro seskupování bis(*tpy*) unimerů s kovovými ionty: tvorba "motýlkových" dimerů $U\text{-}Mt^{z+}\text{-}U$ (U je unimerní jednotka) pro Mt^{z+}/U molární poměry *r* do cca 0.5, tvorba delších MSP řetězců pro *r* od 0.5 do ca 1 a vazba nadbytečných iontů na konce MSP řetězců a rovnovážná depolymerizace řetězců pro $r > 1$. Finální depolymerizace potvrzuje konstitučně-dynamický charakter nových MSP. Nejrychlejší konstituční dynamika byla zjištěna pro Zn-dynamery, nejpomalejší pro Fe-dynamery, které jako jediné z připravených dynamerů vykazují přenosu náboje z kovového iontu na ligand (MLCT). Fotoluminescenční vlatnosti nových *pybox*- and *bzimpy*- MSP jsou kvalitativně obdobné, jako vlastnosti *tpy*-MSP; pouze Zn^{2+}-MSP vykazují intenzivní

fotoluminescenci, zatímco ostatní MSP vykazují jen zhášení luminescence s rostoucí koncentrací kovových iontů v systému.

Nové kationtové konjugované polyelektrolyty byly připraveny modifikacemi poly[3-(6-bromohexyl)thiofen-2,5-diyl bromid]ů s nízkou, střední a vysokou regioregularitou, spočívající v náhradě atomů bromu triethyl- nebo triphenyl-phosphonium bromidovými skupinami. Primární polymery byly připraveny tzv. Grignard metathesis polymerizací jejich regioregularita byla regulována teplotním režimem polymerizace. Studium optických vlastností připravených polyelectrolytů prokázalo jejich solvatochromismus a možnosti ladění jejich luminescence polaritou rozpouštědla. Studováno bylo též zhášení luminescence polyelectrolytů solemi $K_4[Fe(CN)_6]$ a $K_3[Fe(CN)_6]$. Všechny provedené studie jasně prokazují podstatný vliv regioregularity na vlastnosti těchto nových polyelektrolytů, kromě jejich rozpustnosti v polárních rozpouštědlech.

ABBREVIATIONS

CPs	Conjugated polymers
CPE	Conjugated polyelectrolyte
CRU	Constitutional repeating unit
DMF	Dimethylformamide
DMSO	Dimethylsulfoxide
FQ	Fluorescence quenching
FQY	Fluorescence quantum yield
GRIM	Grignard metathesis polymerization
GPC	Gel permeation chromatography
H-T	Head-to-tail regioregularity
IP	Isosbestic point
MLCT	Metal-to-ligand charge-transfer
MSP	Metallo-supramolecular polymer
MW	Molecular weight
PT	Polythiophene
rr	Regioregularity
RU	Repeating unit
SEC	Size exclusion chromatography
THF	Tetrahydrofuran

Symbols of quantities

r	molar ratio
λ_A	wavelength of absorption maximum
λ_F	wavelength of emission maximum
λ_e	wavelength of absorption edge
ε_{max}	molar absorption coefficient
ϕ_F	fluorescence quantum yield
α_{ion}	degree of ionization
ν_S	Stokes shift
τ	reaction time
T_g	glass transition temperature
Đ	dispersity

1 INTRODUCTION

1.1 Origin and aspects of supramolecular chemistry

In the last decades, supramolecular chemistry has become an active field of the polymer research. That fact confirms a large number of published results: articles, reviews, books [1-5]. Establisher or pioneers in this field of chemistry are Donald J. Cram, Jean-Marie Lehn and Charles J. Pedersen which were awarded with the Nobel Prize for chemistry in 1987 "for their development and use of molecules with structure-specific interactions of high selectivity."

Supramolecular chemistry is a special area of chemistry that, in the colloquial usage, is also known as "chemistry beyond the molecule". It is targeted on the study of molecular systems formed by self-assembly process based on the weak and reversible non-covalent interactions between a "host" and "guest" molecules as shown in **Figure 1.1**. Additionally, supramolecular chemistry is also expressed in the literature as "the chemistry of non-covalent bond".

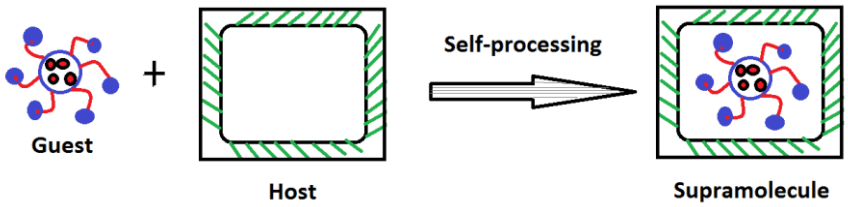

Figure 1.1 Formation of a supramolecular species.

The term "host" is typically used for a larger binding partner such as an enzyme molecule and the term "guest" for a smaller binding partner such as a molecule or an inorganic or organic ion or ion pair. The binding partners (host and guest) mutually interact through hydrogen bonding, or van der Waals interactions, or π-π interactions, or metal coordinations. All these weak and reversible non-covalent interactions play significant and valuable role in biological systems and chemical process.

Hydrogen bond is a special type of dipole-dipole attraction involving a hydrogen atom bonded to a strongly electronegative atom and another electronegative atom with a lone electron pair which is donated to the partly positively charged hydrogen. Hydrogen bonds are generally stronger than ordinary dipole-dipole and dispersion interactions, but weaker than true covalent or ionic bonds. This bonding provides stabilization and formation of

various biological systems including DNA and proteins [6-7] and they are of importance for many catalytic processes and also for complex systems such as some dendrimers [8].

π-π Interactions are typical non-covalent interactions that take place between aromatic molecules. Three types of π-π interactions are observed: *(i)* the T-shaped, *(ii)* parallel displaced, and *(iii)* sendwich ones (see **Figure 1.2**) [9]. π-π interactions especially (parallel displaced) are important in DNA and RNA molecules occurring between the aromatic moieties of adjacent oligonucleotides [10].

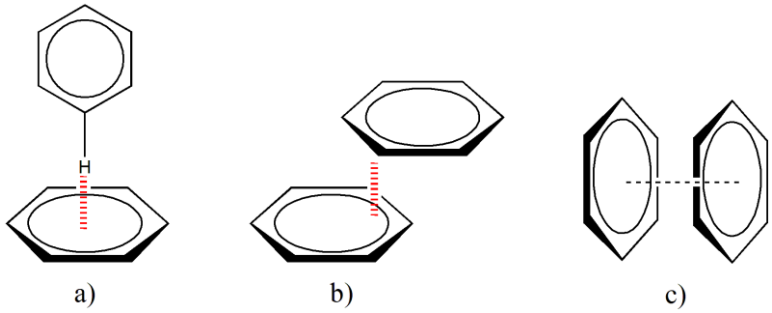

Figure 1.2 Depiction of π-π interactions in the benzene dimer: a) T-shaped; b) parallel displaced, and c) sandwich π-π interactions.

Metal-ligand interactions, i.e., coordination bonds are commonly used in the design of supramolecular complexes formed by a self-assembly process. There are many works related with metal-ligand coordination bonds [11-16]. This type of interactions (metal-ligand) is utilized in this work. The metal-ligand coordination provides a wide range of metallo-supramolecular polymers (MSPs). Since MSPs with significant reversible coordination bonds often exhibit reversible assembly-disassembly process, they are also known in literature as the constitutional dynamic polymers that are an important subclass of dynamers [17]. Dynamic linear MSPs are usually constructed from oligomeric molecules capped with two chelating end-groups (also known as ion selectors) and metal ions often referred to as ion couplers (IC). The coordination of chelating groups to ion coupler is the driving force of the self-assembly process leading to the formation of larger linear chains in solution and long chain in the resulting solid material. Under the dynamics promoting conditions, dynamer molecules are typically composed of only low number of assembled units, most often oligomeric molecules. Such a dynamer is a “superior oligomer” of hierarchically lower oligomer(s). Ambiguity of the term oligomer is thus obvious. Therefore, the term *unimer* (U) for an oligomer utilized as a “monomer” in the preparation of a dynamer was proposed by Ciferri et al. [18].

In MSPs, two building units (U and IC) are held together through reversible non-covalent interactions typically coordination bonds. The above mentioned interactions are represented by reaction in **Figure 1.3**, where formed MSPs exhibit constitutional dynamics either in solution or at increased temperature due to weakening of the interactions between the unimers and metal ion couplers. The self-assembly process is achieved by mixing U and IC in a solution.

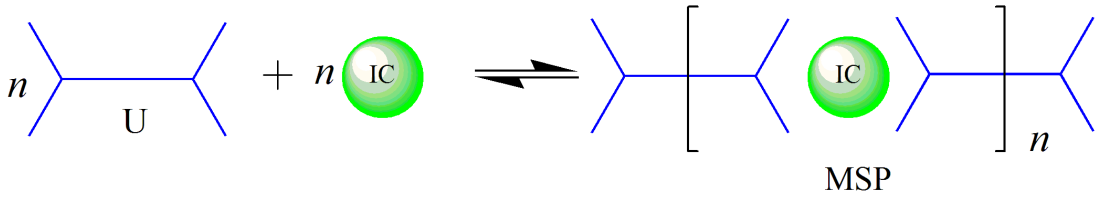

Figure 1.3 Illustration of MSP formation. (U) unimer, (IC) metal ion coupler, MSP metallo-supramolecular polymer.

The constitutional dynamics gives to MSPs attractive properties such as possibility to tune its properties by post-synthesis exchanges of the unimers or ion couplers, or both. The constitutional dynamics of MSPs in solutions is of significant interest [19-22].

1.2 The library of the chelating end-groups of oligomeric molecules and metal ion couplers for MSP preparation

As mentioned before the properties of MSPs are dependent on the nature or origin of metal-ligand or metal-chelating center interactions. Therefore, to know their strength corresponding to the binding constant is a valuable parameter. This constant can be calculated from equation 1,

$$DP \sim (K\,[\mathrm{M}])^{1/2} \qquad (1)$$

where *DP* - degree of polymerization, *K* - binding constant, M - monomer concentration.

It should be stressed, that above indicated equation is suitable only for reversible process. According to equation 1 the high concentration of monomer and the large binding constant lead to the high degree of polymerization, which is required for many applications. Unfortunately, to get high concentration is impossible in many cases due to poor solubility of ligand or unimer. But the high values of binding constant can be achieved by changing of the chelating groups of ligand or metal ion couplers. The significant increase in the binding

constant was experimentally proved for hydrogen-bonded polymers by the use of quadruple hydrogen bonds instead of triple hydrogen bonds [23].

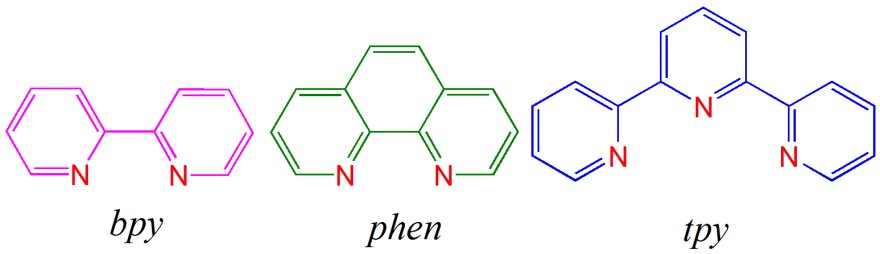

Figure 1.4 Examples of the most used chelating units (single, bidentate and tridentate pyridines).

The most often used chelating ligands in the area of metallo-supramolecular chemistry (2,2'-bipyridine, phenanthroline and 2,2':6'2"-terpyridine) are shown in **Figure 1.4**. They can be combined with different metal ion coupler, which allows tuning the binding constant and dynamics of MSPs. In addition to chelating ligands, simple pyridine ligand has also be examined in the formation of metallo-supramolecular complexes. The coordination of α,ω–bis(pyridine-4-yl) unimers to Ag^{+} ions gave linear coordination polymers (1D inorganic solid-state coordination polymers) [24].

The terpyridine chelating groups especially 2,2':6'2"-terpyridin-4´-yl) referred as (*tpy*) ligand is one of the best suitable groups for MSP formation [25]. This group is capable of forming stable complexes with a high variety of transition metal ions. Besides, the complexation of (*tpy*) ligand gives octahedral geometry of the formed complex linkages, which do not increase the number of enantiomers, as observed in case of phenanthroline and 2,2'-bipyridine ligands shown in Figure 1.4. Moreover, the bis(*tpy*) unimiers allow the formation of linear coordination chains with high degree of polymerization due to high binding constant.

A wide range of transition metal ion couplers has been used for MSP formation. They can be either paramagnetic or diamagnetic and their combination together with the choice of unimers is a good opportunity to change and tune the properties (dynamics) of MSPs prepared. In order to obtain linear coordination polymers, ditopic building blocks should be applied in the complexation with metal ions. This concept was introduced by Constable, who synthesized metallo-supramolecular polymers using α,ω–bis(*tpy*) unimers and Ru^{2+} ion couplers [26]. Transition metal ions such as Fe^{2+}, Co^{2+}, Ni^{2+}, Cu^{2+}, Zn^{2+}, Ru^{2+}, Rh^{2+}, Pd^{2+}, Cd^{2+}, Pt^{2+} form with ditopic terpyridine well-defined octahedral complexes for the building of

linear metallo-supramolecular polymers. The Fe^{2+} ions allow the process of self-assembly at room temperature in water. MSPs based on α,ω –bis(*tpy*) unimers and – Fe^{2+} ions are known as large macromolecular assemblies [27]. α,ω –Bis(*tpy*) unimers also give linear MSPs with Co^{2+}, Ni^{2+} and Zn^{2+} ions due to the high stability constants of formed complex linkages and fast ligand exchange kinetics [28]. For the synthesis of branched MSPs (metal-organic frameworks, metal-organic dendrimers) the use of tris (*tpy*) or tris (*bpy*) unimers is needed [29-32].

Lanthanide ions also undergo complexation with bis(*tpy*) unimers. In contrary to transition-metal, which form 2:1 metal complexes, lanthanides can also give 3:1 complexes and thus act as branching points. The introduction of lanthanides especially Eu^{3+} or Tb^{3+} into MSPs provide outstanding luminescence properties such as high emission quantum yields, narrow emission bands and long excited state lifetime [33]. The main object of study of lanthanides complexes is focused on self-assembled supramolecular metallogels, due to their low stability allowing opening of the branching points upon heating or mechanical stress [34]. However, the solid state study of lanthanide-based coordination polymers is also of interest [35].

The development of new ditopic unimers with novel architecture and properties and their subsequent self-assembly into metallo-supramolecular polymers is one goal of this thesis. The chelating groups based on 2,6-bis(benzimidazol-2-yl) pyridine and 2,6-bis(oxazolyl) pyridine (shown in **Figure 1.5**) have been chosen as the key molecules for the synthesis of desired unimers.

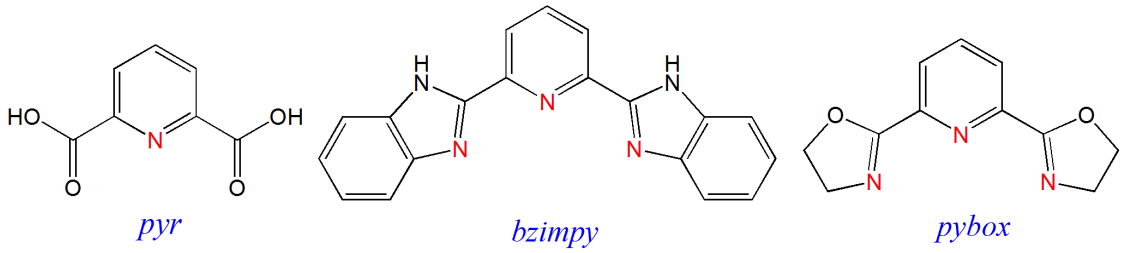

pyr *bzimpy* *pybox*

Figure 1.5 The structures of chelating groups used for the synthesis of unimers.

The chemistry of 2,6-bis(benzimidazol-2-yl) pyridine denoted in literature as (*bzimpy*) is less-known than chemistry of 2,2':6'2"-terpyridines. A molecule of *bzimpy* contains five nitrogen atoms but can act as a tridentate ligand. Also this type of molecules has been investigated in the past two decades [36-44]. The structure of this ligand is a combination of

two aromatic ligands: pyridine and benzimidazole. Therefore, such option can provide unique properties and complexation behavior of *bzimpy* ligands. A research related to the coordination of *bzimpy* with different transition metals ions can be found in some published papers [45-47]. The possibility to introduce various substituents on the nitrogen atom of benzimidazole unit using special chemical reaction is a great advantage of *bzimpy* ligands. There are also reports concerning functionalization N-H atom of the benzimidazole group of *bzimpy* ligand [48-52]. The presence of N-H bonds in benzimidazole group is important for the formation of the hydrogen bonding networks in metallo-supramolecular complexes. Additionally, this type of bonds has strong influence on the rearrangement of individual molecules into supramolecular architecture, such as layers, rods, tubes, sheets [53].

As shown in **Figure 1.5**, pyridine-2,6-dicarboxylic acid (*pyr*) was used as a chelating group. In fact, this rigid molecule due to the presence of carboxylic groups is able to coordinate to metal ions and show better luminescent properties with Eu^{3+} and Tb^{3+} than tridentate *bzimpy* ligands [54-56].

This thesis also deals with the synthesis of unimers bearing 2,6-bis(oxazolyl) pyridine ligand frequently denoted as (*pybox*). The first report about tridentate *pybox* ligand appeared in 1989 [57]. Since that period, metal oxazoline complexes have found various applications in the different fields of chemistry. But the main focus of oxazoline ligand is catalytic chemistry. The different iron-based catalyst were synthesized and applied for various organic reactions such as Mukaiyama-Aldol reaction [58, 59], olefin polymerization [60, 61], the asymmetric Nazarov cyclization of divinyl ketones [62], asymmetric Diels-Alder reaction [63]. Lanthanides-based *pybox* ligands were used for enantioselective catalysis [64-66] and additionally their properties are also used for lanthanide luminescence sensitization [67].

The structure of *pybox* ligand is suitable for derivatization either at 4-position of pyridine moiety or carbon atoms of the oxazoline ring [68, 69]. The incorporation of substituents may increase the selectivity and efficiency of catalytic system. However, the main object of use of oxazoline ligands is asymmetric catalysis. Despite limited use of oxazoline ligands in the synthesis of complexes or metallo-supramolecular polymers, we decided to use the *pybox* skeleton as the chelating groups of unimers for our studies, since various building blocks can easily be introduced at 4-position of pyridine of *pybox* ligand. Therefore, the self-assembly process of the synthesized oxazoline based unimers with different metal ion couplers is

important for exploration of new metallo-supramolecular polymers due to special chelate groups and variable building blocks between *pybox* ligands.

1.3 The architecture of ditopic unimers

The ditopic unimers are important object of this work. In view of the chemical structure, these unimers present the combination of two chelating center (ligands) linked by aromatic or aliphatic central block. The chelating groups of unimers have significant role for the coordination and the formation of supramolecular assemblies as discussed previously. Nevertheless, the second component of a unimer its central block, is also of high importance. The central block can be either rigid (aromatic moieties) or flexible (aliphatic groups), conjugated or not conjugated, and thus give diverse unimers and subsequently MSPs. Unimers with π-conjugated both central blocks and chelating end-groups have a special role, because of they can give MSPs with a high luminescence quantum yields and relatively long emission lifetimes after complexation with heavy metals [70]. It is result of efficient interaction of singlet and triplet excited states.

The structures of central blocks also strongly influence solubility of both unimer and its MSPs. That effect was experimentally proved by Shubert et al., where poor solubility of metal-polymers containing rigid central blocks was solved by the introducing of flexible central blocks [71-73]. A variety of MSPs based on different ditopic unimers with various central blocks bearing groups of the energy-donor or energy-acceptor character are prepared and reported and the most common are collected in **Figure 1.6**. Besides all these examples, novel building blocks can be synthesized using different type of chemical reactions such as Stille coupling [74], Suzuki reaction [75], Sonogashira coupling [76], Kumada coupling [77].

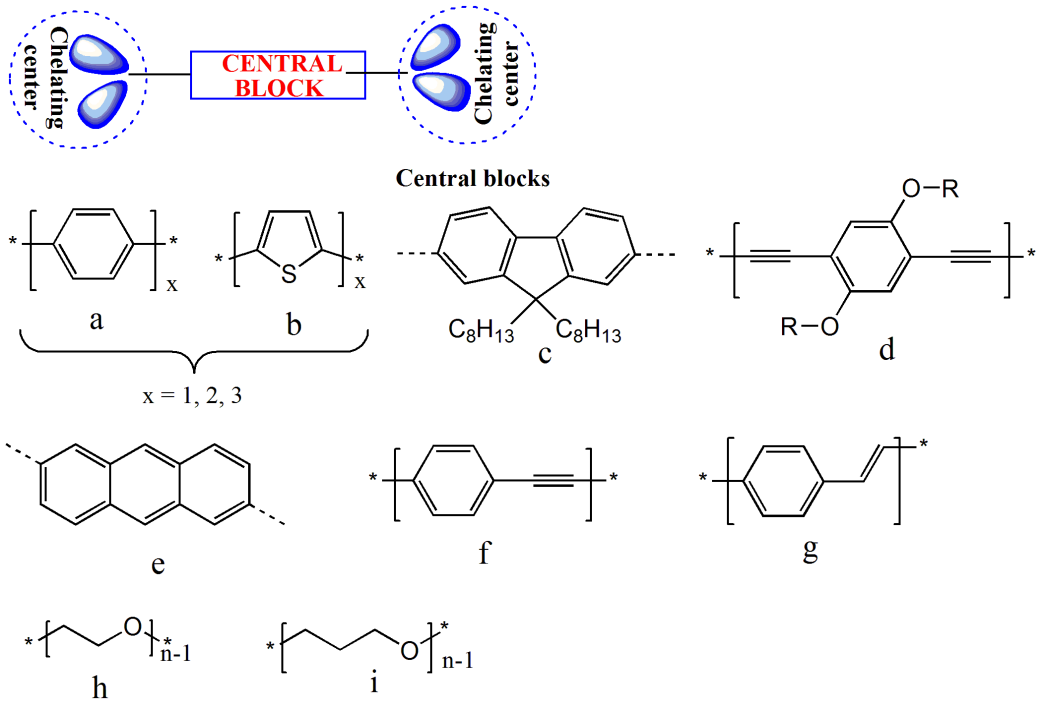

Figure 1.6 The examples of commonly used central blocks.

Thiophene, bithiophene, thienothiophene and terthiophene have been chosen as the building blocks for unimers in this thesis. These compounds constitute a special class of materials referred to as oligothiophenes which exhibits interesting conducting and electronic characteristics [78-80]. These properties of oligothiophenes are used in organic photovoltaic cells [81-83] or organic field effect transistors [84-86]. The incorporation of different substituents into oligothiophene backbone allows the increase of solubility and change in the properties of these materials. However, the substituents at the position 3 of the thiophene unit in oligothiophene form different regioisomers such as: i) head-to-head (HH), ii) tail-to-tail (TT) and iii) head-to-tail (HT). Comparing three types of sequences, oligothiophenes with HT regioregularity show the best performance as materials due to the least steric hindrance of substituents leading to the extended π-conjugation [87]. Additionally, such chosen class of materials is competing with more pronounced conjugated systems – polythiophenes, which are also presented in this thesis. Therefore, combination of oligothiophenes building blocks and various chelating groups allows fine-tuning the properties of ditopic unimers.

1.4 Application and characterization of MSPs

The searching for novel materials with unique properties is very important for industry, electronics, medicine and energy systems [88, 89]. Among all materials, MSPs have a particular role due to their special features based on the electronic interactions between the organic and metallic parts. The incorporation of metal ions into polymeric structure provides unique properties of synthesized materials in optical, electronic, magnetic and catalytic fields [90, 91]. MSPs have attracted scientists due to their stimuli-responsive nature upon application of external stimuli such as heat, pH, photoirradiation and solvent. As a result, self-healing, shape memory and degradability processes are observed in supramolecular polymers [92-95].

MSPs have found application in optoelectronic devices. Electrochemical properties of materials can be tuned by the changing of substituents of the organic ligands [96]. Photoluminescent conjugated MSPs have found usage in the light-emitting diodes [97-99]. The combination of metal ion couplers and functional groups of ligand has significant effect on the fluorescence properties of MSPs. There are self-healing materials which are able to recover their properties after mechanical damages. This effect was confirmed by Rowan and coworkers, where the light-heat conversion for self-healing was studied [100]. Another interesting application of MSPs is in the biomedical field: drug delivery, bioimaging, tissue engineering [101, 102].

The characterization of dynamic MSPs with non-covalent bonds differs from the characterization of traditional covalent polymers, since the conditions such as temperature, concentration and solvent influence the degree of polymerization of metallo-supramolecular systems [103]. GPC analysis is one of the most important tools for the determination of the values of relative molar masses and dispersity of covalent polymers. However, molar mass of an MSP is often a function of the concentration of its components in analyzed solution, which continually changes during the GPC analysis. Therefore, the GPC method is not applicable for the determination of the molar mass characteristics of MSPs that show fast establishing of thermodynamic equilibrium in the solvent used as eluent, i.e., for characterization of MSPs exhibiting fast constitutional dynamics. On the other hand, the GPC method can be used for analyses of the systems exhibiting sufficiently slow constitutional dynamics [104-107].

Another method for the determination of the size of MSPs molecules in solutions is viscometry. This determination is based on the difference of the viscosities of solutions of free unimer and MSPs which indicates formation of a supramolecular system [108-117]. Similarly, light scattering methods, mainly the dynamic one are suitable for the molar mass determination of MSPs [118, 119].

An insight into the morphologic structure of MSPs provides scanning electron microscopy (SEM) and transition electron microscopy (TEM [120] and atomic force microscopy (AFM) [121]. NMR spectroscopy is a useful tool for characterization of MSPs, which allows monitoring the complexation of unimer molecules with metal ions. Kelch and co-workers used this method for the determination of the degree of polymerization of soluble ruthenium-terpyridine polymer [122]. There are also papers reporting the determination of the average degree of polymerization of Fe^{2+} MSPs based on bis(*tpy*) unimers by the NMR end-group analysis [123, 124]. Diffusion ordered spectroscopy (DOSY) NMR has also been used for the characterization of MSPs in solution. This method brings information about the relative size of the assemblies and was experimentally proved for porphyrin based MSPs by Michelsen [125].

The quantitative phosphorescence characteristics (phosphorescence quantum yield, emission lifetime) are also informative and important. As majority of MSPs are π-conjugated systems the incorporation of heavy metal ions into such systems allows the efficient mixing of singlet and triplet excited states causing the efficient increase of the mentioned phosphorescence values [126].

1.5 Conjugated polymers

Covalent conjugated polymers (CPs) are another object of this thesis. The chains of these polymers comprise a sequence of alternating double and single bonds allowing the effective delocalization of π-electrons along chain backbones, which is essential for obtaining organic semiconducting materials. There are different polymer types belonging to the conjugated polymer system. The most frequently studied and used conjugated polymers are polyacetylenes [127], polyphenylenvinylenes [128, 129], polyanilines [130, 131], polythiophenes [132-134] and polyfluorenes [135, 136] (see **Figure 1.7**). They have found

applications namely in the areas such as the light-emitting diodes [137, 138], field-effect transistors [139, 140], photovoltaic cells [141].

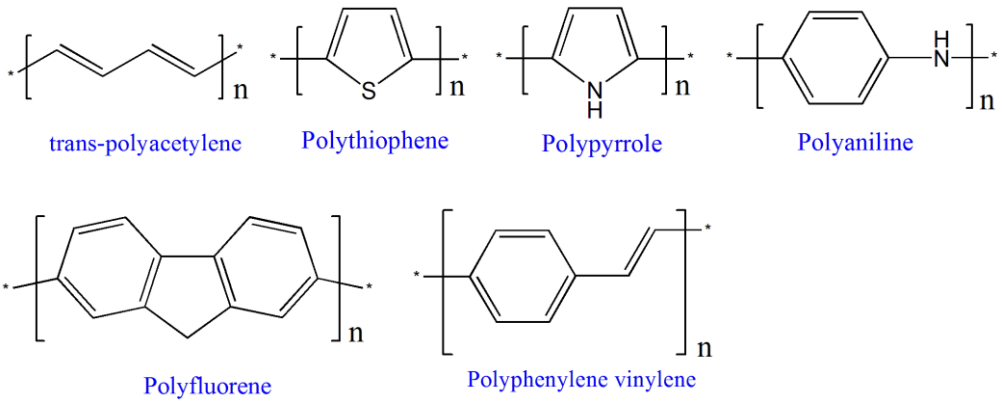

Figure 1.7 The set of frequently used conjugated polymers.

The field of conjugated polymers has developed accidentally when a mistake was made during the preparation of polyacetylene by Ziegler-Natta catalyst using much higher catalyst concentration than usually in the laboratory of prof. H. Shirakawa. As a result, a polyacetylene thin film instead powder material was obtained, which, however, showed only semiconductivity. This observation was taken into account by prof. A. G. MacDiarmid and prof. A. Heeger who investigated this phenomenon more deeply and reported in 1977 that the oxidation of polyacetylene with iodine, also known as a doping reaction, leads to significant increase in conductivity of polyacetylene [142]. Finally, all these three actors were awarded by the Nobel Prize in Chemistry in 2000 for this achievement [143, 144]. The presence of alternating single and double bonds in polyacetylene provides excellent mobility of charged species along polymer chain formed after doping process.

Despite the above successful discovery, scientists were forced to find new conjugated polymers due to the oxidation reaction of polyacetylene by oxygen. Therefore, novel more stable conjugated polymers such as polyanilines, polypyrolles polythiophenes and others were synthesized. Compared to the inorganic semiconducting materials, conjugated polymers have several advantages such as better processability, low cost, flexibility and tunable optoelectronic properties, which allow their use in the low-cost processes like roll-to-roll printing or inkjet printing [145, 146]. On the other hand, conjugated polymers have also serious disadvantages. Their preparation requires the various types of catalytic processes that often result in the formation of structure defects leading to the decrease of charged carrier mobility. The negligible amount of catalyst remnants after purification

strongly influences properties of synthesized material and decreases the performance of optoelectronic devices [147]. Additionally, conjugated polymers suffer from UV irradiation and are susceptible to oxidation process [148]. In general, conjugated polymer materials are less stable than inorganic counterparts.

1.6 Studied conjugated polymers and polyelectrolytes

Polythiophenes (PTs), especially poly(3-hexylthiophene) (P3HT) belongs to the most frequently used conjugated polymers due to their high charge carrier mobility [149]. PTs exhibit good optical and electrical properties and easy processing. Moreover, PTs possess: i) high absorption in the visible spectral range, ii) possibility to tune their properties by the introduction of various substituents or modification of polymer chains. Besides that, they can be regarded as a covalent counterpart of MSPs prepared from bis(*tpy*)oligothiophene unimers studied within this thesis.

The first attempts to synthesize polythiophene were made by Yamamoto and Lin in 1980 [150, 151]. They prepared unsubstituted polythiophene using oxidative polymerization of thiophene with $FeCl_3$. Unfortunately, the synthesized polythiophenes could not be processed due to their insolubility. A few years later, soluble poly(3-alkylthiophenes) were synthesized using polymerization with Ni^{2+} metal catalysts [152]. The presence of side groups provides planarity and processability of overall polythiophene system. However, the attached alkyl side group causes asymmetry of thiophene constitutional units allowing different steric hindrances based on the chain regioregularity. Ideally, the thiophene can be namely linked regularly by the head-to-tail H-T manner, however, if also irregular head-to-head H-H and tail-to-tail T-T linkageges are present (see **Figure 1.8**), the resulting poly(3-alkylthiophene)s cannot acquire optimal conformations allowing a good transport of charge carriers along their chains. In particular, the H-H sequences induce a serious chain distortion as it was shown experimentally as well as by theoretical calculation on short oligo(3-hexylthiophene) chains [153]. Highly regioregular H-T chains allow more efficient three dimensional packing of polymer chains that gives a better performance to these materials [154, 155].

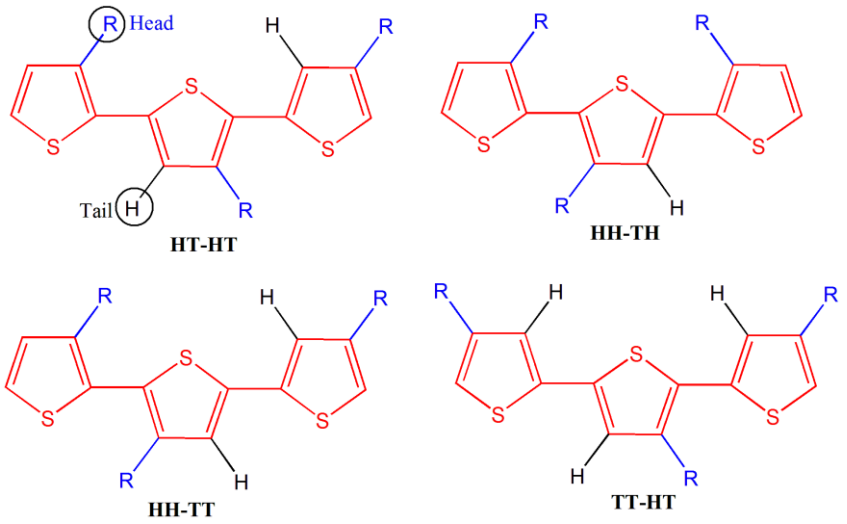

Figure 1.8 H-T isomerism of poly(3-alkylthiophene) chains.

The synthesis of highly regioregular poly(3-alkylthiophene)s was developed by McCullough and co-workers based on the reaction known in the literature as Grignard metathesis polymerization (GRIM) [156]. This polymerization is relatively difficult since it requires special conditions such as argon atmosphere and totally dried reagents. It starts by the reaction of 2,5-dibromo-3-alkylthiophene with one equivalent of the Grignard reagent giving monomer with -MgBr group located predominantly in position 5, which, in the next step, undergoes coupling reaction catalyzed by a suitable nickel (II) catalyst (**Scheme 1**). This method is described to give highly regioregular polythiophenes with up to 98% of (H-T connections of thiophene units.

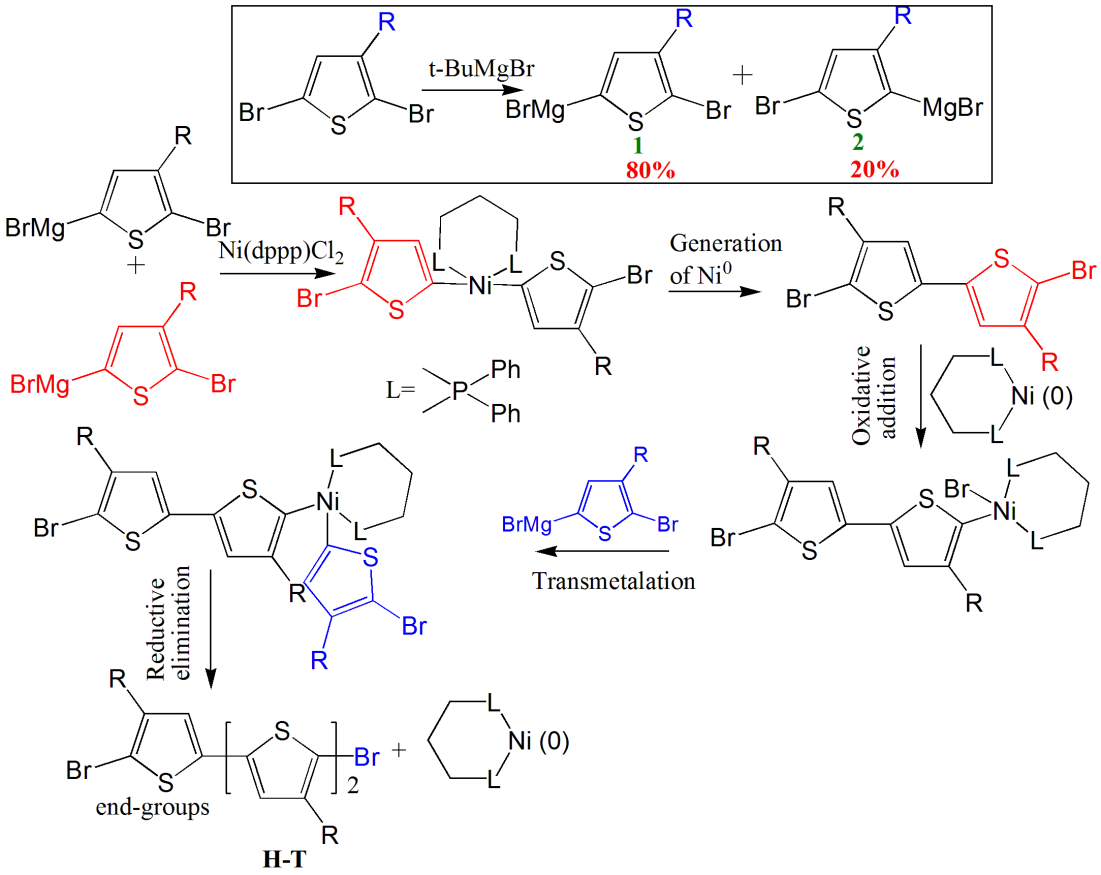

Scheme 1. Mechanism of GRIM polymerization.

The GRIM polymerization has been shown to be efficient also for thiophene with alkyl side chains capped with bromine atoms that were found not to disturbe the GRIM process. In this way a highly regioregular poly[3-(6-bromohexyl)thiophene-2,5-diyl]s have been prepared that can be further modified to obtain a highly regioregular polyelectrolyte with conjugated main chains [157]. The corresponding monomer: 3-(6-bromohexyl)thiophene has been also polymerized oxidatively by $FeCl_3$ giving regio-irregular polymers that are also capable of transformation into polyelectrolytes by the reaction with imidazole derivatives [158].

Conjugated polyelectrolytes (CPEs) are important materials consisting of a π-conjugated backbone and a high content of ionic or ionizable side groups which provide solubility in eco-friendly polar solvents such as water, alcohols and other water-miscible solvents. CPEs are divided on anionic or cationic based on the charge of ionic group. Ionic polymers with charged groups located on the main-chain atoms are referred to as ionenes [159]. Nowadays, the most frequently studied are anionic conjugated polyelectrolytes with ionic

groups such as carboxylate, sulfonate and phosphate groups. Regarding the cationic conjugated polyelectrolytes their ionic groups are mostly based on positively charged nitrogen atom in ammonium, imidazolium and pyridinium moieties [160-164].

Conjugated polyelectrolytes are typically prepared by the modifications of the corresponding conjugated precursor polymers such as poly(phenylene vinylene), polyfluorene or poly(p-phenylene) [165-167] carrying side groups with a reactive site. CPEs have found applications in light-emitting diodes [168] and photovoltaic devices [169]. As a result, they both polymers and polyelectrolytes compete among themselves. The first water soluble conjugated polyelectrolytes were prepared from 3-substituted polythiophenes [170]. Subsequently, this direction to conjugated polyelectrolytes was applied on poly(phenylene vinylene) and polyfluorene based conjugated polyelectrolytes which were properly investigated [171, 172].

Conjugated polyelectrolytes have tendency to interact with oppositely charged species. This ability was used for the development of different fluorescence-based sensors for proteins [173, 174], enzymes [175-177], DNA [178, 179] or biomolecules [180]. In many cases such interactions between polyelectrolytes and oppositely charged species leads to the fluorescence quenching or also called as amplified quenching [181] due to the fluorescence resonance energy transfer from conjugated backbone to negative or positive charged agent. The solubility of CPEs in aqueous media made them suitable for the development of biosensors in living organisms [182].

In this thesis we present cationic π-conjugated polyelectrolytes based on polythiophene bearing imidazolium and phosphonium side groups (see **Figure 1.9**). These materials were prepared by quaternization reaction using (poly[3-(6-bromohexyl)thiophene-2,5-diyl] precursor with N-methyl-imidazole, triethylphosphine and triphenylphosphine.

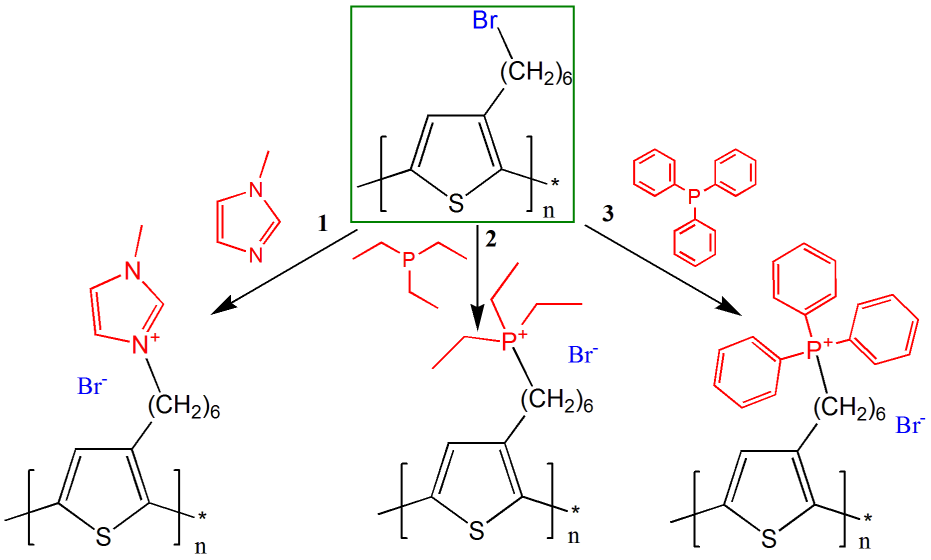

Figure 1.9 Quaternization reactions and structures of studied conjugated polyelectrolytes.

Polyelectrolytes with charged nitrogen (imidazolium based) were already described deeply by Bondarev [157]. Therefore, the discussion of this material is omitted in the current work. In this thesis, novel conjugated polyelectrolytes with phosphonium side groups are presented, which are conterparts of ionic MSPs derived from analogous ionic bis(*tpy*)oligothiophene unimers [107]. Phosphonium salts are known to provide both thermal and chemical stability [183]. The conjugated polyelectrolytes bearing phosphonium groups were examined for fabrication of antibacterial films [184-186]. Therefore, introducing of side phosphonium ionic groups into conjugated polythiophene chain together with simple preparation of phosphonium polyelectrolytes using mild conditions might bring novel properties and, as a result, new applications of these materials.

2 AIMS OF THE THESIS

Targets of my thesis originated from the fact that, in our laboratory, there have recently been developed new MSPs based on the unimers with *tpy* end-groups [107, 153, 187] and ionic side groups.

Therefore, one target of my thesis was the synthesis and characterization of new unimers with different ion selectors (end-groups), specifically those based on the benzimidazole and oxazoline derivatives of pyridine, self-assembly of MSPs from these new unimers and investigation of the properties of the unimers and MSPs.

The second target of my thesis has been the synthesis and characterization of the covalent counterparts of the ionic MSPs: covalent conjugated polyelectrolytes with polythiophene main chains and ionic side groups, and investigation of their properties.

3 RESULTS AND DISCUSSION – Metallo-suporamolecular polymers

The first part of this chapter is devoted to: *(i)* preparation and characterization of new unimers with end-groups derived from a cheap strating compound: chelidamic acid, *(ii)* assembly of these unimers with various ions, and *(iii)* properties of so obtained new MSPs. The second part of this chapter is devoted to the preparation and properties study of new polythiophene polyelectrolytes of different regioregularity.

3.1 Synthesis of ligands and unimers with *bzimpy* end-groups

Abbreviation ***bzimpy*** stands for 2,6-bis(benzimidazol-2-yl)pyridin-4-yl group. The simplest derivative of this class, monotopic ligand ***bzimpy*-OH**, was easily prepared in one step process - by the condensation of chelidamic acid (4-hydroxypyridine-2,6-dicarboxylic acid) and benzene-1,2-diamine, as shown in the first line of **Scheme 2**. Preparation of the second monotopic ligand of this type that is labeled as ***bzimpy*-T** (since it has 2-thienyl group on pyridine ring) required a four-step procedure shown in the next lines of **Scheme 2**. These compounds were chosen as the simplest representatives of the chelating ***bzimpy*** type ligands. The ***bzimpy*-OH** ligand was used as a reference in study on assembling these ligands with metal ions. The second ligand, ***bzimpy*-T**, has more extended system of π-electrons, is more soluble than ***bzimpy*-OH** ligand and can be used for more effective preparation of unimers with oligothiopnene central blocks by different coupling reactions. Knowledge obtained during the synthesis of mono-***bzimpy*** ligands has been exploited in the synthesis of bis(***bzimpy***) unimers. Details of synthetic procedures are summarized in the Experimental section.

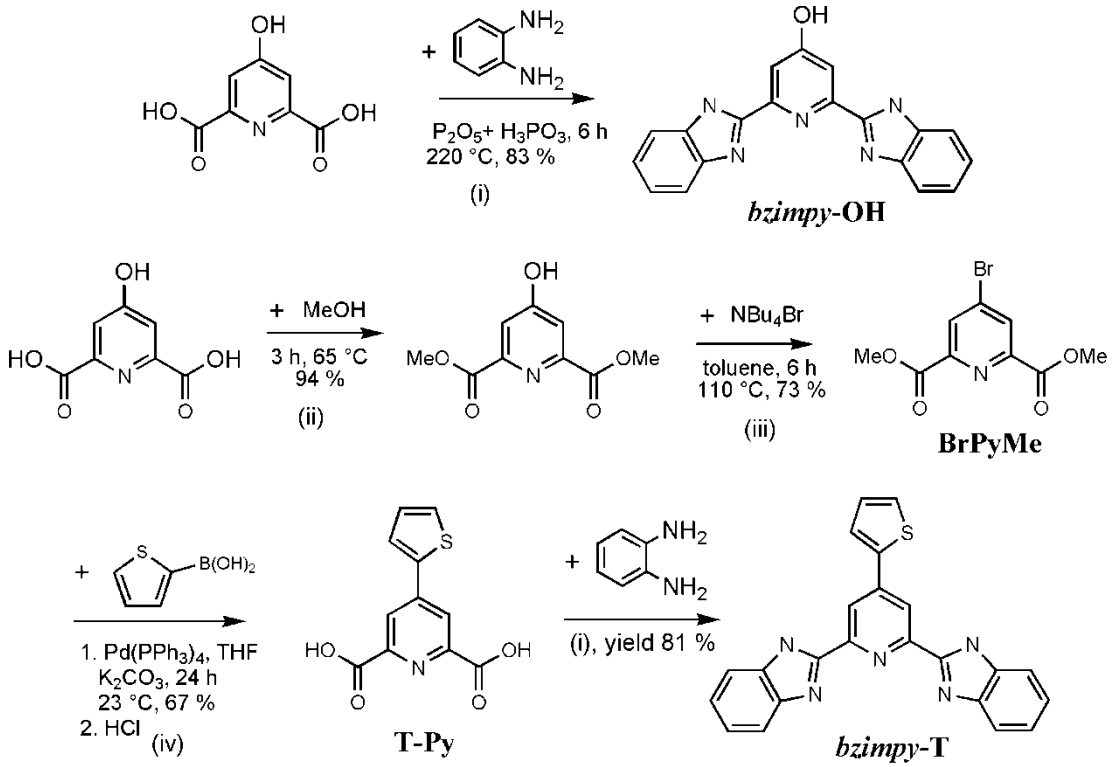

Scheme 2. Synthesis of monotopic ***bzimpy*** ligands.

Bromination of chelidamic acid in order to obtain the brominated precursor for Suzuki coupling with thiophene (see **Scheme 2**) has been found to be a key step of the synthesis of ***bzimpy*-T**. This reaction was first performed using the direct bromination of chelidamic acid with PBr_5 as a bromination agent. However, this approach gave quite low yield of the desired product. Moreover, this bromination agent is quite toxic and thus special safety conditions are required for handling it. Therefore, it was decided to carry out the bromination with tetrabutylammonium bromide reagent. For these reasons, protection of the carbonyl groups of chelidamic acid by methoxy groups was needed as the first reaction step, in order to increase the substrate solubility in nonpolar solvents such as toluene that was used for bromination. Moreover, brominated dimethyl ester of chelidamic acid (**BrPyMe**) is much better derivative for Suzuki coupling reaction compared to the non-protected bromo-chelidamic acid. The obtained **T-PyMe** precursor has been further used not only for the synthesis of ***bzimpy*-T** but also for the synthesis of ***bzimpy*** unimers (see **Scheme 3**).

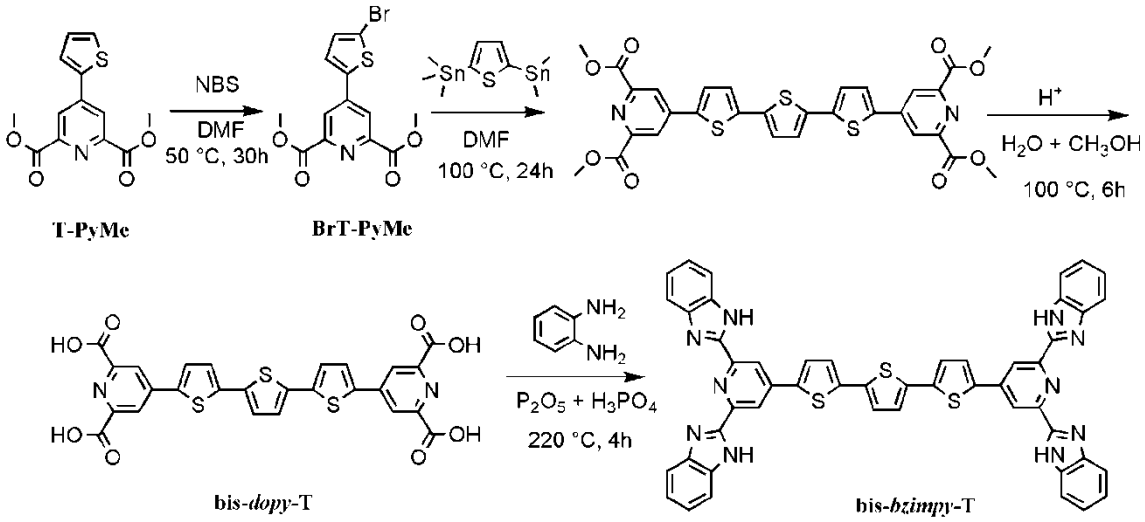

Scheme 3. Synthesis of α,ω-bis(***bzimpy***)terthiophene.

Suzuki coupling and Stille cross-coupling reactions were used as the main tools in the synthesis of unimers. The type of coupling reaction used in Scheme 3 is worth noting. From the synthetic point of view, it is possible to apply Suzuki coupling that uses boronic acid derivative instead of Stille coupling in which toxic 2,5-bis(trimethylstannyl)thiophene is applied. Unfortunately, the attempts to use Suzuki coupling have failed, the most probably owing to a basically catalyzed partial hydrolysis of **BrT-PyMe** to the corresponding carboxylic acid derivative that considerably decreased efficiency of the coupling process. As a result, the Suzuki coupling didn't provide a good yield of the terthiophene unimer. Compounds comprising bithiophene sequences were detected as the dominating product of this coupling. On the contrary, Stille coupling gave quite good yield (of 67 %) of **bis-*dcpy*-T** intermediate that was then effectively hydrolyzed to give the corresponding tetracarboxylic acid derivative **bis-*dopy*-T**, which was finally transformed into the desired unimer **bis-*bzimpy*-T** by the reaction with benzene-1,2-diamine (**Scheme 3**). It should be noted here that the last synthesis step required relatively strong reaction conditions (high temperature and the presence of polyphosphoric acid).

Both ditopic intermediates of the **bis-*bzimpy*-T** synthesis shown in **Scheme 3**: **bis-*dcpy*-T** and **bis-*dopy*-T**, the second one in particular, can be regarded as unimers with four chelating carboxylic groups that can form MSPs by assembling with proper metal ions. However, poor solubility of these ligands disallowed that process, at least at room temperature. Detailed experimental procedures and conditions together with the NMR, IR and other data are summarized in the chapter Experimental part.

3.2 Characteristics and assembling of *bzimpy* ligands and *bzimpy*-T unimer

UV/vis spectra of monotopic ligands ***bzimpy*-OH** and ***bzimpy*-T** are shown in **Figure 2** (black lines). These ligands contain the same coordination site: 2,5-bis(benzimidazol-2-yl)pyridin-4-yl and differ only in the functional group bound to the central pyridine ring at position 4. Thus the differences between their UV/vis spectra should exlusively originate from the effect of the functional group (hydroxyl and 2-thienyl). The spectrum of ***bzimpy*-OH** is bimodal, showing the most intense peak at 314 nm with a blue-arm shoulder at ca 290 nm, almost equally intense satellite peak at 330 nm and the band edge at ca 350 nm. On the other hand, the spectrum of ***bzimpy*-T** shows a single structured band with maximum at 317 nm, a blue-arm shoulder at ca 295 nm, two red-arm shoulders at ca 343 and 358 nm, and the band edge considerably red shifted to ca 400 nm. The observed red-broadening of the absorption band of ***bzimpy*-T** originates from the extension of the system of conjugated double bonds about the bonds of the thiophene ring. The molar absorption coefficient (ε) of ***bzimpy*-T** is also higher than that of ***bzimpy*-OH** (see **Table 1**).

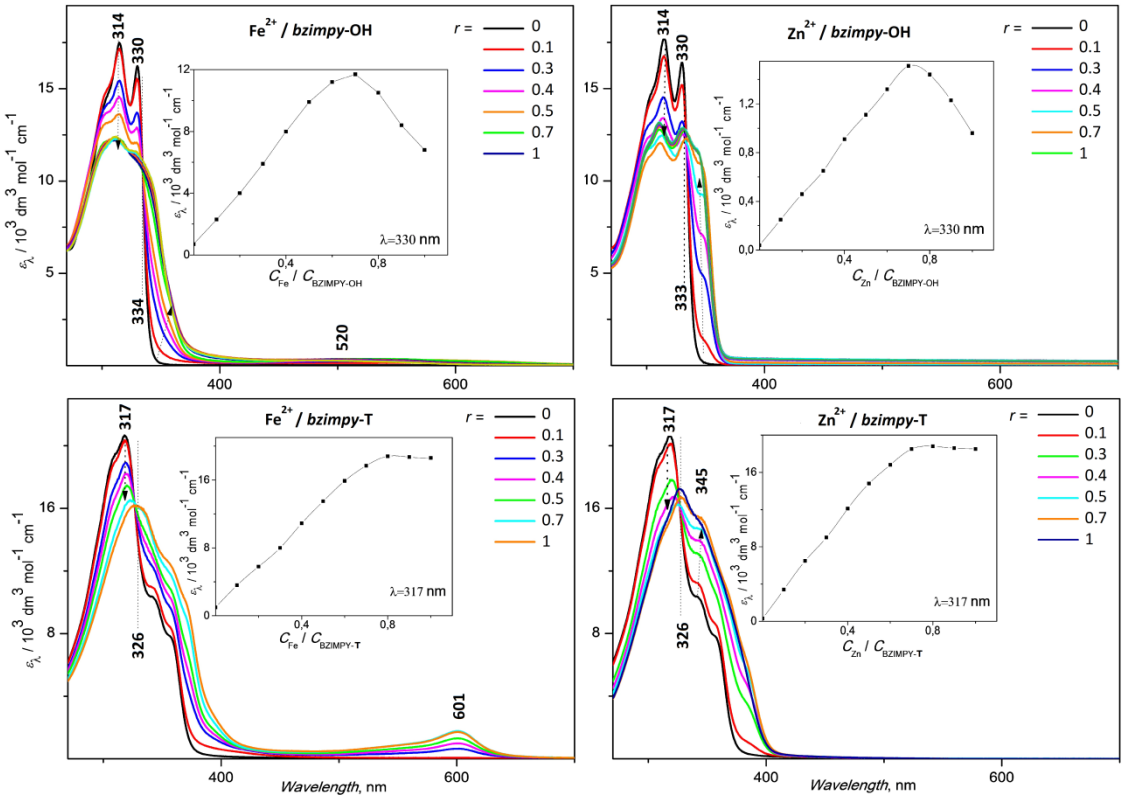

Figure 2. Solution UV/vis spectra of ***bzimpy*-OH** and ***bzimpy*-T** ligands and their changes during titrations with Fe^{2+} and Zn^{2+} ion couplers (4×10^{-2} M). Mixed solvent chloroform/methanol (1/1 by volume), insets show the Job's plots.

The solution photoluminescence spectra of ***bzimpy*-OH**, ***bzimpy*-T** (**Figure 3**, black curves) were taken from the same solutions as their UV/vis spectra. As can be seen, the luminescence spectra of both compounds show a single asymmetric non-structured band with the apexes at 355 nm for ***bzimpy*-OH** and 397 nm for ***bzimpy*-T**, which are nearly equal to the band edge wavelengths of the corresponding UV/vis absorption bands. The Stokes shifts calculated from the measured values of the absorption and emission bands are 2 130 cm^{-1} for ***bzimpy*-OH** and 6 350 cm^{-1} for ***bzimpy*-T**, which proves much more extensive conformational relaxation of the excited ***bzimpy*-T** molecules as compared to the excited ***bzimpy*-OH** molecules. The high Stokes shift value found for ***bzimpy*-T** indicates effective co-planarization of the pyridine and thiophene rings in the excited molecules of this ligand. Similarly high value of the Stokes shift has been observed for the related compound with terpyridine binding site: 4´-(2-thienyl)terpyridine [188].

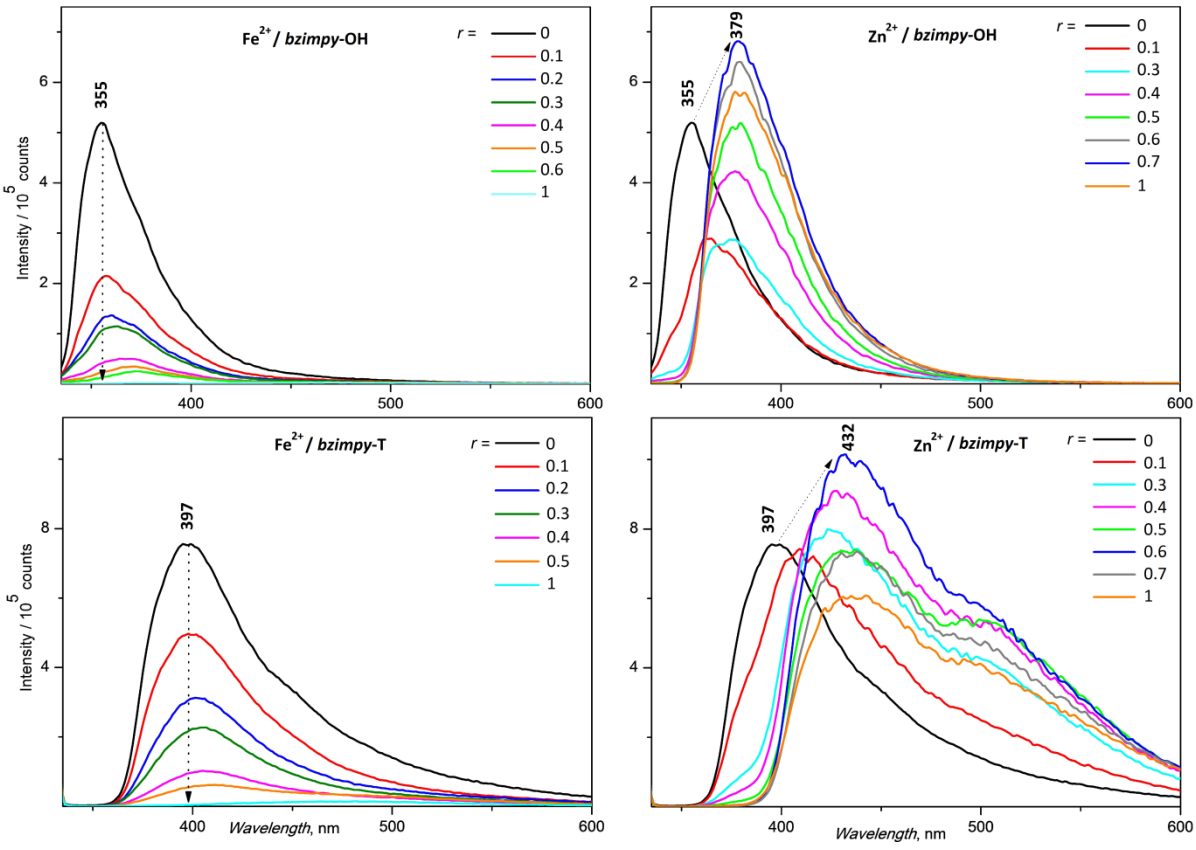

Figure 3. Solution photoluminescence emission spectra of ***bzimpy*-OH** and ***bzimpy*-T** monotopic ligands (black curves) and their changes during titration with Fe^{2+} (left) and Zn^{2+} (right) ions.

Table 1. Spectroscopic characteristics of prepared ligands and their complexes with different ion couplers and molar ratio between ligand to IC: λ_A - wavelength of absorption maximum (nm); ε_{max} - molar absorption coefficient in absorption maxima positions ($m^3\ mol^{-1}\ cm^{-1}$); λ_F - wavelength of emission maximum; ν_S - Stokes shift (cm^{-1}).

Species	***bzimpy*-OH**				***bzimpy*-T**			
	λ_A nm	ε_{max} $m^3\ mol^{-1}\ cm^{-1}$	λ_F nm	ν_S (cm^{-1})	λ_A nm	ε_{max} $m^3\ mol^{-1}\ cm^{-1}$	λ_F nm	ν_S (cm^{-1})
L	314 330	17.5 16.2	355	2130	317	20.5	397	6350
ZnL_2	314 335	12.6 12.1	375	3190	326	16.2	428	7310
ZnL	314 336	12.7 12.5	379	3375	327	17.3	432	7430
FeL_2	314 335	12.2 11.3	374	3110	325	17.8	409	6320
FeL	314 337	12.1 10.9	381	3420	326	16.1	412	6400

Assembling has been studied using the electronic (UV/vis and luminescence) spectra, NMR spectra. For the UV/vis and luminescence spectroscopic studies of the assembling of ligands with metal ions, a set of the ligand solutions in the chloroform/methanol (1/1 by volume) mixed solvent of the constant ligand concentration (4×10^{-4} M) and stepwise increasing ions-to-ligand mole ratio $[Mt^{2+}]/[L] = r$ from 0 to 1 (further referred to as composition ratio, *r*) was prepared for each ligand–ions couple and then their UV/vis and luminescence spectra were taken. The obtained spectra are displayed in Figures 2 (UV/vis) and 3 (luminescence) as a function of the composition ratio *r*.

As can be seen from **Figure 2**, the shorter wavelength part of the ligand UV/vis spectral band attenuates while the longer wavelength part of the band broadens and intensifies with increasing composition ratio *r*. The observed changes in the UV/vis spectral patterns indicate the existence of two stages of complexation process depending on values of *r*. The first stage occurs at the *r* values from 0 to 0.5 and it is characterized by a decrease in the molar absorption coefficient and formation of isosbestic points (IP) indicating transformation of the free ligand molecules into other defined species which, according to the stoichiometry, should be $L\text{-}Mt^{2+}\text{-}L$ species. The second stage that covers *r* values from 0.6 to 1 didn't show any remarkable shift of the absorption maxima or other significant changes. Only negligible

broadening of the absorption bands was observed, which can be ascribed to the equilibrium decomposition of L-Mt^{2+}-L species to the species of the L-Mt^{2+}-(solvent).

The complexation stoichiometry of the ligands with ions was examined by Job plots that confirmed the presence of L-Mt^{2+}-L species ([Mt^{2+}]/[L] = r = 1/2). However, species with different stoichiometry as well as free ligand species are generally also present in solutions. The concentration of each species depends on the thermodynamic stability constant of the species and overall concentration of the solution. The stability constants corresponding to the formation of Mt^{2+}/L (β_{11}) and Mt^{2+}/L_2 (β_{12}) complexes from free components were determined from the sets of UV/vis spectra shown in **Figure 2** using HypSpec software for both ligands: ***bzimpy*-OH** and ***bzimpy*-T** and Fe^{2+} and Zn^{2+} ions. The obtained values of β_{11} and β_{12} are collected in **Table 2**.

Table 2. Stability constants of studied complexes obtained from HypSpec software.

Ligand	Fe^{2+}		Zn^{2+}	
	log (β_{11})	*log* (β_{12})	*log* (β_{11})	*log* (β_{12})
***bzimpy*-OH**	9.55	14.65	6.46	11.53
***bzimpy*-T**	9.56	14.66	6.20	11.00

The UV/vis spectra of Fe^{2+}/L systems showed appearance of new absorption bands at around 520 nm for ***bzimpy*-OH** and 600 nm for ***bzimpy*-T**, which can be assigned to photoinduced charge transfer from Fe^{2+} ions to antibonding orbitals of the bound ligands: Fe(II) → π^*(L),i.e., to the metal to ligand charge trasfer (MLCT) transitions. These transitions proceed between metal ions (atoms) at low oxidation state and ligands with low-lying empty orbitals [189]. Usually, MLCT gives rise to an intense absorption band which, however, can be quenched in some solvents (for example, the band of Fe(II) → π^*(***tpy***) MLCT transition is strong in the chloroform/methanol (1/1 by volume) mixed solvent but quenched in water.

As can be seen in **Figure 2**, the UV/vis spectra of Fe^{2+}/***bzimpy*-OH** systems showed very weak and the spectra of Fe^{2+}/***bzimpy*-T** systems only low-intensity MLCT bands. The shape and position of the MLCT bands in question has been determined by using solutions of the concentration of 4×10^{-3} M that is hundred times higher compared to the concentrations used in the case of ***tpy*** ligands [107, 188] (see **Figure 4**). Job's plot analysis of these spectral series also confirmed the composition ratio r =1/2 of the optimal complex.

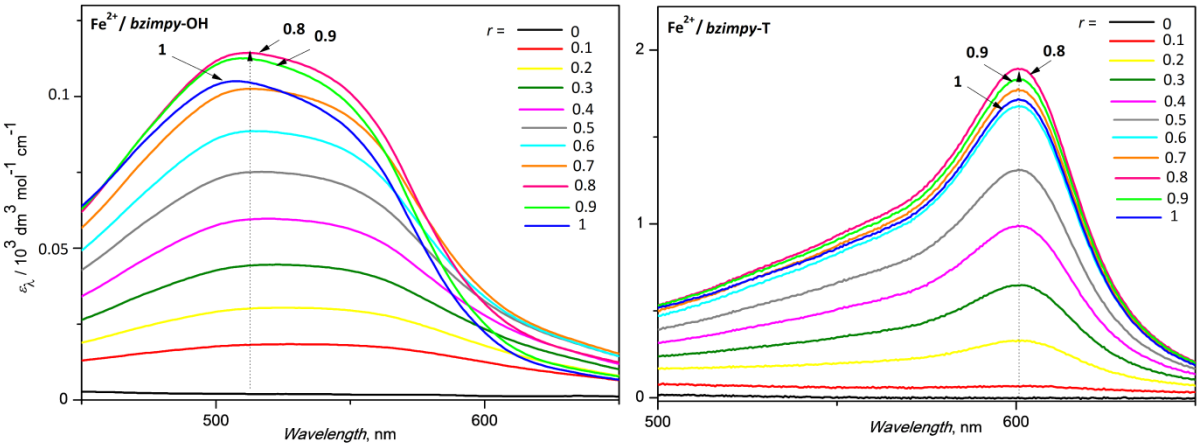

Figure 4. Absorption bands pertaining to MLCT transitions of ***bzimpy*-OH** and ***bzimpy*-T** ligands with Fe^{2+} ion couplers.

The luminescence emission spectra taken from the same solution from which UV/vis spectra showed a gradual decrease in the luminescence intensity for both Fe^{2+}/L systems, but much more complex behavior of the Zn^{2+}/L systems was observed. The latter system has shown an initial decrease in the band intensity accompanied with its read-broadening and red shift of the band maximum, followed by an increase in the band intensity that culminated at ratios *r* of ca 0.6 to 0.7. Further increase in *r* resulted in a decrease in the band intensity that was more pronounced for Zn^{2+}/***bzimpy*-T** system compared to Zn^{2+}/***bzimpy*-OH** system. These results are in a good agreement with results observed from UV/vis analysis.

^{1}H NMR study of assembling of ***bzimpy*-OH** and ***bzimpy*-T** ligands with Zn^{2+} ions was performed using a mixture of deuterated solvents: chloroform and methanol (1/1 by volume). Two sets of the respective ligand solutions (***bzimpy*-OH** and ***bzimpy*-T**) of the constant ligand concentration of 6.1×10^{-3} M and different concentration of Zn^{2+} ions *r* = 0, 0.25, 0.5, 0.75, 1 were prepared and subjected to NMR measurements. As the ligands contain exclusively aromatic moieties (pyridine and benzimidazole), proton signals only in the low field range of the proton scale are expected. The ligand structures with atom numbering are shown in **Figure 5** and the obtained ^{1}H NMR spectra are shown in **Figure 6**.

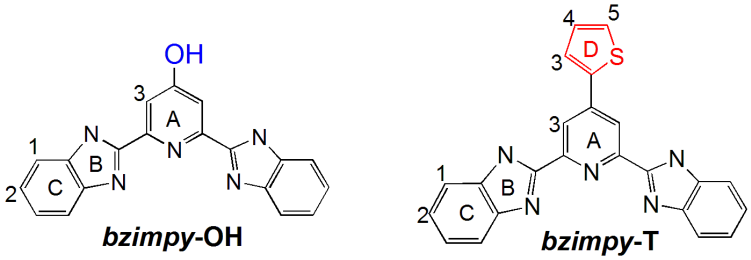

Figure 5. Structures of ligands synthesized and their numbering for NMR.

As can be seen from **Figure 6**, the addition of Zn^{2+} ions resulted in significant shifts of proton signals. The signals pertaining to the pyridine ring hydrogens A^3 shifted from 7.47 to 7.57 ppm for ***bzimpy*-OH** and from 8.26 to 8.34 ppm for ***bzimpy*-T**, respectively (see also **Table 3**). The signals corresponding to the benzimidazole groups including proton signals of the thiophene ring of ***bzimpy*-T** ligand were also shifted down-field. The above mentioned shifts of the proton signals are caused by the deprotonation of the (N-H) proton of the benzimidazole part of ligands leading to the accumulation of electron density on the carbon C^1 and C^2 (see **Figure 5**). Moreover, the shifts of the proton signals are also accompanied by the appearance of the new set of signals corresponding to complexes species and broadening of NMR signals, indicating the constitutional dynamics in solution.

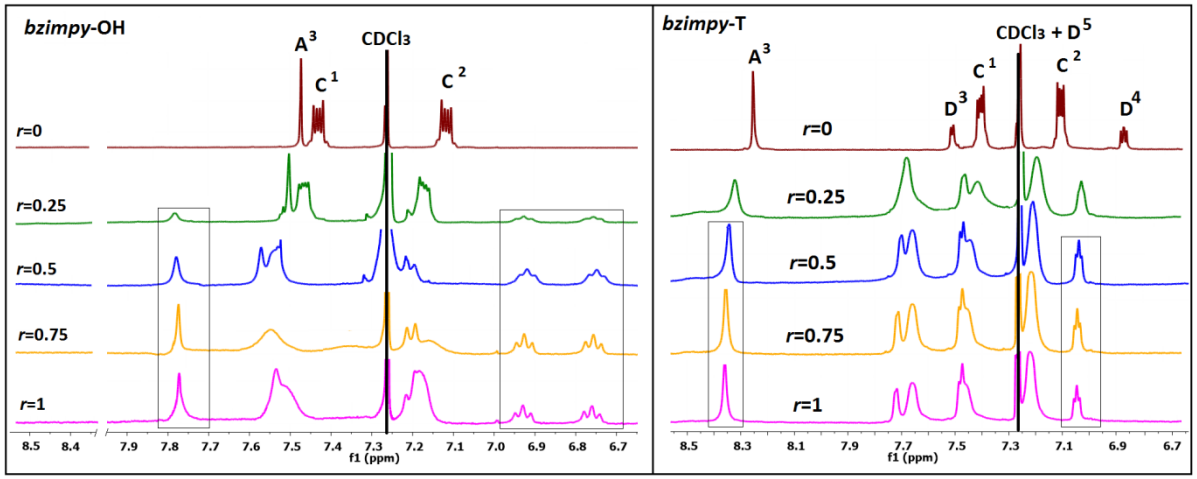

Figure 6. ^{1}H NMR spectra Zn^{2+}/L systems of various composition ratio *r*.

Table 3. ^{1}H NMR signal in ppm of ***bzimpy*-OH**, ***bzimpy*-T** ligands and their complexes with Zn^{2+} (IC)s at *r* = 0.5 and 1.

Species	A^3	A^{OH}	C^1	C^2	D^3	D^4	D^5
***bzimpy*-OH**	7.47		7.41	7.12			
$[ZnL_2]$	7.57	7.78	7.52	7.21			
[ZnL]	7.55	7.7	7.55	7.23			
***bzimpy*-T**	8.26		7.4	7.12	7.51	6.85	7.26
$[ZnL_2]$	8.34		7.65	7.20	7.69	7.03	7.46
[ZnL]	8.36		7.66	7.22	7.7	7.05	7.47

The ***bzimpy*-OH** ligand undergoes the keto-enol tautomerization consisting in the proton exchanges between oxygen atom of OH group and nitrogen atom of pyridine ring. The ligand

complexation to Zn^{2+} ions favorizes the enol tautomeric form with hydroxyl group at 4-position of pyridine with the proton signal at 7.78 ppm. NMR spectra of both Zn^{2+} systems are consistent with a stepwise formation of $[ZnL_2]^{2+}$ and $[ZnL]^{2+}$ species if the concentration of zinc ions in the system is increased: $[ZnL_2]^{2+}$ species dominate at r = 0.5 whereas $[ZnL]^{2+}$ species at r = 1. Thus the results obtained from NMR spectra are in a good agreement with the results obtained from the UV/vis and fluorescence spectra of the studied systems.

Bis-*bzimpy*-T unimer with terthiophene central block exhibited quite low solubility in majority of tested solvents. Therefore, its assembling with metal ions has been studied only marginally, using dilute solution in DMSO and UV/vis and luminescence spectroscopy. The UV/vis spectra obtained for Zn^{2+}/**bis-*bzimpy*-T** systems showed only small marginal changes as shown in **Figure 7** and similarly small changes has been observed also for the systems with Fe^{2+} ions. On the other hand, luminescence spectra of Zn^{2+}/**bis-*bzimpy*-T** systems showed a gradual increase of intensity with increasing of the composition ratio value *r*. Change in the luminescence of the system were observable visually by naked eyes. A change of coloration from bright blue-green into bright yellow was easily observed though the measured spectral changes accompanying this assembly not too progressive. Assembling with Fe^{2+} ions resulted in similarly small changes in the UV/vis spectra of the system when *r* value is increased and a parallel decrease to quenching of the luminescence.

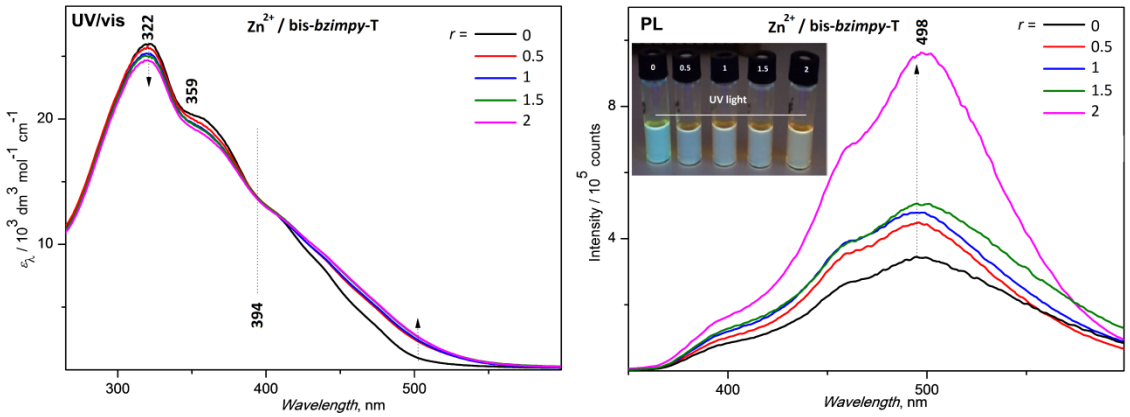

Figure 7. Absorption and emission spectra of Zn^{2+}/**bis-*bzimpy*-T** systems measured in DMSO.

Assembling with Fe^{2+} and Zn^{2+}metal ion couplers was also examined for **bis-*dopy*-T** unimer, precursor of the **bis-*bzimpy*-T** unimer. However, the complexation of **bis-*dopy*-T** with Zn^{2+} ions resulted in the formation of a precipitate, which disallowed spectral

monitoring of this process. Therefore, only results concerning the assembling with Fe^{2+} ions are presented in **Figure 8**.

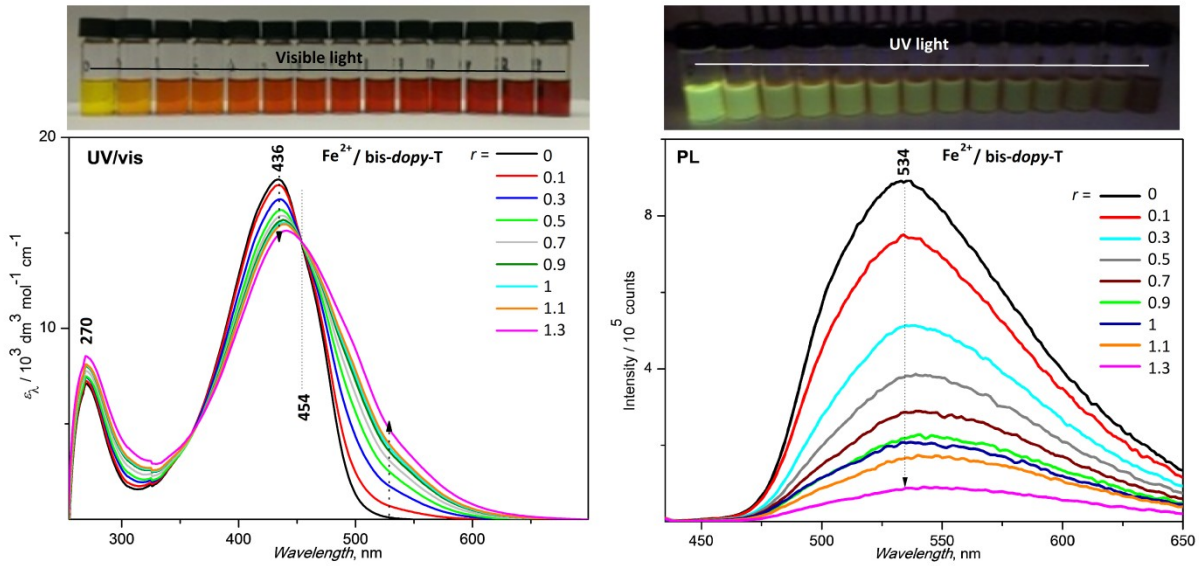

Figure 8. UV/vis and fluorescence titration spectra of bis-*dopy*-T (2×10^{-4} M) with Fe^{2+} ion couplers (2×10^{-2} M).

The solution UV/vis spectrum of **bis-*dopy*-T** unimer (**Figure 8**) showed a band of chelidamic end-groups centered at 270 nm and the main absorption band at 436 nm pertaining to transitions within terthiophene central block. The self-assembling with Fe^{2+} ions was accompanied by a small red shift of the main band with the appearance of a shoulder at around 530 nm which might but need not be related to the MLCT transition. Moreover, the UV/vis spectra showed an isosbestic point indicating the transformation of the free unimer species into another well-defined species. The luminescence spectra of the Fe^{2+}/**bis-*dopy*-T** systems showed only gradual luminescence quenching with increasing *r* but fairly not as progressive as that observed for related systems ***bzimpy*-T** or bis(***tpy***) unimers [187, 188].

3.3 Synthesis of ligands and unimers with 2,6-bis(oxazolyl)pyridine (*pybox*) group

Poor solubility of *bzimpy* unimer significantly reduces their potential practical usage. Therefore, to overcome this disadvantage, we have been searching for another, more favorable unimers capable of self-assembling in solutions. We have decided to synthesize

compounds bearing tridentate ligand 2,6-bis(oxazolyl)pyridine (***pybox***) as a chelating end-group. The decision to use this type of ligands was taken due to the following factors: i) better solubility; ii) possibility to introduce and change substituents at the 4-position of the pyridine rings of the ***pybox*** ligands. Besides that, complexes consisting of oxazoline moieties are widely used in microelectronics and in some catalytic systems [190, 191].

In order to check the method of preparation of ***pybox*** ligands, we have examined the synthesis of the simplest representative of ***pybox*** family - 2,6-bis(oxazolyl-2-yl)pyridine using 2,6-pyridine dicarboxylic (chelidamic) acid as a starting material. The synthetic path is shown in **Scheme 4**, where the 3-step procedure to the trial ligand is described. The first and second step of this path were accomplished as a one-pot synthetic procedure at which compound **2** was immediately used for further reaction with chlorethylamine due to strong hydrophobic effect of 2,6-pyridinedicarbonyl dichloride formed in the first step. The successful preparation of ***pybox*** ligand opened the door for the synthesis of new ligands and unimers with ***pybox*** chelating groups. Since this ligand has no novelty in complexation process with metal ions it was omitted from the study in the current work.

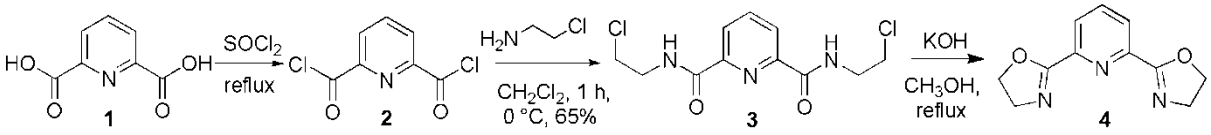

Scheme 4. Synthetic path to the simplest ***pybox*** ligand.

The synthesis of ***pybox*** ligands started from cheap chelidamic acid (same as in the case of *bzimpy*-based compounds), which was firstly transformed into dimethyl 4-bromopyridine-2,6-dicarboxylate further denoted as **BrPyMe** (see **Scheme 2**). The key ligand 2,6 bis(oxazoline-2-yl)-4-(2-thienyl)pyridine referred as ***pybox*-Th** was prepared using Suzuki coupling reaction (**Scheme 5**, route B) [192]. The purity and identity of ***pybox*-Th** ligand was confirmed by NMR and elemental analysis. More information on the synthesis, extraction and purification of the synthesized ligand and intermediate compounds can be found in Experimental section.

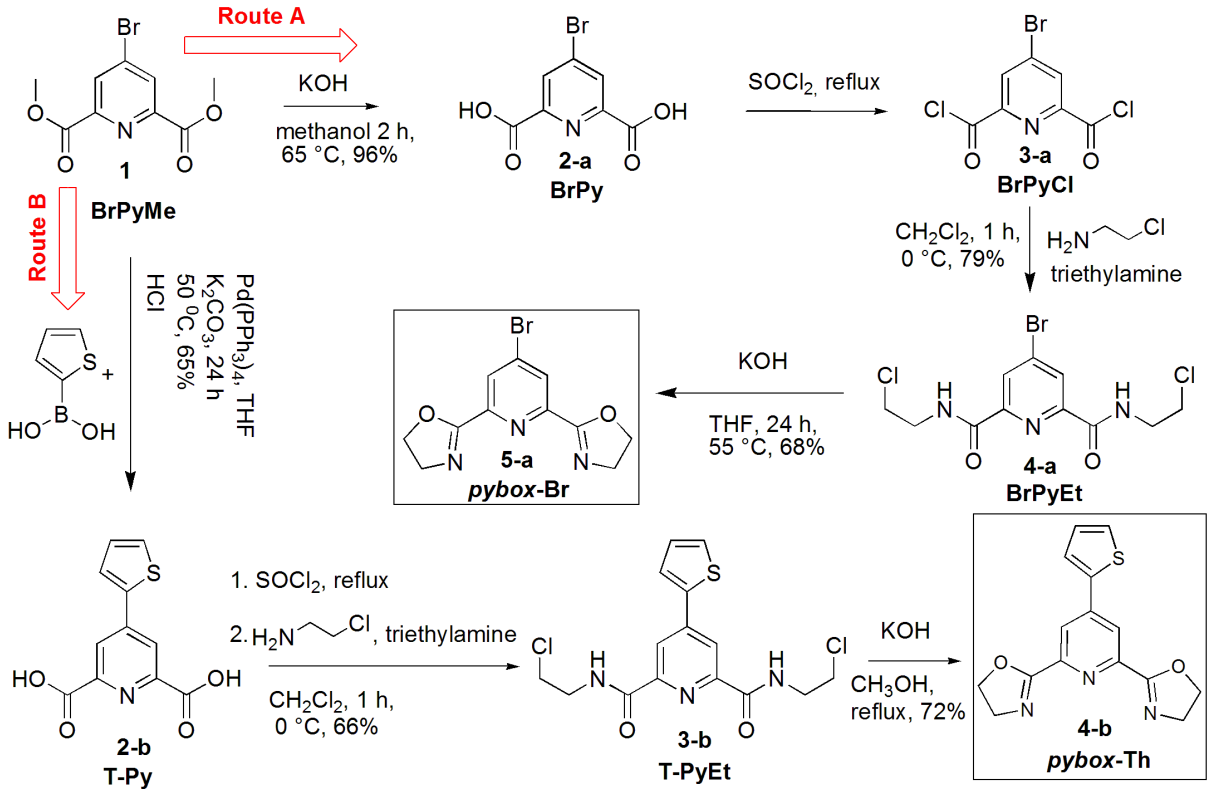

Scheme 5. Synthetic routes to ***pybox*-Th** ligand and a key bromo-***pybox*** precursor ***pybox*-Br**.

Another synthetic path to ***pybox*** ligand (compound) is described in Scheme 5 as the route A. This way provides 4-bromo-2,6 bis(4,5-dihydro-2-oxazolyl) pyridine (***pybox*-Br**) as the key intermediate: activated end-group which can be further connected to an oligomeric central block of a desired unimer. It should be stressed here that the last reaction step (cyclization with KOH) was necessary to optimize (modify compared to literature procedure) by using THF instead of methanol as the solvent owing to S_N1 substitution reaction taking place between methanol and intermediate **BrPyEt**.

The ***pybox*-Br** precursor allows different combinations of catalytic coupling reactions due to the presence of active Br group at the 4-position of pyridine. Originally, Suzuki cross-coupling of ***pybox*-Br** with various α,ω-dibromooligothiophenes available in our group was considered as the main reaction for the preparation of unimers with ***pybox*** end-groups. Therefore, ***pybox*-Br** has been reacted with bis(pinacolato)diboron reagent and thus successfully transformed into corresponding boronic acid pinacol ester. Unfortunately, consecutive Suzuki couplings of the pinacol ester with 2,5-dibromothiophene as well as other dibromo derivatives of the unimer central blocks failed. Variations of the reaction temperature, time and solvents did not led to an effective formation of the desired unimers

with ***pybox*** end-groups. Therefore, Stille coupling was chosen as an alternative way to bis(***pybox***) unimers. Direct couplings of ***pybox*-Br** with 2,5-bis(trimethylstannyl)thiophene, 5,5'-bis(trimethylstannyl)-2,2'-bithiophene or 2,5-bis(trimethylstannyl)-thieno[3,2-b]thiophene lead to the successful formation of the following unimers with relatively high isolated yields: α,ω-bis(2,6-bis(oxazoline-2-yl)pyridin-4-yl)thiophene (**P-Th**), α,ω-bis(2,6-bis(oxazoline-2-yl)pyridin-4-yl)bithiophene (**P-Bt**) and α,ω-bis(2,6-bis(oxazoline-2-yl)pyridin-4-yl)thieno[3,2-b]thiophene (**P-Te**), see **Scheme 6**. For details see Experimental part.

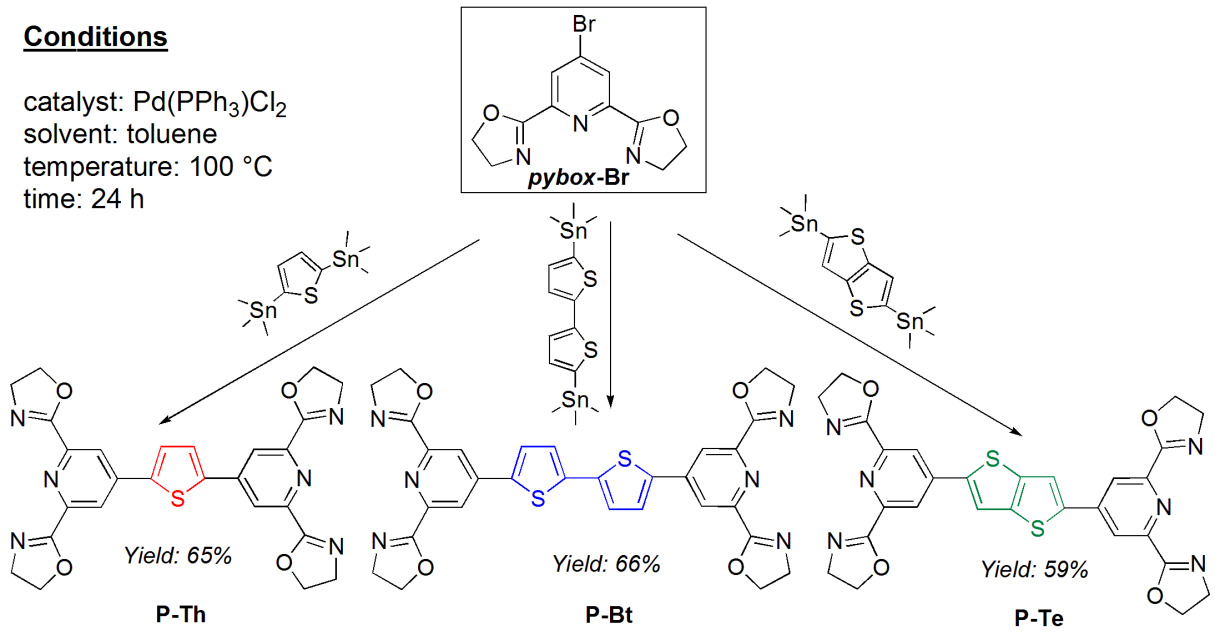

Scheme 6. Synthetic routes to conjugated unimers bearing ***pybox*** chelate end groups.

All unimers synthesized showed a good solubility in organic solvents especially in the mixtures of polar and non-polar solvents such as chloroform/methanol, which allowed their self-assembling with a wide range of metal ions leading to the formation of various MSPs. Good solubility also enabled casting of the films of unimers as well as their MSPs for the following analyses of their solid-state properties. The synthesized ***pybox*** unimers are absolutely new materials never studied before that show different photophysical properties and can be used for tuning the properties of corresponding MSPs through differences in the extent of delocalization of electrons within their building blocks and in the block´s stiffness.

3.4 Characteristics and assembling of monotopic *pybox*-Th ligand

The UV/vis spectrum of monotopic ligand ***pybox*-Th** shows a band of intraring π-π* and n-π* electronic transitions at 270 nm and the band of HOMO-LUMO transitions centered at 310 nm (**Figure 9**). The ligand coordination to Fe^{2+} as well as Zn^{2+} ions results to a blue shift of the former band to ca 250 nm, attenuation of the free ligand band (at 310 nm) and development of a new HOMO-LUMO band of the formed complex species located at 348 nm for Fe^{2+}/***pybox*-Th** and 352 nm for Zn^{2+}/***pybox*-Th**. The spectra of Fe^{2+}/***pybox*-Th** system show an additional band that can be attributed to the MLCT transitions within the formed complex species. Lowered wavelength of the HOMO-LUMO band of Fe^{2+}/***pybox*-Th** species compared to that of the for Zn^{2+}/***pybox*-Th** species can be explained by the fact that a part of the HOMO-LUMO transitions contributes to the MLCT band as it was observed for Fe-MSPs derived from bis(***tpy***)oligothiophene unimers [107]. Photos of vials filled with the measured samples shown in **Figure 9** demonstrate blue luminescence of Zn^{2+}/***pybox*-Th** systems and its absence for Fe^{2+}/***pybox*-Th** systems for which, on the other hand, the violet color typical of the MLCT transitions within Fe^{2+} complexes of this family of ligands.

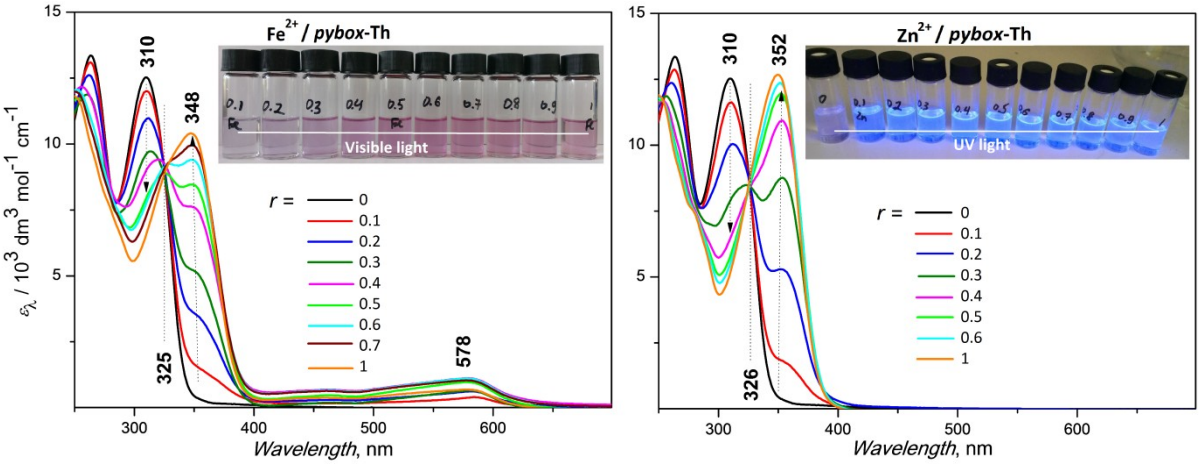

Figure 9. UV/vis spectra of systems Fe^{2+}/***pybox*-Th** and Zn^{2+}/***pybox*-Th** of various composition ratio *r*.

The UV/vis spectral sets of the studied systems show isosbestic points at almost identical wavelengths: 325 nm for the Fe^{2+}/***pybox*-Th** spectral set and 326 nm for the Zn^{2+}/***pybox*-Th** spectral set. As already mentioned above for ***bzimpy*** complexes, the presence of isosbestic points indicates a transformation of the defined original species into another defined species. Here, within experimental errors, we see only a single isosbestic

point for each Mt^{2+}/***pybox*-Th** system though the overall transformation should proceed in two distinct steps:

(i) $Mt^{2+} + 2L \rightarrow [MtL_2]^{2+}$ at $r \leq 0.5$, and

(ii) $[MtL_2]^{2+} + Mt^{2+} \rightarrow 2\,[MtL]^{2+}$ at r above 0.5.

This indicates coincidence of isosbestic points belonging to the above two consecutive transformations, which has already been also observed for some complexes and MSPs derived from bis(***tpy***) ligands and unimers [188]. The second possibility is that the ***pybox*** moiety does not form $[MtL_2]^{2+}$ species, which are referred to as "butterfly dimer" species, but only directly species $[MtL]^{2+}$.

Regarding the above uncertainty, ^{1}H NMR spectra of the Zn^{2+}/***pybox*-Th** systems have been measured in order to obtain supplementary data elucidating the formation of complex species. This experiment was performed in the following manner. A solution of Zn^{2+} ions (2×10^{-2} M) was prepared in a deuterated mixture of chloroform and methanol (1/1 by volume) and subsequently added to the prepared set of the solutions of ***pybox*-Th** (0.2 M) in the same solvent mixture in the amount to obtain solutions of the composition ratios equal to 0, 0.5 and 1. The series of prepared samples was left to equilibrate for 24 hrs them before NMR measurements, the results of which are shown in **Figure 10** and **Table 4**. Main information on the complex structure can be obtained from the signals of protons C2 and C3, because these protons occur in close vicinity of the central atom and thus they are most influenced by the complex structure. The spectrum taken from the system of r = 0.5, when the highest concentration of the butterfly dimer species is assumed to be present, shows the signal of C3 protons shift to lower fileds (from 4.01 to 4.85 ppm) due to the decreased electron density in coordinated oxazole rings. On the contrary, the signal of C2 protons is shift to higher fields (from 4.46 to 3.77 ppm) due to mutual shielding of C2-H bonds belonging to two different ligands bound to the same zinc atom perpendicularly (octahedral geometry). The spectrum of the system with r = 1 shows unchanged position of the signal of C3 but the almost disappearance of the signal at 3.77 ppm which is shift to 4 ppm where it is overlapped by the solvent signal. Nevertheless, some residual signals are apparent in the region between 3.77 and 4 ppm, which is indicates constitutional dynamics of the system, i.e., effective equilibrium exchanges described by the above shown reaction *(ii)*. Thus the NMR spectra proved the formation of species $[ZnL_2]^{2+}$ from zinc ions and molecules of

pybox*-Th**, which is of high importance for the formation of MSPs by the assembling of unimers with ***pybox end-groups with metal ions.

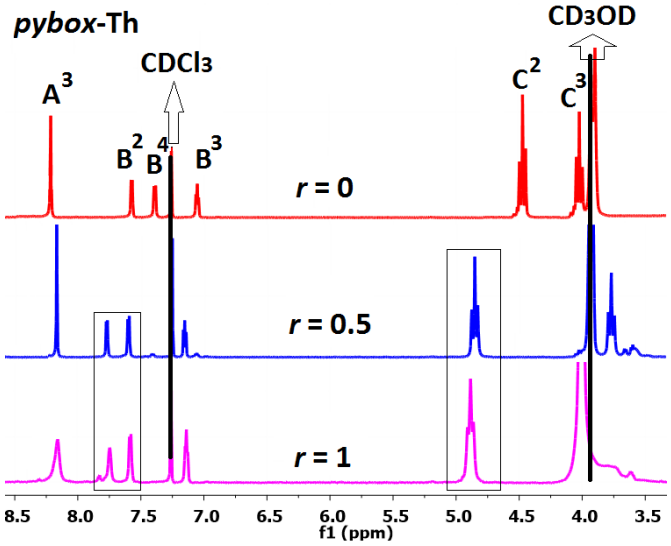

Figure 10. ^{1}H NMR data for ***pybox*-Th** and its complexes with Zn^{2+} ions.

Table 4. ^{1}H NMR chemical shifts (in ppm) for free ***pybox*-Th** and its complexes with Zn^{2+} ions.

Structure	Species	A^3	B^2	B^3	B^4	C^2	C^3
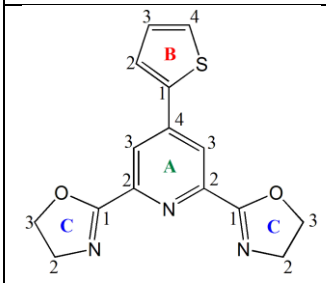	L	8.22	7.65	7.05	7.47	4.46	4.01
	ZnL	8.19	7.78	7.16	7.6	3.77	4.85
	ZnL_2	8.15	7.74	7.13	7.57	4.01	4.88

3.5 Characteristics and assembling of unimers with *pybox* end-groups

The solution and solid-state UV/vis spectra of ***pybox*** unimers are displayed in **Figure 11**. As can be seen, the band of HOMO-LUMO transitions is a function of the structure of the unimer central block. The lowest absorption band wavelength (λ_A = 350 nm) shows unimer **P-Th** with a single thiophene ring, medium: λ_A = 377 nm unimer **P-Te** with thieno[3,2-b]thiophene bicyclic structure and the highest λ_A = 377 nm unimer **P-Bt** with bithiophene sequence in the central block.

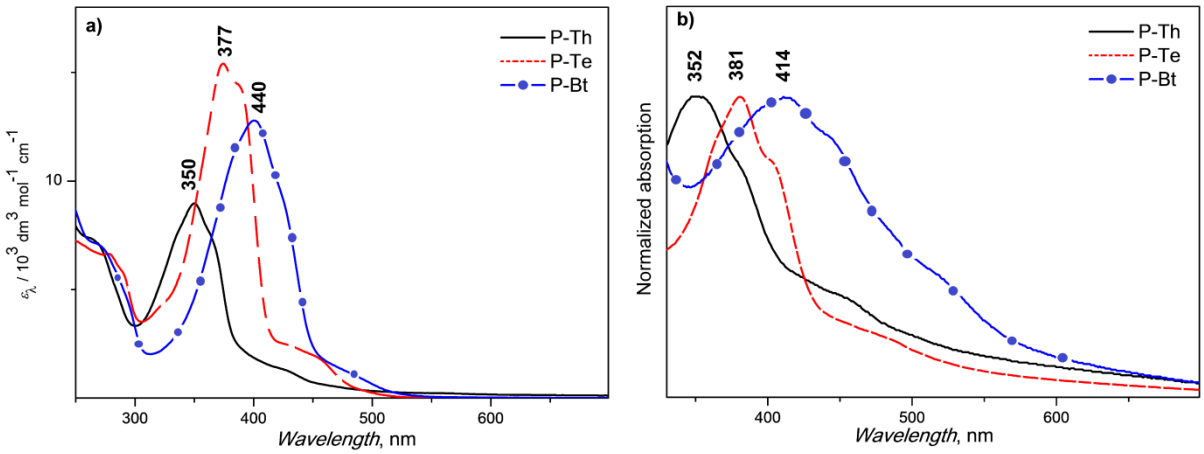

Figure 11. Absorption spectra of ***pybox*** unimers in solution (a) and solid state (thin films, b).

The observed positions of the absorption maxima are in a good accord with the extent of delocalization of valence electrons within unimer molecules. The energy of the HOMO-LUMO transitions decreases in the order: **P-Th** > **P-Te** > **P-Bt**. The lowest transition energy is observed for **P-Bt** with the largest system of conjugated double bonds and the highest transition energy for **P-Th** with smallest conjugated system. As it is evident, prolongation of the central block about only single thiophene ring drastically increased the λ_A value about 50 nm and, in addition, significantly increased the value of the molar absorption coefficients ε. On the other hand, the difference in λ_A between **P-Th** and **P-Te** is smaller but the increase in the ε value is much higher (doubled) when going from monocyclic thiophene-2,5-diyl to bicyclic thieno[3,2-b]thiophene-2,6-diyl unit in the central block.

Somewhat surprising are relatively small red shifts of the UV/vis absorption bands when going from solution to the solid state. The bands of the solid-state spectra of oligothiophenes are namely usually more redshifted with respect to their solution spectra due to the increased planarization of their main chains in the solid state [193]. Nevertheless, the absorption band should be evaluated not only as to its position but also as to its width, particularly its red broadening. As can be seen from **Figure 11 b**, the solid state spectra of all unimers are substantially red-broadened, the highest red broadening being observed for **P-Bt** indicating a high content of chromophores with the lowered band-gap energy, i.e., with increased extent of the delocalization of electrons.

The solution and solid-state luminescence spectra of ***pybox*** unimers are displayed in **Figure 12**. The solution spectra show two (**P-Th**) to four (**P-Bt** and **P-Te**) modal emission bands with maxima at wavelengths λ_F increasing in the same order as absorption maxima λ_A:

P-Th > **P-Te** > **P-Bt** (see **Table 5**). Unlike the solution spectra, the solid-state luminescence emission spectra of unimers showed unimodal bands with maxima λ_F substantially red shifted with respect to their values for solution spectra. The highest red shift with respect to the solution showed the band of the simplest unimer **P-Th**. As a result of this, the value of λ_F for the solid-state spectra increases in the order: **P-Te** > **P-Th** > **P-Bt** that differs from the order found for the solution spectra.

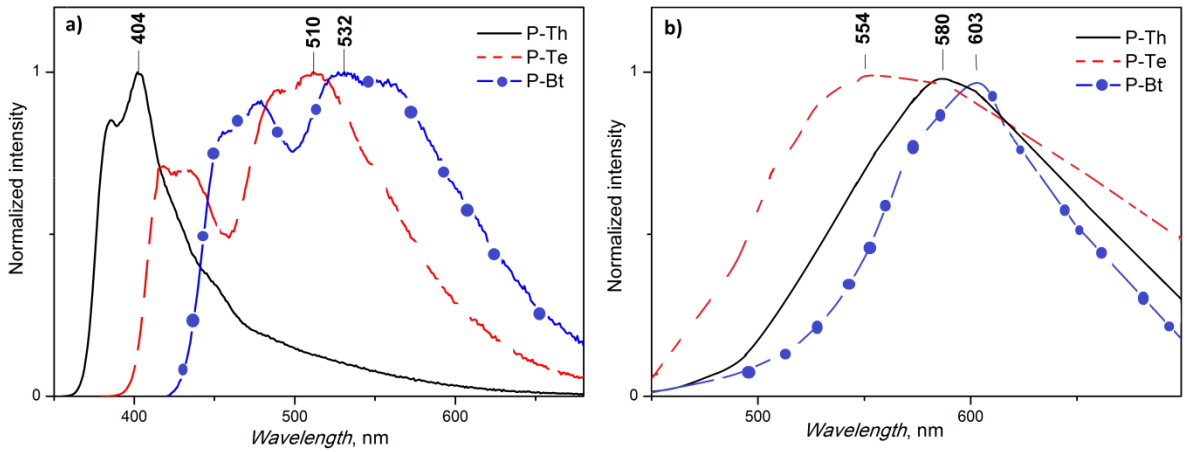

Figure 12. Photoluminescence spectra of ***pybox*** unimers in solution (a) and in the solid state (b).

The energy difference between emission and absorption bands of a given compound is known as the Stokes shift ν_S. This shift is a measure of the energy relaxation of excited molecules prior to their radiative transition to the ground state. As can be seen from **Table 5**, the Stokes shift values of **P-Te** and **P-Bt** determined for solutions and films relatively little differ from each other (6 200 to 8 200 cm^{-1}), the ν_S value for film being cca about 1000 cm^{-1} higher compared to the value for solution. In contrast, **P-Th** showed clearly the smallest ν_S in solution (of only 3 800 cm^{-1}) but clearly the highest ν_S in the solid state (11 170 cm^{-1})! Similarly high Stokes shift has been recently observed for bis(***tpy***)terthiophene and proved to be due to the formation of excimers [153, 194, 195]. However, so high Stokes shift can also originate from the high extent of the conformational relaxation of excited molecules. Therefor, we examined the morphology of the prepared unimers (**P-Th**, **P-Bt**, **P-Te**) using the powder X-ray diffraction (XRD) which provides information on the degree of crystallinity of measured samples.

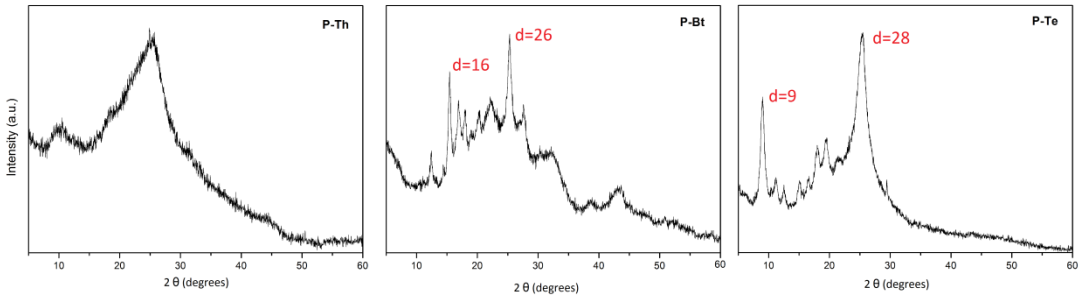

Figure 13. XRD spectra of ***pybox*** unimers.

The obtained XRD spectra of unimers are shown in **Figure 13**. As can be seen, the XRD pattern of **P-Th** does not contain any sharp reflection indicating the presence of crystallites. Thus this unimer can be regarded as an amorphous solid. On the other hand, the XRD patterns of the **P-Bt** and **P-Te** unimers showed sharp reflections: **P-Bt** at 2ϑ = 16° (first order reflection) corresponding to a *d* spacing of 5.7 Å and at 2ϑ = 26° corresponding to a *d* spacing of 3.5 Å; **P-Te** at 2ϑ = 9° and 28°, corresponding to a *d* spacing of 10 °A and 3.3 °A, respectively. In addition, the presence of reflections of low-intensity but high sharpness is observed in the XRD patterns of both these unimers. These observations indicate a rather high degree of crystallinity of the solid **P-Bt** and **P-Te** unimers. Though we do not know (based on the XRD data) how the unimer molecules are packed in the crystallites, it seems reasonable that they cannot undergo extensive conformational relaxation upon excitation because they are somehow anchored in the crystallites. On the other hand, excited **P-Th** molecules occurring in amorphous environment should be more weekly anchored and thus supposed to undergo more extensive conformational relaxation in exctid states. Nevertheless, the formation of excimers during these relaxations is not excluded.

The fluorescence quantum yield (ϕ_F) values were determined to be ca 13 to 14 % for solutions and about 1.5 % for films of unimers with mono- and bi-thiophene central blocks (**P-Th** and **P-Bt,** see **Table 5**). The **P-Bt** unimer showed significantly but not too much lower values of ϕ_F: 7.3 % for solution and 1.2 % for film, which indicates that the rigid bithiophene central block somewhat more favors a non-radiative decay of the excited states.

Table 5. Spectroscopic data for ***pybox*** unimers; λ_A - absorption maximum wavelength (nm); ε_{max} - molar absorption coefficient ($m^3\ mol^{-1}\ cm^{-1}$); λ_F - emission maximum wavelength (nm); ν_S - Stokes shift (cm^{-1}); ϕ_F - fluorescence quantum yield (%).

Sample	λ_A, nm		ε	λ_F, nm		ν_S, cm^{-1}		Φ, %	
	solution	film	solution	solution	film	solution	film	solution	film
P-Th	350	352	8.9	404	580	3 820	11 170	12.8	1.57
P-Bt	400	414	12.6	532	603	6 210	7 570	7.3	1.17
P-Te	373	381	15.3	510	554	7 210	8 200	14.3	1.45

3.6 Assembling of *pybox* unimers with metal ions

The process of self-assembling of ***pybox*** unimers with various metal ions such as Fe^{2+}, Zn^{2+}, Ni^{2+}, Cu^{2+} (all with ClO_4^- counterions) and lanthanides Eu^{3+} or Tb^{3+} (with Cl^- counterions) to MSPs in solutions was monitored by the UV/vis and photoluminescence spectroscopy, NMR spectroscopy and size-exclusion chromatography (SEC).

For the UV/vis spectroscopic monitoring, a set of solutions of each unimer (**P-Th**, **P-Bt** and **P-Te)** of the constant unimer concentration (2×10^{-4} M) but different composition ratio *r* from 0.1 to 1.5 had been prepared in the chloroform/methanol (1/1 by volume) mixed solvent and allowed to equilibrate for 24 hrs before recording the spectra. This solvent mixture, consisting of a polar and a non-polar solvent that together form a positive azeotrope, has been found suitable for dissolving unimers as well as all used metal salts.

The UV/vis spectral changes caused by the gradual increase in the ratio *r* are shown in **Figures 14** to **16**. They are characterized by attenuation of absorption bands of the free unimer and occurrence of new bands attributed to the formed MSPs oligomers (at low *r* values) and polymers (at higher *r* values). Crossings of the spectra indicating the presence of isosbestic points indicating the transformation of free unimer species into other well-defined species have been also observed. The assembling can be divided into three stages, same as assembling of bis(***tpy***) unimers described in literature [107]: *(i)* formation of butterfly dimers U-Mt^{2+}-U in systems with $r < 0.5$, *(ii)* growth of MSP chains [-Mt^{2+}-U-]$_n$ in systems with *r* from 0.5 to ca 1, and *(iii)* equilibrium dissociation of the longer MSP chains to shorter chains end capped with excess of Mt^{2+} ions in systems with $r > 1$. The systems with Fe^{2+} ion couplers have shown the MLCT band at relatively high positions from 629 to 635 nm, which are even higher than λ_{MLCT} determined for Fe-MSPs with phosphole rings in the central block [194].

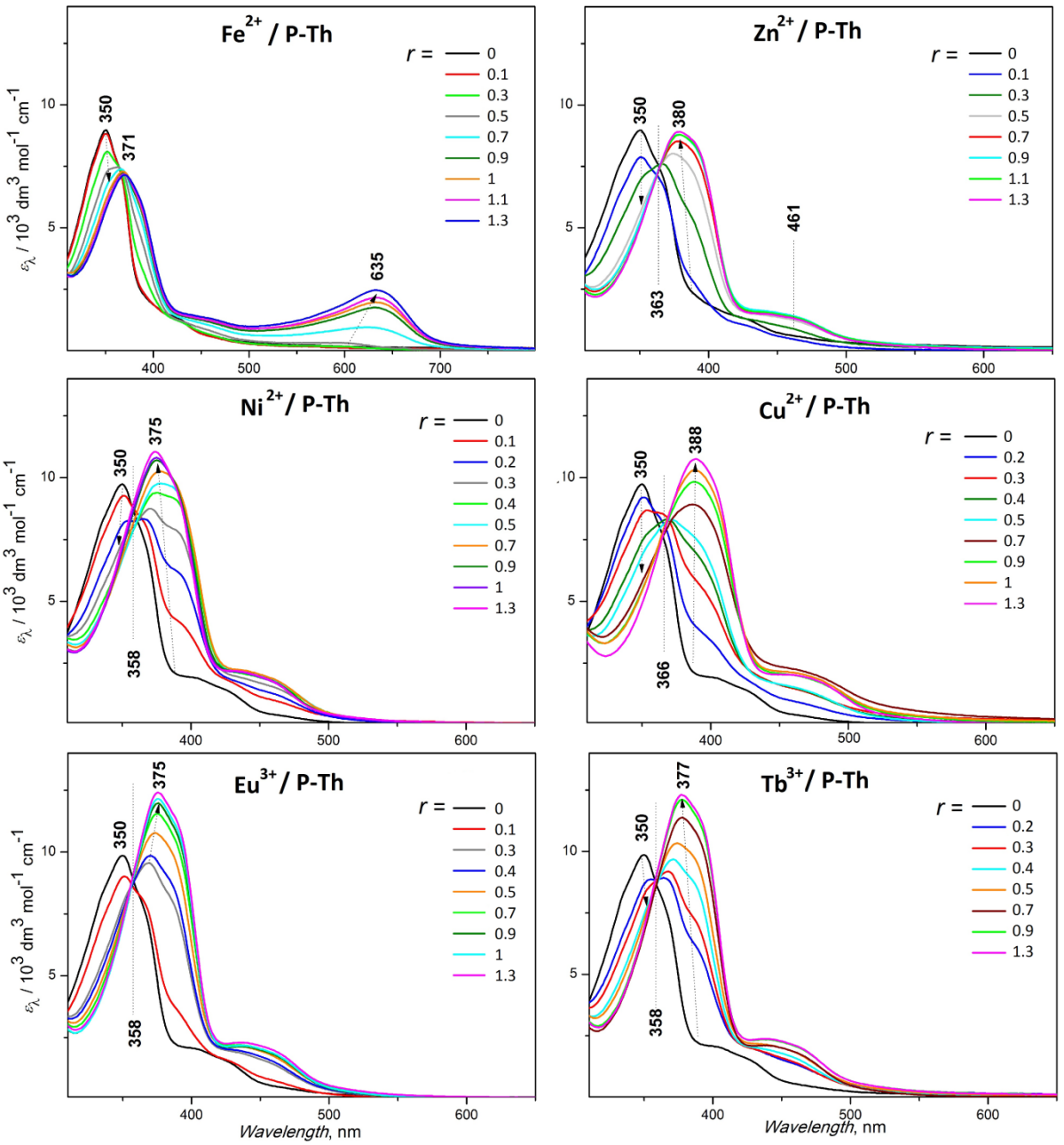

Figure 14. UV/vis spectra of Mt^{2+}/**P-Th** systems of various composition ratio *r*.

The positions of absorption maxima of formed MSPs strongly depend on the metal ion couplers used. The differences between absorption maxima position of unimers and their MSPs with various ions at *r* = 1 are collected in **Table 6** and the round diagrams of **Figure 17**. The highest red shifts when going from free unimer to its MSP were observed for Cu^{2+}-MSPs, the lowest one for Fe^{2+}-MSPs, which can be ascribed to partial transfer of the corresponding transitions to the MLCT band of these MSPs, as observed for other systems, too [153, 194].

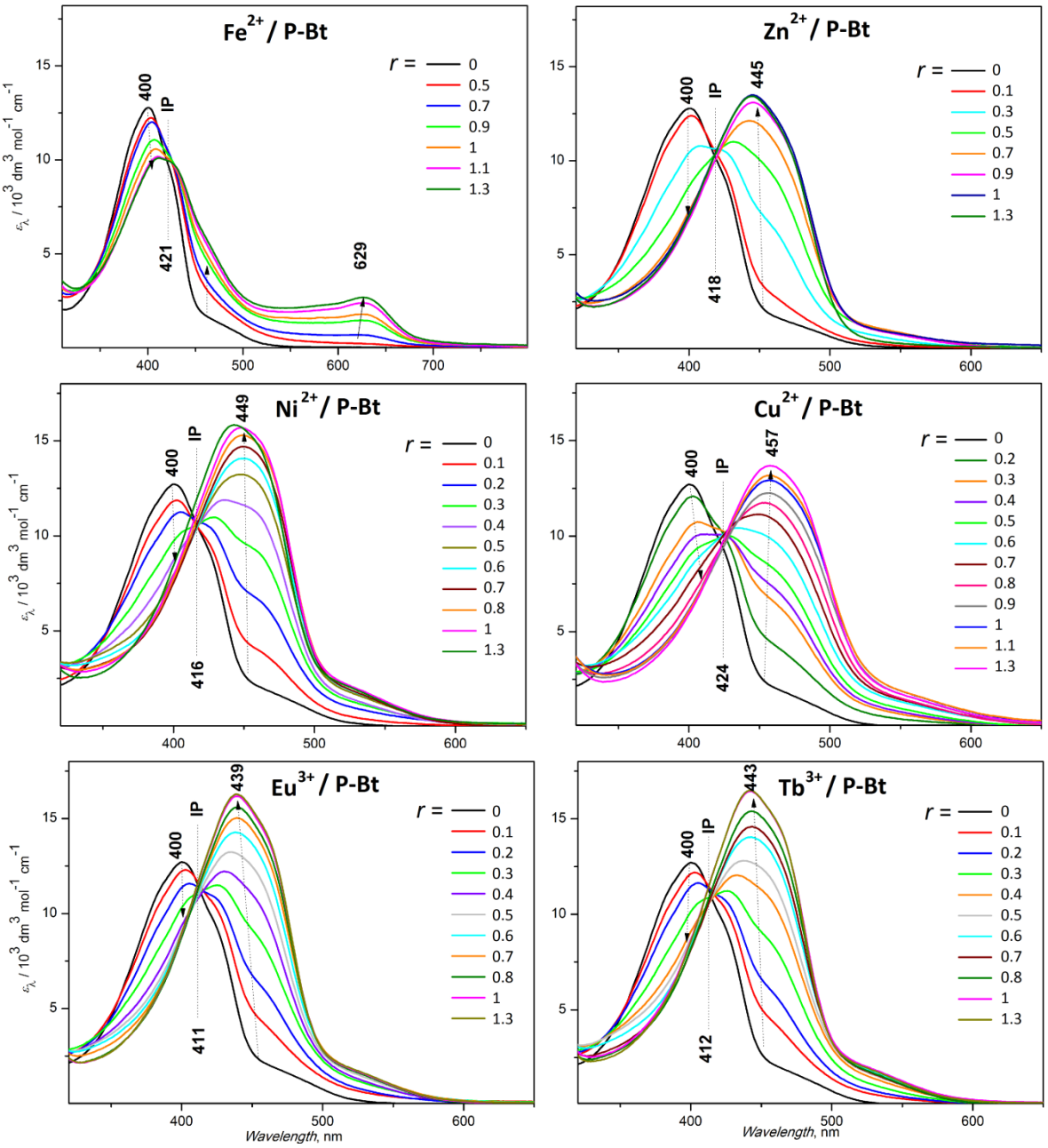

Figure 15. UV/vis spectra of Mt^{2+}/**P-Bt** systems of various composition ratio *r*.

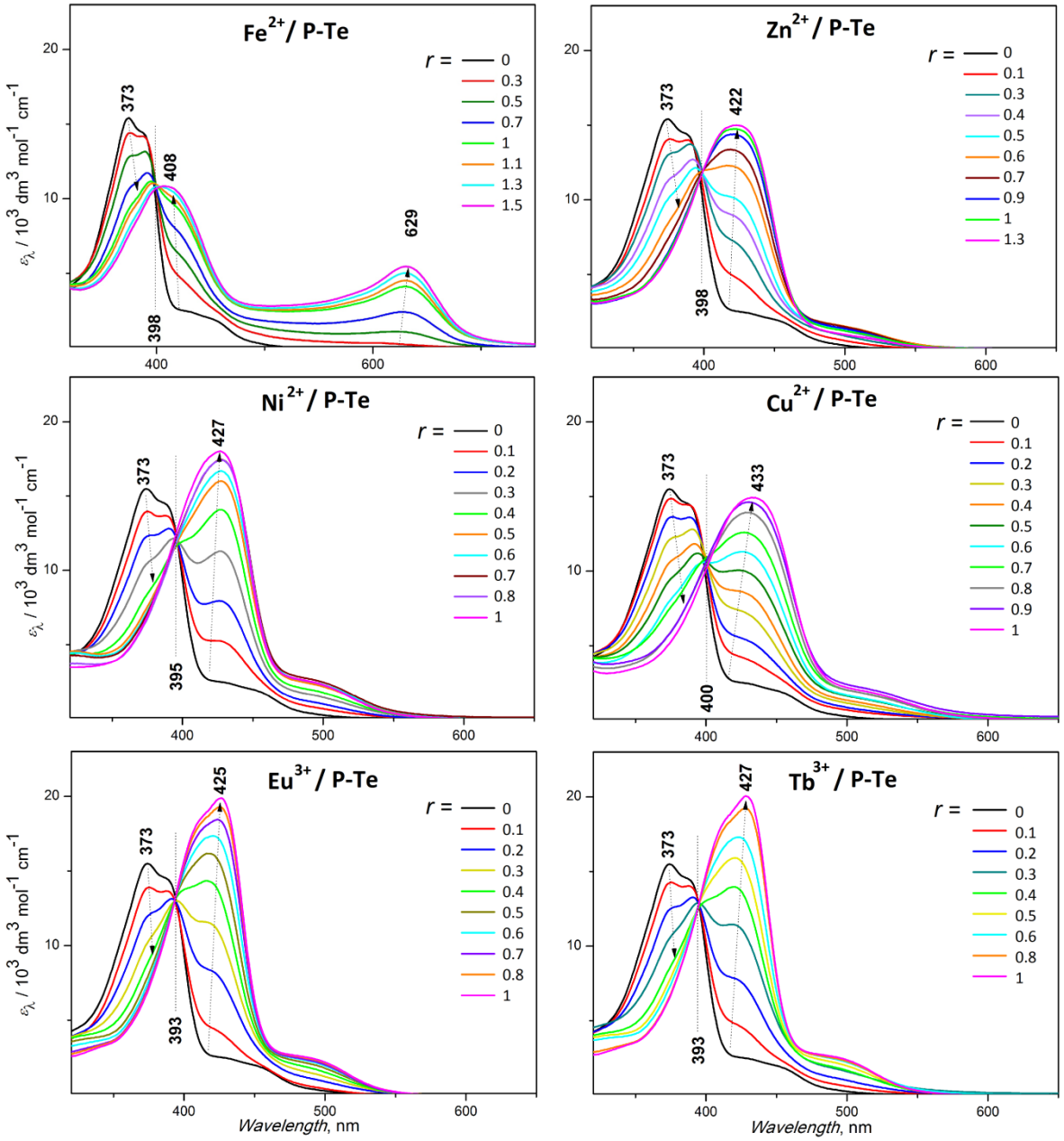

Figure 16. UV/vis spectra of Mt^{2+}/**P-Te** systems of various composition ratio *r*.

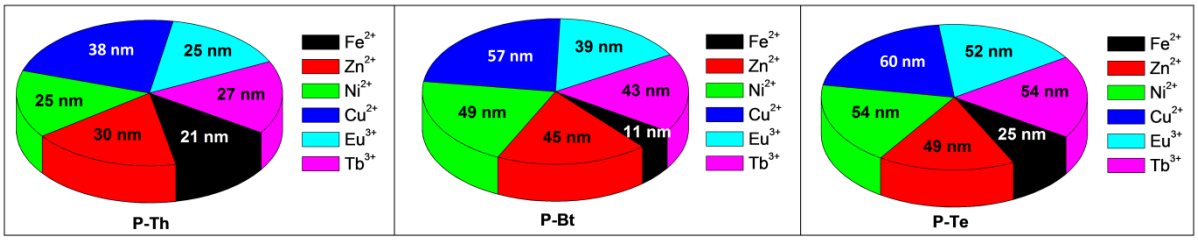

Figure 17. Red shifts of λ_A when going from the unimer to its MSPs with various ion couplers.

Dynamic nature of MSPs has been examined by the "*end-capping experiment*" at which the ***pybox*-Th** monotopic ligand has been added to the solution of Zn^{2+}/**P-Bt** MSPs (r = 1). The occurrence of an additional (new) absorption band with λ_A equal to that determined for the dimer species ***pybox*-Th**-Zn^{2+}-***pybox*-Th** was observed. This observation can be explained by partial disassembling and/or end-capping of MSP chains with ***pybox*-Th** ligands as well as by the formation of the butterfly dimer species on account of the MSP chains. In any case the result of this experiment proves constitutional dynamics of the ***pybox*** type Zn-MSPs. Unfortunately, the dynamics of the MSPs in solution has been found so fast that it disallowed a GPC/SEC analysis of the prepared MSPs.

Table 6. UV/vis spectral data for ***pybox*** MSPs (r = 1) with different metal ions: λ_A - wavelength (nm); ε_{max} - molar absorption coefficient of absorption maximum (m^3 mol^{-1} cm^{-1}); λ_e - absorption edge wavelength; λ_F - wavelength of emission maximum (nm); ν_S - Stokes shift (cm^{-1}).

Metal	P-Th					P-Bt					P-Te				
	λ_A nm	λ_e nm	ε_{max}	λ_F nm	ν_S cm^{-1}	λ_A nm	λ_e nm	ε_{max}	λ_F nm	ν_S cm^{-1}	λ_A nm	λ_e nm	ε_{max}	λ_F nm	ν_S cm^{-1}
U	**350**	**491**	**8.9**	**404**	**3820**	**400**	**526**	**12.6**	**532**	**6210**	**373**	**516**	**15.3**	**510**	**7210**
Fe^{2+}	371	698	7.2	408	2445	411	687	10.5	480	3490	398	702	10.9	440	2390
Zn^{2+}	380	516	8.7	434	3270	445	625	13.3	542	4020	422	566	14.6	483	2990
Ni^{2+}	375	523	10.6	409	2210	449	594	15.6	496	2110	427	567	17.9	465	1910
Cu^{2+}	388	538	10.2	421	2020	457	632	12.8	501	1920	433	583	14.9	474	1990
Eu^{3+}	375	505	12.1	415	2570	439	583	16.2	502	2860	425	543	19.8	460	1790
Tb^{3+}	377	509	12.0	421	2770	443	594	16.3	513	3080	427	550	19.8	468	2050

The luminescence spectra of the unimer/Mt^{2+} systems were taken from the same solutions from which UV/vis spectra were taken. The examples of the spectra obtained for the systems derived from unimer **P-Th** are shown in **Figure 18**. As can be seen, the coordination of unimer to metal Zn^{2+} ion couplers resulted in the attenuation of the emission band of free **P-Th** (λ_F = 404 nm) and simultaneous occurrence of a new band with maximum at 433 nm, which can be assigned to the formed Zn-MSP chains. In contrast, all systems with the other used ion couplers exhibited only attenuation and a small red or blue shift of the emission band maximum but not any formation of a new emission band. Qualitatively similar behavior has been observed for the MSPs derived from bis(***tpy***) unimers with phosphole ring in the central block [194] and, if only difference between Zn- and Fe-MSPs is concerned, for many bis(***tpy***) unimers with oligothiophene and oligoarylene central blocks [107, 153, 188]. However, there is a significant difference between systems with ***tpy*** and ***pybox*** unimers as to

the extent of the luminescence attenuation at higher values of the composition ratio *r*. The ***pybox*** systems show only more or less pronounced luminescence attenuation but not its total quenching which is otherwise typical of almost all Fe^{2+}/bis(***tpy***) unimer systems. This observation points to a substantial difference between MSPs derived from the ***pybox*** and the ***tpy*** type unimers concerning the relaxation of the electronically excited states in these MSPs.

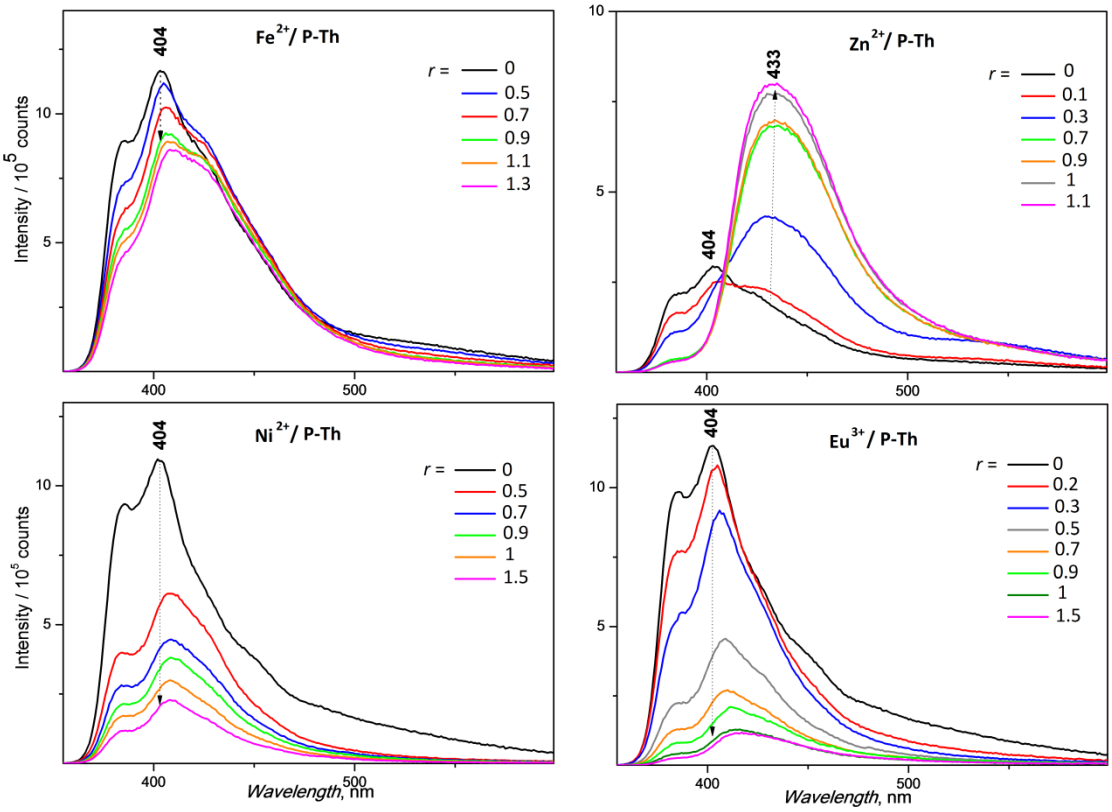

Figure 18. Photoluminescence spectra of different Mt^{2+}/**P-Bt** systems as a function of the ratio *r*.

Table 7. Fluorescence emission maxima (λ_F, nm) and quantum yields (ϕ_F, %) of the dissolved and solid state Zn-MSPs (*r* = 1) derived from ***pybox*** unimers.

	P-Th + Zn^{2+}		**P-Bt + Zn^{2+}**		**P-Te + Zn^{2+}**	
	λ_F, nm	ϕ_F, %	λ_F, nm	ϕ_F, %	λ_F, nm	ϕ_F, %
solution	434	22.2	542	34.2	483	17.4
film	614	2.02	635	1.99	618	1.51

The values of the luminescence band maxima λ_F and quantum yields ϕ_F for both the dissolved and the solid state Zn-MSPs derived from ***pybox*** unimers are summarized in **Table 7**. As can be seen, all systems exhibited a significant red shift of the absorption band when

going from solution to the solid state, the highest shift (+180 nm) being observed for Zn^{2+}/**P-Th** polymer and the lowest one (+90 nm) for Zn^{2+}/**P-Te** polymer. It is worth noting here that also in this respect the ***pybox*** MSPs substantially differ from the ***tpy*** MSPs which typically show rather small red shift or even blue shift of the emission band when going from solution to the solid state [107, 153].

3.7 Mode of the coordination of *pybox* end-groups to metal ions and morphology of MSPs

The ***pybox*** end-group contains oxazoline ring that can coordinate to a metal ion by N or O atom. The coordination mode of the oxazoline moiety has been determined by the X-ray photoelectron spectroscopy (XPS) measurements on free unimers and their Cu^{2+} based MSPs. The samples of Cu-MSPs were prepared by mixing equimolar amounts of a given unimer and Cu^{2+} perchlorate in chloroform/methanol mixture (concentration of 0.02 M) followed by isolation and drying in vacuum of the formed precipitate of corresponding MSPs.

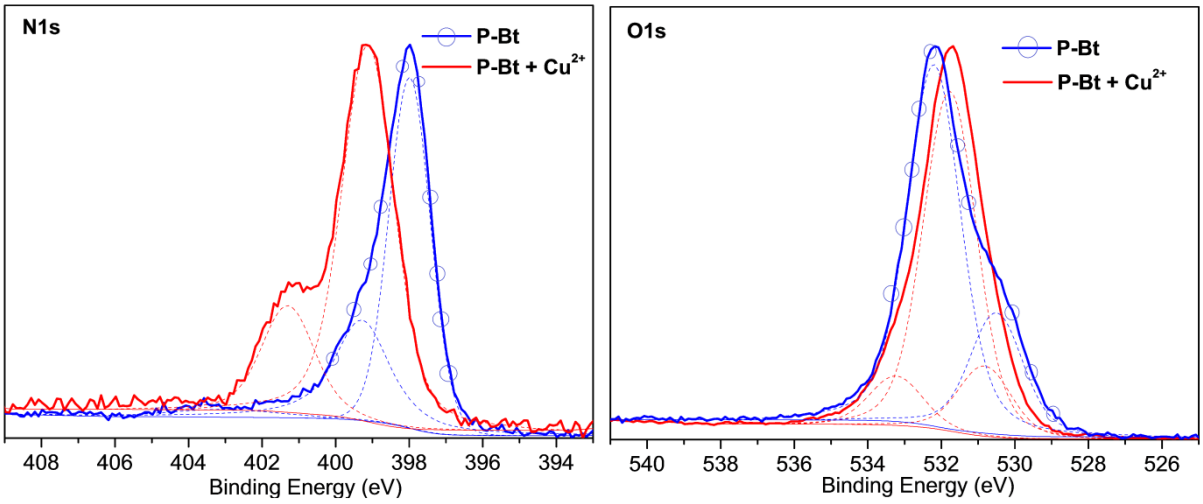

Figure 19. XPS spectra of **P-Bt** and its Cu-MSP (*r* = 1).

The results of XPS measurements done on **P-Bt** and its Cu-MSP (as an example) are shown in **Figure 19**. For all unimers studied (**P-Th**, **P-Bt** and **P-Te**), a shift of the peaks to a higher binding energy (1.1–2 eV) was observed in the N1s XPS spectra (see left part of **Figure 19**). This shift is caused by the electron withdrawing capacity of Cu^{2+} ions, which decreases electron density on the nitrogen atoms in the pyridine and oxazoline rings. This results in the enhancement of the effective nuclear charge experienced by the core-electron, thereby

increasing the electron binding energy. Unlike the N1s XPS spectra, the O1s XPS spectra showed a shift of the XPS band to a lower electron binding energy. This unambiguously indicates predominant coordination of the oxazoline rings through the nitrogen atoms.

The prepared Cu-MSPs were also investigated as their solid-state structure by the XRD method. Cu^{2+}-MSPs were chosen because they exhibit the highest shifts of the UV/vis absorption maxima to lower energies when going from a unimer to its MSPs. As can be seen from **Figure 20**, the XRD patterns of Cu-MSPs do not exhibit any sharp reflection but only extensive broadening of peaks indicating the amorphous character of self-assembled Cu-MSPs.

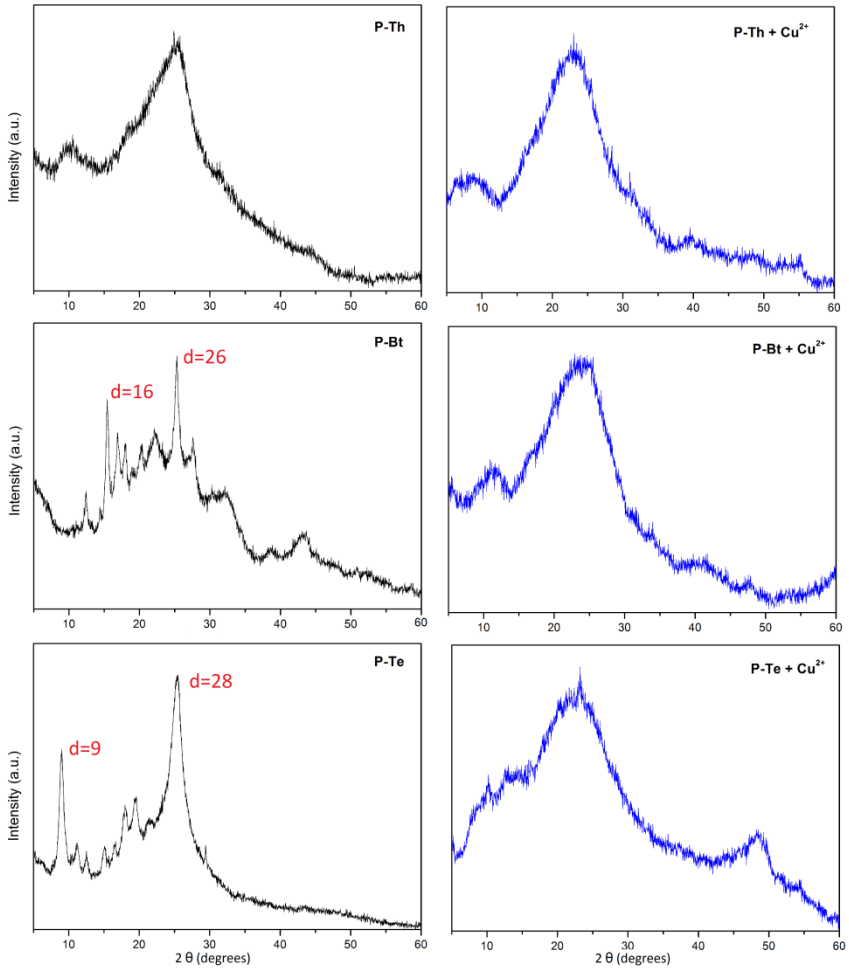

Figure 20. XRD spectra of ***pybox*** Cu-MSPs (right). For a comparison, the patterns of ***pybox*** unimers copied from Fig. 13 are presented as well.

4 RESULTS AND DISCUSSION – Polythiophene based polyelectrolytes

4.1 Synthesis of cationic polythiophene polyelectrolytes

New conjugated cationic polyelectrolytes with phosphonium side groups have been prepared using the modification strategy already applied at our laboratory for the preparation of polythiophene based polyelectrolyte with imidazolium side groups [158]. First precursor polythiophenes of different regioregularity that contained reactive 6-bromohexyl side groups: poly[3-(6-bromohexyl)thiophene-2,5-diyl] further abbreviated as **PHT-Br**, have been prepared, isolated and characterized and then they were subjected to the reactions with triethylphosphine or thiphenylphosphine.

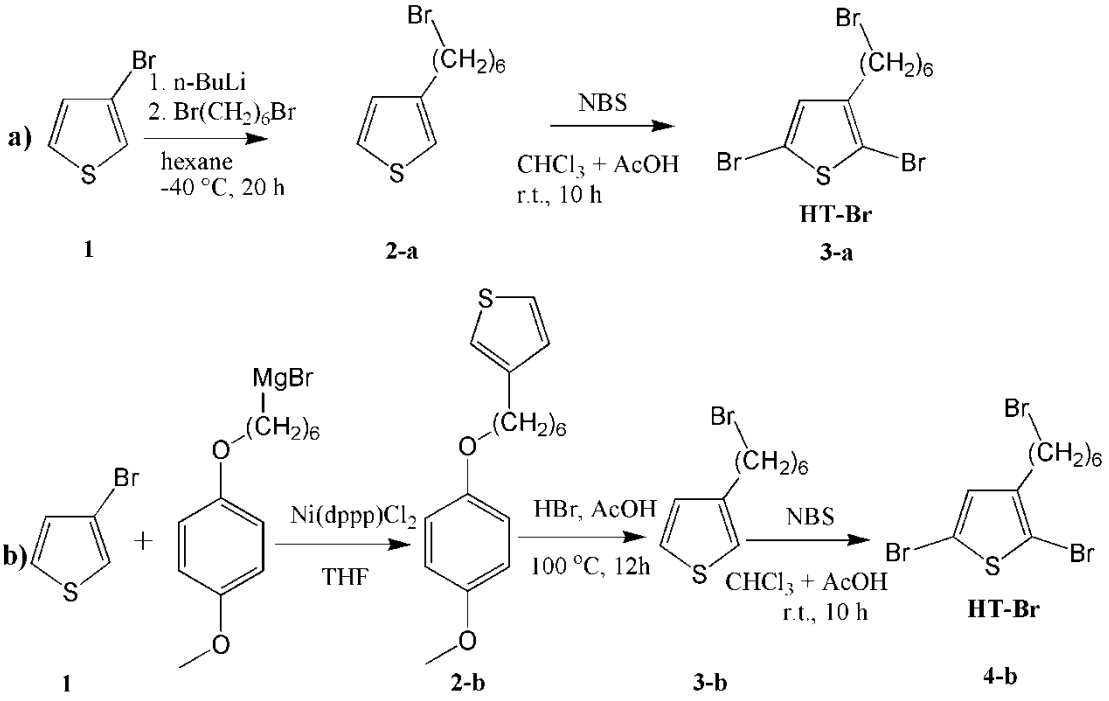

Scheme 7. Synthetic routes to the key monomer 3-(6-bromohexyl)thiophene.

The preparation of **PHT-Br** started with the synthesis of the corresponding monomer: 2,5-dibromo-3-(6-bromohexyl)thiophene. Two synthesis paths shown in **Scheme 7** have been examined. The synthetic path a) is shorter but requires an effective high vacuum distillation after the first reaction step in order to separate the desired product: **HT-Br** from the side product formed by substitution of both bromine atoms of 1,6-dibromohexane with 3-thienyl groups. The amount of side product in the reaction mixture could be reduced by

the dropwise adding of the solution of 3-thienyl lithium into a high excess of relatively cheap 1,6-dibromohexane. If this reaction step was done using the sufficiently large amounts of reactants, the separation of the resulting reaction mixture by vacuum distillation was found to effective. The second reaction path as b) that already has been used in our group is more complicated. The main difficulties concerning this path have been found in its second step: reaction of **2-b** with HBr.

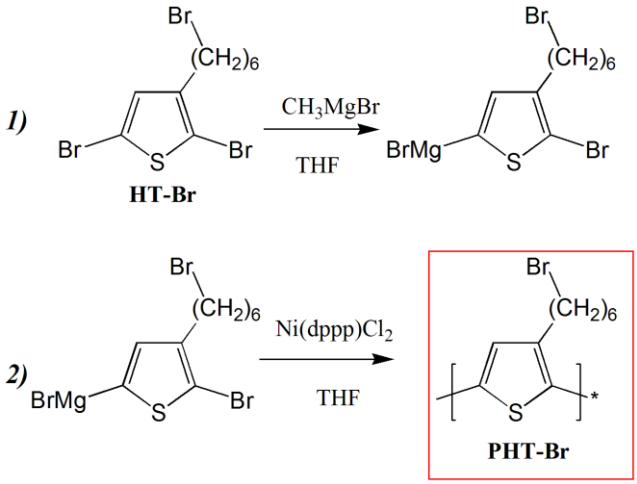

Scheme 8. Synthesis of poly[3-(6-bromohexyl)thiophene-2,5-diyl] by GRIM polymerization.

Polymerization of **HT-Br** was performed using Grignard metathesis polymerization usually referred to as GRIM polymerization. The GRIM polymerization is mostly used for the preparation of highly regioregular poly(3-alkyl)thiophenes. However, modification of the reaction temperature of the second step of polymerization procedure (**Scheme 8**) allowed us to synthesize **PHT-Br** with different values of the molecular weight (MW) and head-to-tail (H-T) regioregularity. **PHT-Br** of the lowest MW as well as regioregularity, further referred to as **PL-Br**, was prepared in such a way that the reaction mixture obtained by adding CH_3MgBr into **HT-Br** solution in dry THF at 0° C was slowly heated up and finally kept under reflux for two hours. After that, the reaction mixture was cooled down to room temperature, $Ni(dppp)Cl_2$ catalyst was added and the mixture heated up and stirred under reflux (65° C) for next two hours. The formed **PL-Br** was then precipitated with methanol and repeatedly reprecipitated in order to remove low-MW fractions and catalyst remnants. The precursor polymer **(PHT-Br**) of medium MW and regioregularity (**PM-Br)** was prepared using the polymerization temperature of 25 °C and the precursor polymer of the highest MW and

regioregularity (**PH-Br**) using the lowest polymerization temperature of only 5 °C. The synthetic procedures are in detail described in the Experimental section.

The simple quaternization reactions of the precursor polymers with triethylphosphine or triphenylphosphine (**Scheme 9**) gave corresponding conjugated polyelectrolytes: poly {3-[6-(triethylphosphonium)hexyl]-thiophene-2,5-diyl bromide} and poly {3-[6-(triphenyl-phosphonium)hexyl]-thiophene-2,5-diyl bromide}, respectively, of different (low, medium and high) both MW and regioregularity. Polyelectrolytes bearing triethylphosphonium side groups are further denoted as **PL-EtP$^+$**, **PM-EtP$^+$** and **PH-EtP$^+$** while those with triphenylphosphonium side groups as **PL-PhP$^+$**, **PM-PhP$^+$** and **PH-PhP$^+$**. Polyelectrolytes with N-methylimidazolium side groups were prepared using the procedure described in ref. [196]. Details of the preparation of polyelectrolytes are given in the Experimental part.

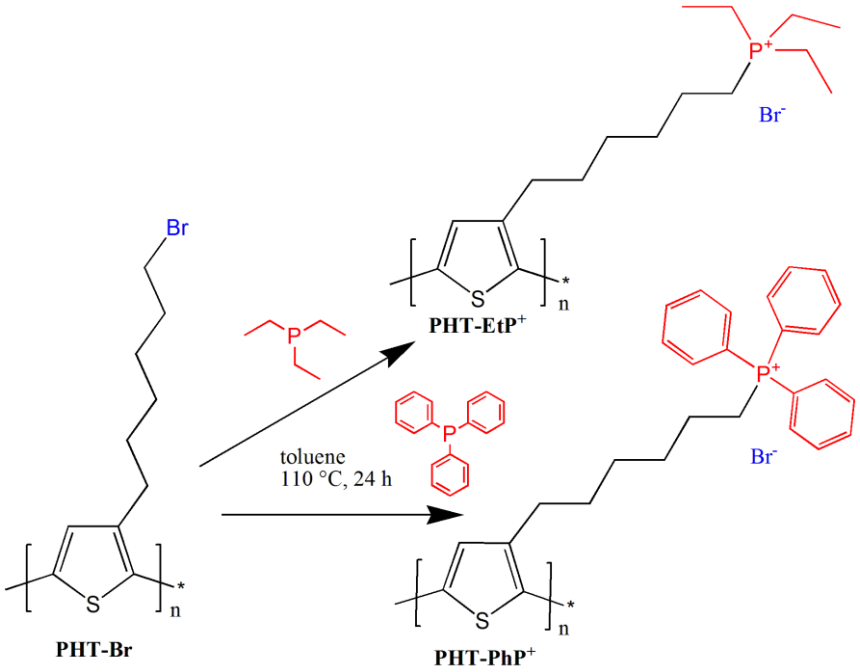

Scheme 9. Synthetic routes to polythiophene polyelectrolytes with phosphonium side groups.

4.2 Characterization of precursor polymers and related polyelectrolytes

The synthesized **PL-Br**, **PM-Br** and **PH-Br** polymer precursors were reproducibly obtained by GRIM reaction catalyzed by Ni(dppp)Cl_2. As indicated above, a remarkable dependence of MW and H-T regioregularity of the precursor polymers on the reaction temperature has been observed (see **Table 8**).

Table 8. Polymerization data for **PHT-Br.** *T* is polymerization temperature; M_w - weight-average molar mass; M_n - number-average molar mass; *Đ* - dispersity; *rr* - H-T regioregularity.

Sample	*T*, °C	M_w kg mol^{-1}	M_n kg mol^{-1}	*Đ*	*rr* %
PL-Br	65	7.20	4.6	1.6	62
PM-Br	25	11.8	6.8	1.7	78
PH-Br	5	13.2	8.7	1.5	94

^{1}H NMR spectra of the precursor polymers are presented in **Figure 21**. ^{1}H NMR allows determination of regioregularity of poly[(3-alkyl)thiophenes] from the integral intensity ratio of NMR signals at 2.8 and 2.6 ppm pertaining to H-T and HH-TT sequences, respectively. The signal at 2.8 ppm is attributed to α-methylene protons of regioregular polymer and signal at 2.6 ppm to irregular sequences including the end units of polymer chains. The regioregularity has been estimated (calculated) as the ratio: *a*/*a*+*b*, where *a* is integral intensity of the signal at 2.8 ppm (H-T sequence) and *b* integral intensity of the signal at 2.6 ppm. Calculated regioregularities are collected in **Table 8**. ^{1}H NMR spectra of the **PHT-Br** precursor polymers also showed a singlet signal at 6.98 ppm corresponding to the thiophene-ring protons with a weak shoulder at 7.0 ppm (see **Figure 21**). The presence of this shoulder also indicates the presence of the fraction of irregular sequences in polymer chains.

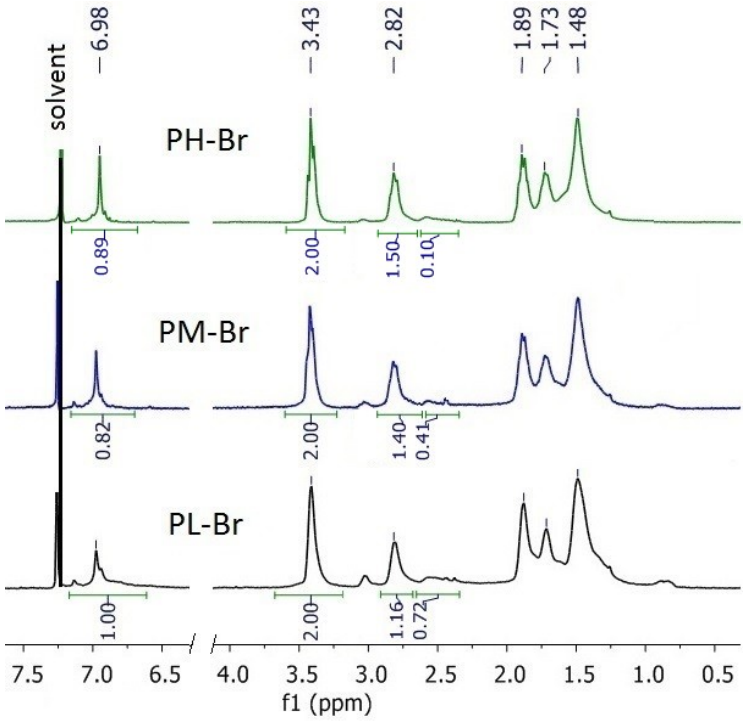

Figure 21. Proton NMR spectra of the **PHT-Br** precursor polymers ($CDCl_3$, room temperature).

The quaternization reaction has been supposed to proceed without a change of the structure of the polymer main chains. Therefore, the values of MW and regioregularity found for the **PHT-Br** precursor polymers has been directly applied to the corresponding polyelectrolytes with side groups capped with **EtP$^+$** or **PhP$^+$** ionic groups instead of bromine atom.

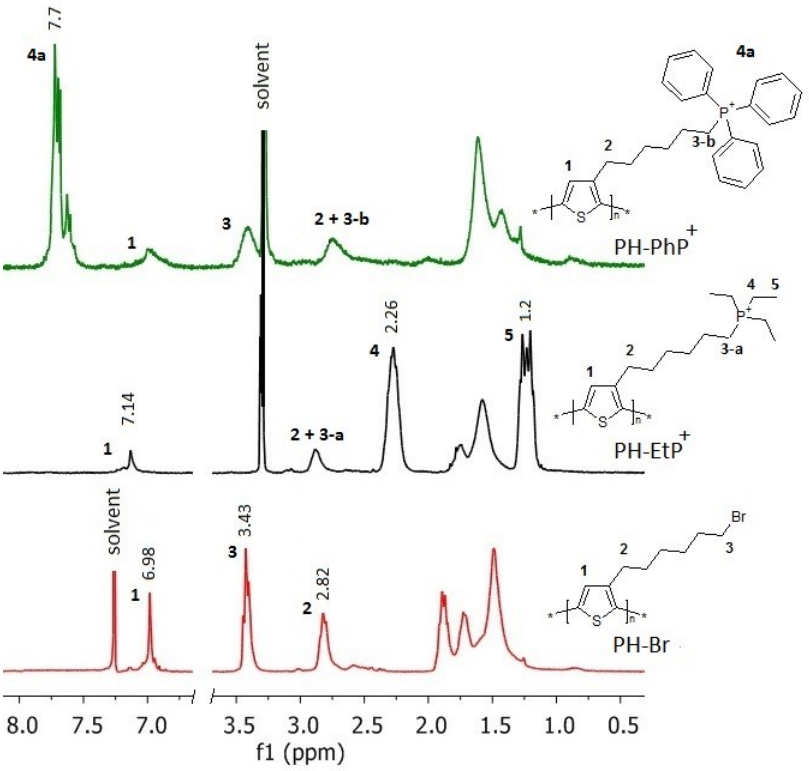

Figure 22. ^{1}H NMR spectra of the precursor polymer **PH-Br** ($CDCl_3$, r.t) and corresponding CPEs **PH-EtP$^+$** and **PH-PhP$^+$** (both measured in CD_3OD, r.t).

NMR spectroscopy has been also used for the monitoring of the transformation of the **PHT-Br** precursor polymers into corresponding conjugated polyelectrolytes and estimation of the degree of quaternization (ionization, α_{ion}) of the obtained conjugated polyelectrolytes. Examples of the ^{1}H NMR spectra of the prepared CPEs are presented in **Figure 22** together with the formulas of the corresponding constitutional repeating units for polymers of the highest regioregularity: **PH-Br**, **PH-EtP$^+$**and **PH-PhP$^+$**. Comparison of these NMR spectra of the starting polymer precursor and final polyelectrolytes provided valuable information concerning these materials.

As can be seen (**Figure 22**, black spectrum), the signal at 3.43 ppm that corresponds to protons 3 in bromomethylene group CH_2Br capping the side hexyl groups (see **Figure 22**, red spectrum) has completely disappeared in the spectrum of **PH-EtP$^+$**. Simultaneously, a new signal at 2.26 ppm that belongs to the protons 3-a in CH_2 groups directly linked to phosphorus atom in Et_3P^+ (and also to protons 2 of the methylene groups next to thiophene ring) has appeared in the spectrum of **PH-EtP$^+$**. In addition, the latter spectrum also show a new ^{1}H NMR signal at 1.2 ppm that belongs to the protons of the methyl groups of triethylphosphine moiety denoted as protons 4. These observations clearly prove that the

quaternization reaction of **PHT-Br** (**Figure 22**, red spectrum) with triethylphosphine took place practically quantitatively, i.e., that practicallyall 6-bromohexyl groups have been successfully transformed into triethylphosphonium pendant groups.

Unlike the ^{1}H NMR spectrum of **PH-EtP^{+}**, the spectrum of **PH-PhP^{+}** showed only attenuated signal at 3.43 ppm belonging to protons 3 of the CH_2Br groups and correspondingly relatively weaker signal of CH_2 groups next to the ionic group and thiophene ring. The signal at 7.8 ppm in the spectrum of **PH-PhP^{+}** belong to the aromatic protons 4a of phenyl group. Certain shifts in position of other signal are also apparent in this spectrum. The evaluation of integrated NMR signals of the spectra of polyelectrolytes with **–**Ph_3P^{+} groups the values of the degree of ionization α_{ion} for these polymers: α_{ion} was found to be 0.5 for **PL-PhP^{+},** 0.55 for **PM-PhP^{+}**and 0.57 for **PH-PhP^{+}**. The observed incomplete ionization of polymers with -Ph_3P^{+} groups can be ascribed to the steric hindrances originating from bulkiness of triphenylphosphine molecules. Additionally, the measured ^{31}P NMR spectra confirmed the presence of phosphonium groups in the prepared CPEs.

4.3 Electronic spectra of precursor polymers – effect of regioregularity

UV/vis and photoluminescence spectra of the solutions of the **PHT-Br** polymer precursors (10^{-3} M with respect to monomeric unit) with various MW and H-T regioregularity are shown in **Figure 23** and the values of relevant spectral characteristics are summarized in **Table 9**. As expected, the position of as well as the molar absorption coefficient of the absorption maximum band and also the wavelength of the emission band maximum increase with the H-T-regioregularity of the polymer. The UV/vis spectra of the precursor polymers showed absorption maxima at positions from 408 nm for **PL-Br** to 427 nm for **PH-Br**. The highest molar absorption coefficient as well as the highest wavelength of the absorption edge also exhibited the precursor polymer **PH-Br** indicated that this material really is the most regioregular polymer of the prepared precursor polymers, i.e., that it contains the highest portion of (H-T) sequences. Nevertheless, the least regioregular precursor polymer **PL-Br** has also showed a significant absorption in the range 520-560 nm indicating the presence of a not negligible portion of longer regioregular sequences of monomeric units in the chains of this polymer. As a result, the differences between band gap wavelengths of the

precursor polymers of different regioregularity are negligible. The presence of longer regioregular sequences in polymers of decreased regioregularity also explains similarity of the positions of the luminescence maxima of the precursor polymers that are all in the very narrow region from 572 to 580 nm. The reason for it consists in the preferred relaxation of the excitation energy to excited states with the lowest energy, whose are just the states of the highest regioregularity. As such sequences (and thus also the states) are present even in the precursor polymer **PL-Br**, the emission from these states is important even for this polymer. The fluorescence quantum yields (ϕ_F) of the **PHT-Br** precursor polymers were measured in $CHCl_3$ solutions and their values are collected in **Table 9**. The highest value of ϕ_F was observed for **PH-Br** sample and the lowest one for **PL-Br**, respectively. The values of Stokes shift showed a slight decrease accompanied by a shift of the positions of emission maxima to lower energies with the increasing polymer MW and H-T regioregularity.

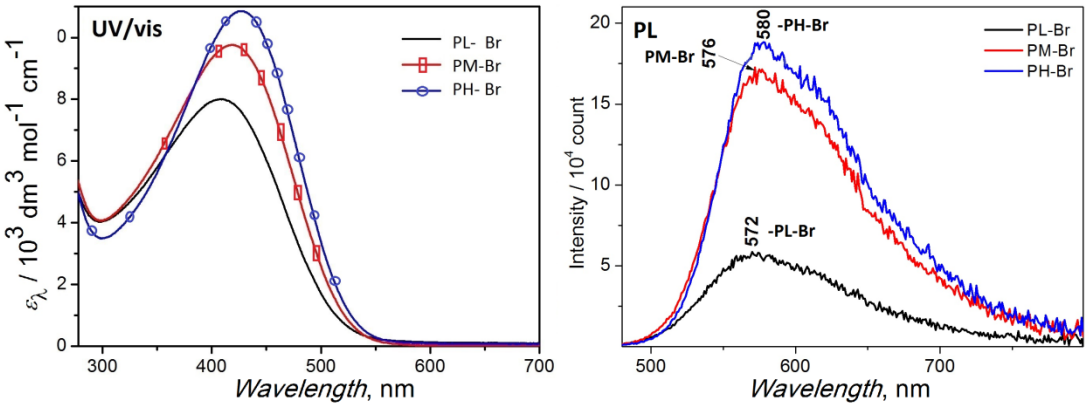

Figure 23. UV/vis and luminescence spectra of the solutions of precursor polymers.

Table 9. Spectroscopic data for the precursor polymers: λ_A – wavelength of absorption band maximum (nm); ε_{max} - molar absorption coefficient of absorption band maximum (m^3 mol^{-1} cm^{-1}); λ_e - edge wavelength (nm); E_g - band-gap calculated from λ_e (*eV*); λ_F - emission maximum wavelength; ϕ_F - fluorescence quantum yield (%); ν_S - Stokes shift.

Sample	λ_A nm	λ_e nm	E_g *eV*	ε_{max} m^3 mol^{-1} cm^{-1}	λ_F nm	ϕ_F %	ν_S (cm^{-1})
PL-Br	408	520	2.38	7.9	572	10	7030
PM-Br	417	535	2.31	9.6	576	11	6620
PH-Br	426	540	2.29	10.8	580	15	6230

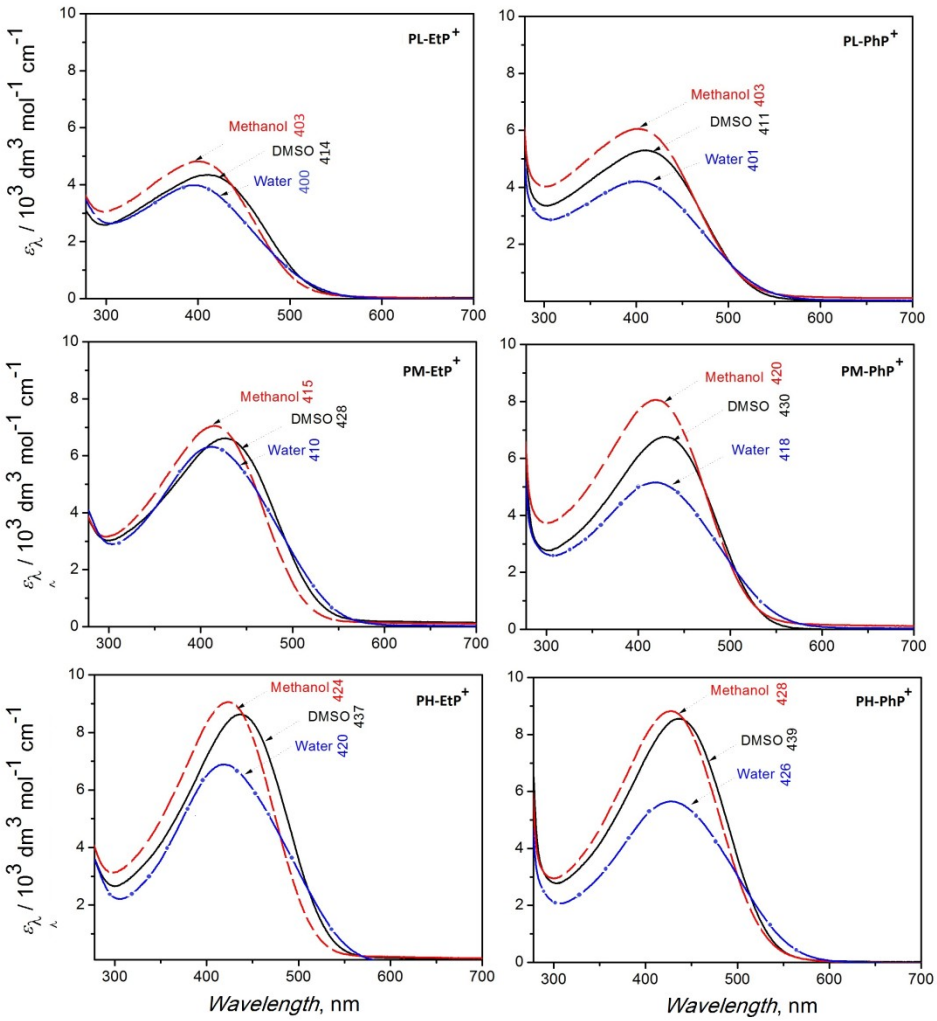

Figure 24. UV/vis spectra of **PHT-EtP$^+$** and **PHT-PhP$^+$** polyelectrolytes in indicated solvents.

4.4 Electronic spectra of conjugated polyelectrolytes of different regioregularity

The solubility in water and water miscible solvents is the most important property of that gives to CPEs great processing advantages compared to non-ionic conjugated polymers. Therefore, the spectroscopic characteristics of the here prepared CPEs have been studied in water, methanol and DMSO.

The UV/vis absorption spectra of the synthesized CPEs exhibited broad bands, corresponding to the π-π^* and n-π^* electronic transitions taking place dominantly in the conjugated polythiophene backbones. As can be seen from **Figure 24**, the optical spectra of the prepared CPEs with both Et_3P^+ and Ph_3P^+ pendant chain-capping groups depend not only on the ionic group but also on the solvent used. All studied CPEs exhibited slight but significant shift of the absorption maximum (λ_A) upon a change of the solvent, i.e., they

exhibited a slight solvatochromism. The highest value of λ_A showed solutions in DMSO while the lowest one showed aqueous solutions of all prepared CPEs. On the other hand, the molar absorption coefficient of the particular CPE has been found to decrease in the solvent order: methanol > DMSO > water (see **Table 10**).

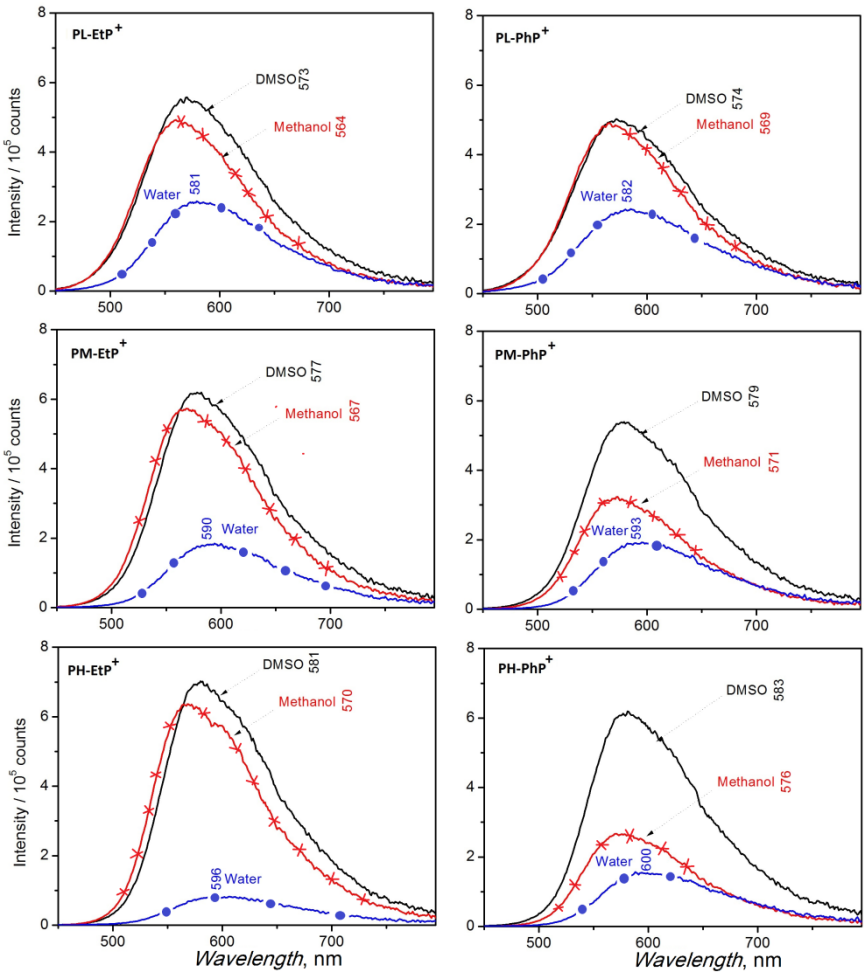

Figure 25. Photoluminescence spectra of **PHT-EtP$^+$** and **PHT-PhP$^+$** in indicated solvents.

Photoluminescence spectra of studied CPEs taken from different solvents are shown in **Figure 25**. As expected, the emission band wavelength showed a regular increase with increasing regioregularity of the CPE chains. However, the spectral characteristics did not exhibit clear dependences on the solvent. As can be seen, the λ_F value is the highest for aqueous solutions and the lowest for methanol solutions for all prepared CPEs, which is somewhat suprising because the solvent order observed for λ_F: water > DMSO > methanol is different from the order: DMSO > methanol > water observed for the λ_A values relating to the absorption bands. As a result, the Stokes shifts obtained for aqueous solutions are

considerably higher than the shifts for the other two solutions. The solvent order concerning the luminescence intensity measured under equal experimental conditions is the same as the solvent order found for λ_A: DMSO > methanol > water, i.e., different from the solvent order: methanol > DMSO > water observed for ε_λ that might be regarded as more relevant as to the luminescence intensity. These irregularities indicate high complexity of the relaxation processes in the excited molecules of studied CPEs.

Table 10. Optical data of CPEs with different MW: λ_A - wavelength of absorption maximum (nm); λ_F - wavelength of emission maximum (nm); ε_{max} - the molar absorption coefficient ($m^3\ mol^{-1}\ cm^{-1}$); ν_S - Stokes shift (cm^{-1}); ϕ_F **-**fluorescence quantum yields measured in methanol (%).

Sample	Solvent	λ_A nm	λ_e nm	ε_{max} $m^3\ mol^{-1}\ cm^{-1}$	λ_F nm	ϕ_F, %	ν_S (cm^{-1})
PL-EtP$^+$	Water	400	531	3.9	581	-	7790
	Methanol	403	513	4.8	564	11	7080
	DMSO	414	524	4.3	573	-	6700
PL-PhP$^+$	Water	401	541	4.1	582	-	7760
	Methanol	403	522	6.0	569	10	7240
	DMSO	411	527	5.2	574	-	6910
PM-EtP$^+$	Water	410	550	6.3	590	-	7440
	Methanol	415	518	7.0	567	16	6460
	DMSO	428	533	6.5	577	-	6030
PM-PhP$^+$	Water	418	554	5.1	593	-	7060
	Methanol	420	525	8.0	571	14	6300
	DMSO	430	535	6.7	579	-	5990
PH-EtP$^+$	Water	420	557	6.8	596	-	7030
	Methanol	424	518	9.0	570	22	6040
	DMSO	437	532	8.6	581	-	5670
PH-PhP$^+$	Water	426	561	5.6	600	-	6810
	Methanol	428	531	8.8	576	15	5420
	DMSO	439	540	8.5	583	-	6210

4.5 Aggregation of polyelectrolytes in aqueous solutions

The lowest λ_A value found for aqueous solutions is consistent with the increased coiling of CPE molecules in these solutions due to hydrophobic nature of their main chains that favors aggregation main chain moieties. On the other hand, the polar organic solvents such as DMSO and methanol can better interact with CPE chain backbones and simultaneously

good interact with ionic side groups, which makes them thermodynamically better solvents of studied CPEs compared to water. Low fluorescence intensity of **PH-EtP$^+$** in aqueous solutions can be also ascribed to the aggregation and/or collaps of their chains which support the luminescence quenching. Actually, CPEs are known to aggregate in aqueous solution due to the hydrophobicity of their backbones. Repulsion of charged pendant ionic groups acts against this aggregation proces [197, 198]. Consequently, optical properties of CPEs should depend on thermodynamic quality of the solvent. To obtain a better insight into behavior of our CPEs in solutions, the aggregation study was done in the water/DMSO system, since this behavior should depend on the thermodynamically good solvent added to the CPE aqueous solution.

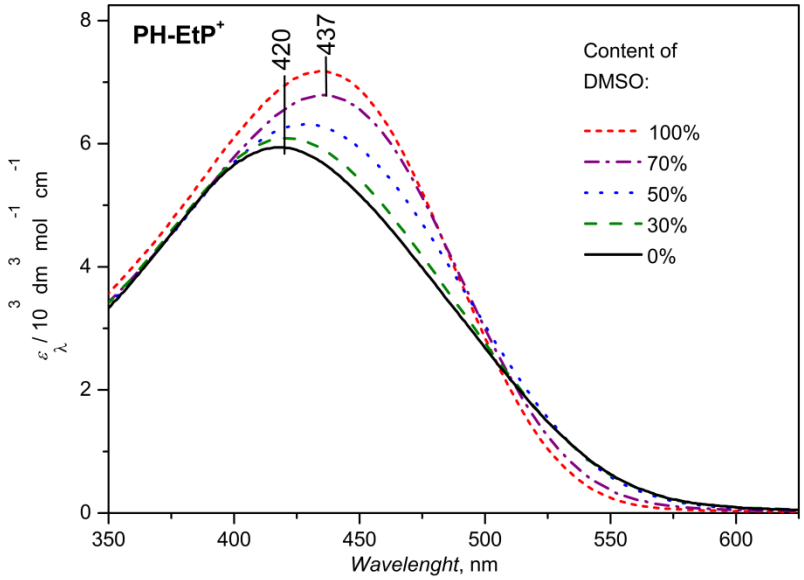

Figure 26. Absorption spectra of **PH-EtP$^+$** as a function of the DMSO content in aqueous solution.

The aggregation of the CPEs can be monitorred through the changes in UV/vis spectra caused by the changes in the solvent composition [199]. The spectra displayed in **Figure 26** clearly show how the values of ε_λ and λ_A increase with the increasing concentration of DMSO in aqueous solution. The thermodynamically ‘‘better” co-solvent plays a key role consisting in the breaking of polymer aggregates. The increase in both ε_λ and λ_A confirms that more aggregated systems exhibit absorption at higher energies. Additional figures depicting visual changes of the polyelectrolyte solutions with the increasing DMSO concentration together with appropriatetrend in emission spectra are presented in the paper published [200]. Similar behavior of the absorption as well as luminescence spectra was observed in our group during study of regioregular polyalkylthiophene with ionic side groups [157, 201].

4.6 Stern-Volmer study of luminescence quenching of CPEs in aqueous solutions

Conjugated polyelectrolytes are able to interact with various species such as metal ions, proteins or nanoparticles due to the presence either positively or negatively charged moieties. Such interactions change photophysical behavior of CPEs. The fluorescence quenching is of particular interest in the field of sensors.

Quenching of the fluorescence of CPE can be best achieved by the addition of oppositely charged quenching species to the solution of the CPE. Keeping in mind the above mentioned facts, fluorescence quenching study of the cationic conjugated polyelectrolytes **PL-EtP$^+$** and **PH-EtP$^+$** with model quenchers such as $K_4[Fe(CN)_6]$ and $K_3[Fe(CN)_6]$ was performed using Stern-Volmer methodology. The CPEs bearing Et_3P^+ pendant groups were chosen due to their better solubility in pure water compared to the solubility of CPEs with Ph_3P^+ groups and also due to their higher degree of ionization (100 %). The fluorescence quenching experiments were performed using a set of concentrations of a quencher (potassium ferrocyanide or potassium ferricyanide) from 10^{-8} M to 10^{-4} M. The solutions of CPEs of the concentration of 10^{-3} M (with respect to polymer repeating units) were used in order to avoid the concentration-dependent aggregation. Moreover, low concentration of a sensing material is always an important advantage. The photoluminescence spectra were measured after the addition of quencher and the changes in luminescence intensity (mainly decreasing of fluorescence) were analyzed using the Stern-Volmer equation in order to obtain the value of Stern-Volmer constant K_{SV} that is a quantitative measure of the fluorescence quenching. The calculated values of K_{SV} are summarized in **Table 11** and illustrated in **Figure 27.**

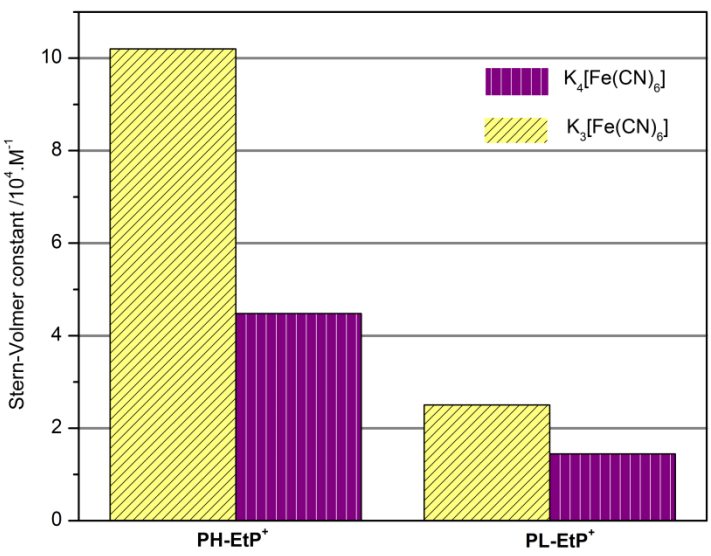

Figure 27. Stern-Volmer constants K_{SV} for quenching of the luminescence of **PL-EtP$^+$** and **PH-EtP$^+$** by $K_4[Fe(CN)_6]$ and $K_3[Fe(CN)_6]$, respectively, in aqueous solutions.

Table 11. Stern-Volmer constants K_{SV} for quenching the luminescence of **PL-EtP$^+$** and **PH-EtP$^+$** by $K_4[Fe(CN)_6]$ and $K_3[Fe(CN)_6]$.

CPEs/quencher	**PL-EtP$^+$**		**PH-EtP$^+$**	
	$K_3[Fe(CN)_6]$	$K_4[Fe(CN)_6]$	$K_3[Fe(CN)_6]$	$K_4[Fe(CN)_6]$
K_{SV}	2.5×10^4 M^{-1}	1.44×10^4 M^{-1}	1.02×10^5 M^{-1}	4.48×10^4 M^{-1}

The data in **Table 11** show that $K_3[Fe(CN)_6]$ quenches fluorescence more efficiently than $K_4[Fe(CN)_6$ (more than twice as much). Besides, **PH-EtP$^+$** shows K_{SV} three times higher for $K_4[Fe(CN)_6$ and five times higher for $K_3[Fe(CN)_6]$ than **PL-EtP$^+$**. These results indicate that the CPEs of high regioregularity are more effective quenchers than CPEs of lower regioregularity. This effect is probably caused by easier and faster energy migration along better ordered conjugated main-chains. The luminescence spectra showed a quick decrease of the fluorescence intensity at low concentrations of the quenchers. Thus fast responses are promising for the development of highly sensitive bio- or chemosensors. More detailed information about the Stern-Volmer experimentsis collected in the published paper [200].

5 EXPERIMENTAL PART

5.1 Materials

Solvents

Methanol, tetrahydrofuran (THF), dimethyl sulfoxide (DMSO), dimethylformamide (DMF), hexane, toluene were purchased from Sigma-Aldrich. Solvents used for the reactions with catalysts or n-BuLi such as toluene, tetrahydrofurane (THF) and hexane were dried and distilled by standard methods and stored under argon. Toluene was distilled under argon from sodium/benzophenone prior to use, THF was distilled from $LiAlH_4$ before use and hexane was dried over molecular sieves 4Å. The second series of solvents such as dichloromethane, chloroform, diethyl ether, acetic acid, hydrochloric acid, sulphuric acid and orthophosphoric acid were purchased from Lachner and used as received without further purification.

Chemical compounds used for the synthesis of unimers, corresponding metallo-supramolecular polymers and cationic conjugated polyelectrolytes

4-hydroxypyridine-2,6-dicarboxylic (chelidamic) acid, benzene-1,2-diamine, thiophene-2-boronic acid, tetrabutylammonium bromide, thionyl chloride, 2-chloroethylamine hydrochloride, triethylamine, 2,5-bis(trimethylstannyl)thiophene, 5,5'-bis(trimethylstannyl)-2,2'-bithiophene, 2,5-bis(trimethylstannyl)-thieno[3,2-b]thiophene, 1,3-bis(diphenylphosphino)propane nickel (II) chloride [$Ni(dppp)Cl_2$], tetrakis(triphenylphosphine)palladium(0) $Pd(PPh_3)_4$, 3-bromothiophene, 1,6-dibromohexane, *n*-butyllithium solution (2.5 M in hexane), methylmagnesium bromide, *N*-bromosuccinimide (NBS), triphenylphosphine, triethylphosphine solution (1.0 M in THF), potassium carbonate, potassium hydroxide, sodium sulfate, magnesium sulfate, sodium bicarbonate, phosphorus pentoxide, zinc (II) perchlorate hexahydrate, iron (II) perchlorate hydrate, nickel (II) perchlorate hexahydrate, copper (II) perchlorate hexahydrate, europium (III) chloride hexahydrate, terbium (III) chloride hexahydrate were all purchased from Sigma-Aldrich and used as received.

5.2 Methods

Nuclear magnetic resonance spectroscopy (NMR)

^{1}H, ^{13}C and ^{31}P NMR spectra were recorded on a Varian ^{UNITY}INOVA 400 or Varian SYSTEM 300 instruments in $CDCl_3$, d_6-DMSO, CD_3OD and referenced to the solvent signal (δ): 7.25 ppm ($CDCl_3$), 2.50 ppm (d_6-DMSO) or 3.33, 4.78 ppm (CD_3OD) for ^{1}H and 77.0 ppm ($CDCl_3$), 49.15 ppm (CD_3OD) ppm for ^{13}C spectra. Coupling constants, *J* (in Hz), were obtained by the first-order analysis.

Infrared (IR) and Raman spectroscopy

Infrared spectra were recorded on a Thermo Nicolet 7600 FTIR spectrometer equipped with a Spectra Tech InspectIR Plus microscopic accessory using KBr-diluted samples and diffuse reflectance technique (DRIFT) (128 or more scans at resolution 4 cm^{-1}). Raman spectra were recorded on a DXR Raman microscope (Thermo Scientific) using extended range of excitation from 445 nm to 780 nm (usual laser power at the sample 0.1 to 0.4 mW).

UV/vis spectroscopy

UV/vis spectra were recorded on Shimadzu UV-2401PC using solvent mixture chloroform/methanol (1/1 by vol.) or methanol, DMSO and water solutions of the prepared compounds. The solid state samples were prepared using coating method via slow solvent evaporation technique on the surface of the quartz plate.

Photoluminescence spectroscopy

Photoluminescence spectra were measured on a Fluorolog 3-22 Jobin Yvon Spex instrument (Jobin Yvon Instruments S. A., Inc., USA) in solutions using four-window quartz cuvette (1 cm). Samples prepared in thin film were measured using the methodology mentioned above for UV/vis spectra. The emission spectra were excited using the wavelength, λ_{ex}, equal to the position of the absorption maxima of particular compound. Quantum luminescence yields, ϕ_F, of photoluminescence were measured using integration sphere Quanta-ϕ F-3029 Horriba Jobin Yvon.

Size exclusion chromatography (SEC)

SEC analyses were performed on a Spectra Physics Analytical HPLC instrument fitted with two SEC columns Polymer Labs (Bristol, UK) Mixed-D, Mixed-E and THERMO UV6000 DAD detector, using THF as mobile phase; apparent molar mass averages related to the polystyrene standards are reported.

SEC records of MSPs were obtained using a Spectra Physics Analytical HPLC pump P1000 with two SEC columns: Polymer Labs (Bristol, USA) Mixed-Dand Mixed-E. The system was equipped with a Thermo UV6000 DAD detector. 0.05 M tetrabutylammoniumhexafluoro-phosphate in chloroform/methanol (1/1, v/v, CHROMASOLV, Riedel-deHaen) was used as an eluent (0.7 mL min^{-1}).

X-ray photoelectron spectroscopy (XPS)

X-ray photoelectron spectroscopy (XPS) measurements were carried out with a K-Alpha^{+} spectrometer (ThermoFisher Scientific, East Grinstead, UK). The samples were analyzed using a micro-focused, monochromated Al Kα X-ray source (400 µm spot size) at an angle of incidence of 30° (measured from the surface) and an emission angle normal to the surface. The kinetic energy of the electrons was measured using a 180° hemispherical energy analyzer operated in the constant analyzer energy mode (CAE) at 50 eV pass energy for the high resolution spectra. Data acquisition and processing were performed using Thermo Advantage software. XPS spectra were fitted with Voigt profiles obtained by convolving Lorentzian and Gaussian functions. The analyzer transmission function, Scofield sensitivity factors, and effective attenuation lengths (EALs) for photoelectrons were applied for quantification. EALs were calculated using the standard TPP-2M formalism. All spectra were referenced to the C1s sp^2 peak at 284.2 eV. The BE scale was controlled by the well-known position of the photoelectron C-C and C-H, C-O and C(=O)-O peaks of polyethylene terephthalate and Cu 2p, Ag 3d, and Au 4f peaks of metallic Cu, Ag and Au, respectively. The BE uncertainty of the reported measurements and analysis is in the range of ±0.1 eV.

X-ray diffraction spectroscopy (XRD)

X-ray diffraction studies were performed using Bragg-Brentano geometry on a PanAlytical X'Pert PRO MPD X-ray diffraction system equipped with PIXcel detector using Cu-anode (Cu-Ka; l ¼ 1.5418 Å).

Elemental spectroscopy

This analysis was performed by Dr. Bondarev on Department of Polymer Engineering, Tomas Bata University in Zlin.

Gas chromatography

Conversion and purity of reactants in the syntheses of unimers and monomer compounds for the synthesis of polymer precursors were checked by GC-2010 Gas Chromatograph, Shimadzu.

5.3 Syntheses

5.3.1 Synthesis of *bzimpy*-based compounds

2,6-bis(benzimidazol-2-yl)-4-hydroxypyridine (***bzimpy*-OH**)

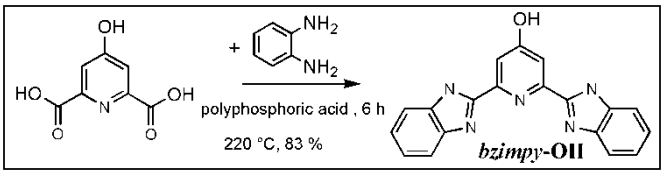

4-hydroxypyridine-2,6-dicarboxylic (chelidamic) acid (4 g, 20 mmol) and benzene-1,2-diamine (5.2 g, 48 mmol) were suspended in polyphosphoric acid (50 mL), the resulting mixture was stirred at 220 ^{0}C for 6 h, then cooled down to room temperature, poured into ice-water (500 mL) and obtained solution was titrated with aqueous ammonia to pH 8-9. The excluded crude product was isolated by filtration and recrystallized from methanol. Yield 5.93 g (83%). ^{1}H NMR (300 MHz, DMSO-d_6, ppm) δ 12.89 (s, NH), 11.43 (s, OH), 7.75 (d, 2H), 7.72 (d, 4H), 7.34-7.27 (d-t, 4H). ^{13}C NMR (101 MHz, DMSO-d_6) δ 171.41, 156.07, 154.70, 149.48, 139.67, 128.97, 127.46, 125.15, 117.16, 114.14, 85.52, 84.68, 83.69. IR (DRIFT), cm^{-1}: 3608 (s), 3297 (s), 1614 (s), 1575 (m), 1449 (s), 1412 (m), 1197 (m), 923 (w), 859 (w), 736 (s), 603 (w). Anal calculated for $C_{19}H_{13}N_5O$ (*M*W 327.11 g.mol^{-1}), C, 69.71; H, 4.00; N, 21.39; O, 4.89, found: C, 69.07; H, 4.11; N, 21.04.

Dimethyl 4-bromopyridine-2,6-dicarboxylate (**BrPyMe**)

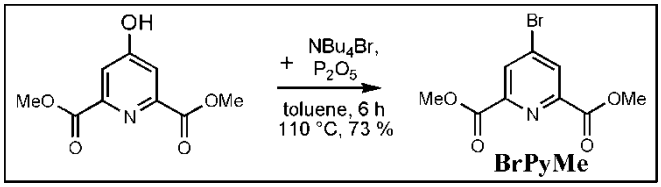

Tetrabutylammonium bromide (20 g, 60 mmol) and P_2O_5 (16 g, 113 mmol) were dissolved in toluene (100 mL) in a round bottle flask (250 mL) and dimethyl ester of chelidamic acid (5 g, 20 mmol) was slowly added. The mixture was stirred for 6 h at 110 ^{0}C and, upon partial cooling, toluene was removed by a rotary evaporator. The remained yellow oil was then mixed with distilled water (60 mL) and the product was extracted with dichloromethane (2x50mL). The organic phase was washed with water (3x40 mL), dried with Na_2SO_4, and the crude product obtained by evaporation of dichloromethane was recrystallized from methanol to obtain a white solid **BrPyMe** (yield 4.75 g, 73%). ^{1}H NMR (300 MHz, DMSO-d_6,

ppm) δ 8.4 (s, 2H), 3.92 [s, 6H-$(OCH_3)_2$]. IR (DRIFT), cm^{-1}: 3105 (w), 2950 (w), 7727 (s), 1601 (m), 1445 (s), 1360 (m), 1266 (s), 1129 (m), 988 (m), 780 (m), 645 (w), 466 (s). Anal calculated for $C_9H_8BrNO_4$ (*M*W 272.96 $g.mol^{-1}$), C, 39.44; H, 2.94; Br, 29.15; N, 5.11; O, 23.35, found: C, 38.95; H, 2.98; Br, 29.02; N, 5.01.

4-(2-thienyl)pyridine-2,6-dicarboxylic acid (**T-Py**)

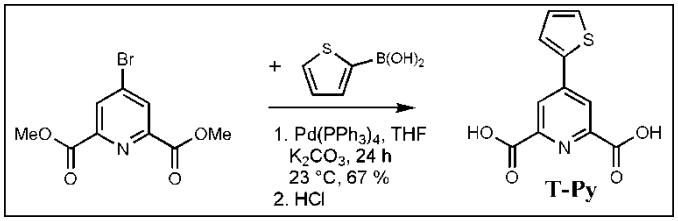

BrPyMe (1 g, 3 mmol), 2-thienylboronic acid (0.7 g, 5 mmol) and $Pd(PPh_3)_4$ (0.06 g, 0.05 mmol) were dissolved in distilled THF (70 mL), an aqueous solution (20 mL) of K_2CO_3 (5 g, 0.03 mmol) was added and the reaction mixture was stirred for 24 h at 80 ^{0}C. Then the reaction mixture was cooled down to room temperature, THF was distilled off and the remaining dark solution was acidified by hydrochloric acid to pH 3-4 because of basic condition of reaction leads to hydrolysis of dimethyl dicarboxylate groups of **BrPyMe** compound. Formed white precipitate was subsequently filtered off and recrystallized from propan-2-ol. Yield: 0.6 g, 67%. ^{1}H NMR (300 MHz, DMSO-d_6, ppm) δ 8.37 (s, 2H), 8.05 (d, 1H), 7.85 (d, 1H), 7.26 (t, 1H). ^{13}C NMR (101 MHz, DMSO-d_6) δ 170.93, 155.20, 148.78, 144.27, 135.17, 134.81, 133.50, 127.58. IR (DRIFT), cm^{-1}: 3278 (s), 1737 (s), 1610 (m), 1526 (w), 1390 (s), 1225 (m), 901 (w), 727 (s), 495 (w).

2,6-bis(benzimidazole-2-yl)-4-(2-thienyl)pyridine (***bzimpy*-T**)

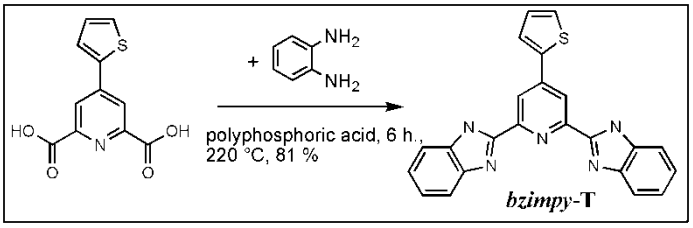

This compound was prepared by the same procedure as was mentioned for the preparation of ***bzimpy*-OH**, using **T-Py** (0.27 g, 1 mmol), benzene-1,2-diamine (0.25 g, 2 mmol) and polyphosphoric acid (15 mL). The procedure gave a yellow solid with yield 0.34 g, 81%. ^{1}H NMR (300 MHz, DMSO-d_6, ppm) δ 8.51 (s, 2H), 8.13-8.12 (d-d, 1H), 7.88-7.87 (d-d, 1H), 7.78

(s, 4H), 7.32 (s, 4H), 7.31 (q, 1H). ^{13}C NMR (101 MHz, DMSO-d_6) δ 150.23, 148.64, 143.33, 139.52, 129.35, 127.69, 123.76, 122.29, 119.67, 116.27, 11.95. IR (DRIFT), cm^{-1}: 3196 (s), 1607 (s), 1561 (m), 1463 (s), 1233 (w), 956 (w), 734 (s), 694 (m), 522 (w). Anal calculated for $C_{23}H_{15}N_5S$ (*M*W 393.1 g.mol^{-1}), C, 70.21; H, 3.84; N, 17.80; S, 8.15, found: C, 69.97; H, 3.91; N, 17.62; S, 8.03.

4-(2-thienyl)pyridine-2,6-dicarboxylate (**T-PyMe**)

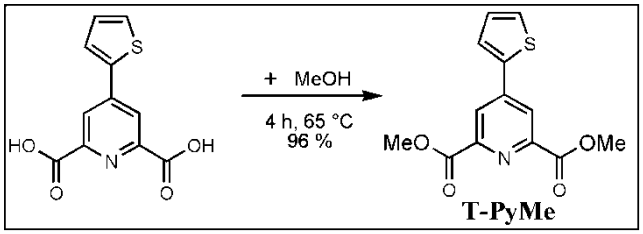

T-Py (1 g, 4 mmol) was added to methanol (150 mL) and this mixture was refluxed for 4 hours in the presence of H_2SO_4 (0.1 mL). After that reaction mixture was cooled down to room temperature and remnants of methanol were removed by a rotary evaporator. The crude product was recrystallized from methanol and gave a white solid with yield 1.07 g, 96%. ^{1}H NMR (300 MHz, DMSO-d_6, ppm) δ 8.37 (s, 2H), 8.05 (d, 1H), 7.86 (d, 1H), 7.27 (t, 1H), 3.94 [s, 6H-$(OCH_3)_2$].

4-(5-bromo-2-thienyl)pyridine-2,6-dicarboxylate (**BrT-PyMe**)

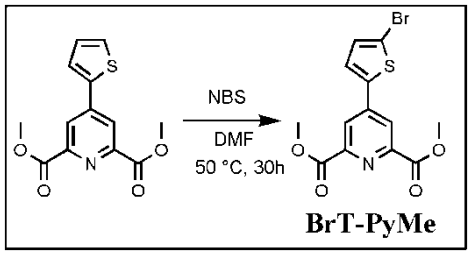

A solution of **T-PyMe** (1 g, 3 mmol) in 25 mL of dimethylformamide (DMF) was stirred at 50 °C while N-bromosuccinimide (0.96 g, 5 mmol) was added and the resulting mixture was allowed to stirring for 24 h. After cooling, methanol (40 mL) was added to the solution and white solid was precipitated and filtered off. Yield: 1.32 g, 97%. ^{1}H NMR (400 MHz, DMSO d_6, ppm) δ 8.29 (s, 2H), 7.79 (d, 1H), 7.37 (d, 1H), 3.97 [s, 6H-$(OCH_3)_2$]. ^{13}C NMR (101 MHz, DMSO-d_6) δ 159.70, 144.51, 137.79, 135.57, 127.65, 124.16, 117.77, 110.33. IR (DRIFT), cm^{-1}:

3105 (w), 2950 (w), 1727 (s), 1601 (m), 1445 (s), 1360 (m), 1266 (s), 988 (m), 780 (m), 645 (w), 466 (m).

α,ω-*bis(2,6-dicarboxylatepyridin-4-yl)terthiophene* (**bis-*dcpy*-T**)

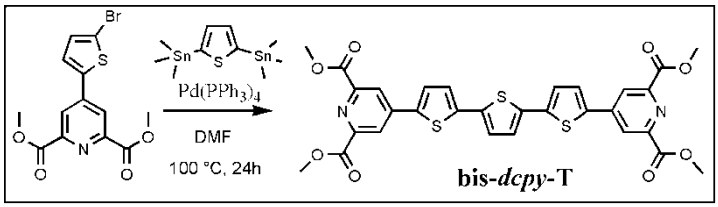

BrT-PyMe (1 g, 2 mmol) and 2,5-bis(trimethylstannyl)thiophene were added to DMF (50 mL) degassed with argon prior to use. The reaction mixture was heated to 100 °C and then $Pd(PPh_3)_4$ was added and stirred under argon for 24 hours. The stirring was accompanied by precipitating of orange solid product. Then the reaction mixture was cooled to the room temperature and precipitate was filtered off and washed with methanol (3x20 mL). Yield: 1.2 g, 67%. Unfortunately, extremely fast precipitation of **bis-*dcpy*-T** in all deuterated solvents even at high temperature disallowed NMR measurement.

α,ω-*bis(2,6-dicarboxylicpyridin-4-yl)terthiophene* (**bis-*dopy*-T**)

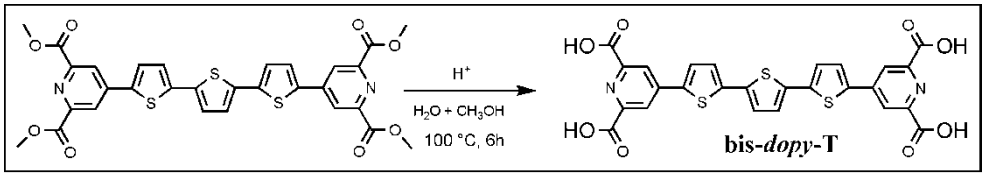

Acid hydrolysis was carried out for obtaining **bis-*dopy*-T** compound. **Bis-*dcpy*-T** (1.2 g, 1 mmol) was added to mixed solvent (50 mL) (HCl/H_2O). Subsequently, this mixture was heated to reflux and maintained at such conditions for 4 hours. After cooling to room temperature, dark precipitate was filtered off. Yield: 0.8 g, 80%. ^{1}H NMR (400 MHz, DMSO-d_6, ppm) δ 8.28 (s, 4H), 7.92 (d, 2H), 7.39 (s, 4H). ^{13}C NMR (101 MHz, DMSO-d_6) δ 165.76, 149.75, 143.47, 139.45, 138.17, 136.19, 130.08, 126.96, 122.73. IR (DRIFT), cm^{-1}: 3251 (w), 1746 (s), 1597 (s), 1511 (w), 1383 (s), 1226 (s), 1022 (m), 898 (w), 783 (m), 459 (w). Anal calculated for $C_{26}H_{14}N_2O_8S_3$ (*M*W 577.99 g.mol^{-1}), C, 53.97; H, 2.44; N, 4.84; O, 22.12; S, 16.63, found: C, 53.02; H, 2.53; N, 4.53; S, 16.48.

α,ω-*bis(2,6-bis(imidazol-2-yl)pyridin-4-yl)terthiophene* (**bis-*bzimpy*-T**)

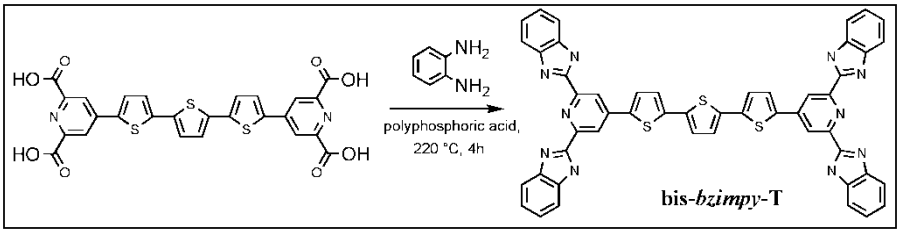

For the synthesis of this compound we used the same procedure as was described above for ***bzimpy*-OH** or ***bzimpy*-T** ligands, using **bis-*dopy*-T** (0.5 g, 0.8 mmol), benzene-1,2-diamine (0.37 g, 4 mmol) and polyphosphoric acid (25 mL). The dark yellow solid product was obtained with yield 0.4 g, 53%. ^{1}H NMR (300 MHz, DMSO-d_6, ppm) δ 8.37 (s, 4H), 7.76 (s, 8H), 7.22 (s, 10H), 6.49 (d, 2H), 6.37 (d, 2H). IR (DRIFT), cm^{-1}: 3062 (w), 1602 (s), 1452 (m), 742 (s), 514 (w), 433 (w). Anal calculated for $C_{50}H_{30}N_{10}S_3$ (*M*W 866.18 g.mol^{-1}), C, 60.26; H, 3.49; N, 16.15; S, 11.09, found: C, 59.87; H, 3.41; N, 15.82; S, 11.04.

5.3.2 Synthesis of *pybox*-based compounds

4-(2-thienyl)-N^2,N^6-bis(2-chloroethyl)pyridine-2,6-dicarboxamide (**T-PyEt**)

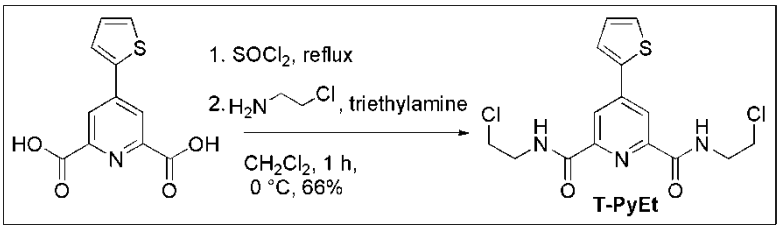

T-Py (synthesis see above) (1 g, 4 mmol), thionyl chloride (7 g, 59 mmol) and DMF (0.1 mL) were placed into a 100 mL round bottom flask and refluxed with stirring for 1 h. The remnants of $SOCl_2$ were removed in vacuum and the formed product of reaction was washed by toluene with further evaporation by a rotary evaporator. The crude product (1.12 g, 4 mmol) was dissolved in CH_2Cl_2 (10 mL) and added to the solution of chlorethylamine hydrochloride (1.16 g, 10 mmol) and triethylamine (1.6 g, 16 mmol) in CH_2Cl_2 (50 mL) at 0 °C. The resulting mixture was stirred for 1 h at room temperature. After that CH_2Cl_2 was removed by a rotary evaporator and water (60 mL) was added into flask. The mixture was extracted with dichlormethane (4×30 mL). The combined organic extracts were dried over $MgSO_4$. The solvent was evaporated and formed product was recrystallized from methanol.

Yield: 1.17 g, 81%. ^{1}H NMR (300 MHz, $CDCl_3$, ppm) δ 8.52 (s, 2H-pyH), 8.22 (br s, 2H- NH), 7.70 (d, 1H-Th), 7.49 (d, 1H-Th), 7.17 (t, 1H-Th), 3.90 (m, 4H-CH_2N), 3.77 (t, 4H-CH_2Cl).

2,6-bis(oxazoline-2-yl)-4-(2-thienyl)pyridine (***pybox*-Th**)

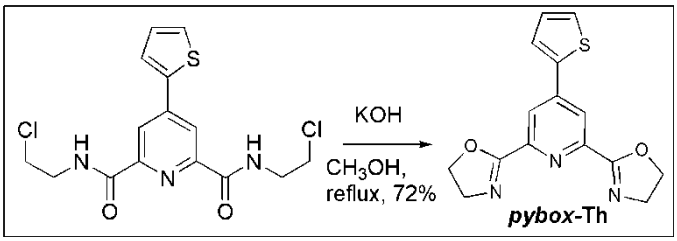

The **T-PyEt** compound (1 g, 2.7 mmol) was dissolved in THF (25 mL) and mixed with 25 % water solution of KOH (0.58 g, 10.8 mmol). The resulting mixture was stirred at 50 °C for 48 h. Then the reaction mixture was cooled down and solvent (THF) was evaporated. The obtained product was filtered off and subsequently recrystallized from ethanol. Yield: 0.56 g, 71%. ^{1}H NMR (300 MHz, $CDCl_3$, ppm) δ 8.33 (s, 2H-pyH), 7.65 (d, 1H-Th), 7.47 (d, 1H-Th), 7.33 (t, 1H-Th), 4.55 (t, 4H-CH_2N), 4.14 (t, 4H-CH_2O). Anal calculated for $C_{15}H_{13}N_3O_2S$ (*M*W 299.07 g.mol^{-1}), C, 60.18; H, 4.38; N, 14.04; O, 10.69; S, 10.71, found: C, 59.47; H, 4.49; N, 13.76; S, 10.42.

4-bromopyridine-2,6-dicarboxylic acid (**BrPy**)

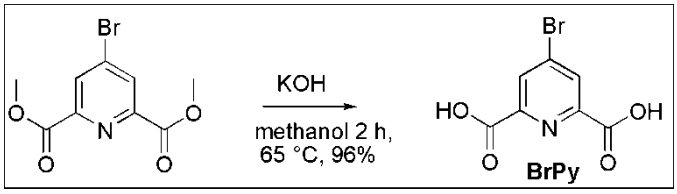

BrPyMe previously synthesized (see above) (4 g, 15 mmol) was dissolved in methanol (150 mL) and subsequently potassium hydroxide (1.79 g, 32 mmol) dissolved also in methanol (50 mL) was added. The reaction mixture was slightly heated and allowed for stirring (2 h). After that, reaction mixture was cooled down to room temperature. Methanol was evaporated to get the potassium salt of 4-bromopyridine-2,6-dicarboxylic acid. The salt obtained was dissolved in water (50 mL) and solution was concentrated by aqueous hydrogen chloride solution (37%) in order to get pH=1-3. The white precipitate formed was filtered off, washed with water (3×50 mL) and dried under vacuum. Yield: 3.4 g, 94%. ^{1}H NMR (300 MHz, DMSO-d_6, ppm) δ 8.36 (s, 2H-pyH).

4-bromopyridine-2,6-dicarbonyl dichloride (**BrPyCl**)

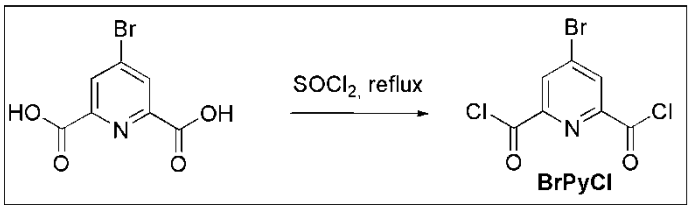

BrPy (3 g, 12 mmol), thionyl chloride (20 g, 168 mmol) and DMF (0.2 mL) were placed into a 100 mL round bottom flask. The resulting mixture was refluxed and stirred for 1 h. The residual thionyl chloride was removed in vacuum to give the crude product as a yellow powder. Yield: 3.4 g, 98%.

4-bromo-N^2,N^6-bis(2-chloroethyl)pyridine-2,6-dicarboxamide (**BrPyEt**)

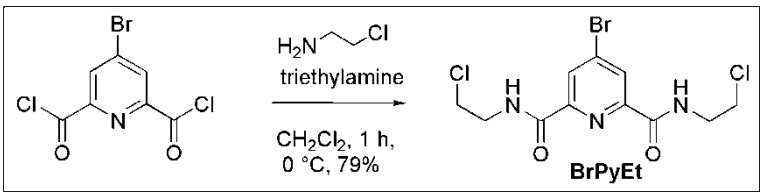

A solution of chlorethylamine hydrochloride (3.48 g, 30 mmol) and triethylamine (4.85 g, 48 mmol) in CH_2Cl_2 was prepared and cooled down to 0 °C. The crude **BrPyCl** product (3.4 g, 12 mmol) in dichloromethane was slowly added to the above prepared solution at 0 °C. The mixture was stirred for 1 h at room temperature. Than the solvent was removed by rotary evaporation and water (50 mL) was infused into flask. The mixture was extracted with dichlormethane (3×30 mL). The combined organic extracts were dried over $MgSO_4$. Evaporation of solvent and crystallization from methanol gave the product as white powder (3.5 g, 79%). ^{1}H NMR (300 MHz, $CDCl_3$, ppm) δ 8.51 (s, 2H-pyH), 8.12 (br s, 2H- NH), 3.84 (m, 4H-CH_2N), 3.75 (t, 4H-CH_2Cl).

4-bromo-2,6-bis(4,5-dihydro-2-oxazolyl)-pyridine (***pybox*-Br**)

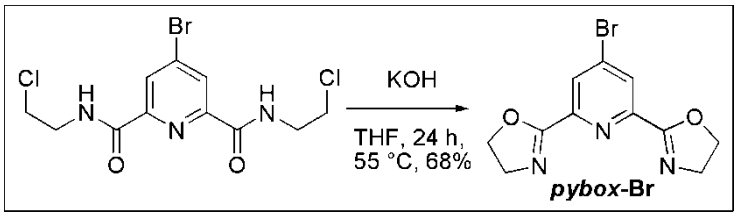

The **BrPyEt** compound (3.5 g, 9.5 mmol) dissolved in THF (50 mL) and 25 % water solution of KOH (2.1 g, 38 mmol) were mixed and stirred at 50 °C for 48 h. After that the solvent (THF) was evaporated and residue was purified by recrystallization from ethanol. Yield: 2.1 g, 68%. ^{1}H NMR (300 MHz, $CDCl_3$, ppm) δ 8.32 (s, 2H-pyH), 4.53 (t, 4H-CH_2N), 4.11 (t, 4H-CH_2O). Anal calculated for $C_{11}H_{10}BrN_3O_2$ (*M*W 295 g.mol^{-1}), C, 44.62; H, 3.40; Br, 26.98; N, 14.19; O, 10.81, found: C, 44.02; H, 3.48; Br, 26.52; N, 13.82.

2,5-bis(2,6-bis(4,5-dihydrooxazol-2-yl)pyridin-4-yl)thiophene (**P-Th**)

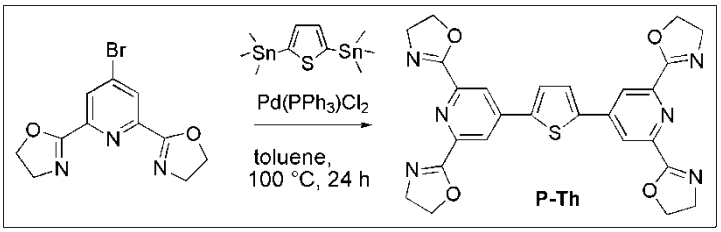

The ***pybox*-Br** compound previously synthesized (0.4 g, 1.35 mmol) was added to the mixture of $Pd(PPh_3)_2Cl_2$ (0.02 g, 0.03 mmol) and 2,5-bis(trimethylstannyl)thiophene (0.24 g, 0.58 mmol) in freshly distilled toluene (10 mL). The resulting mixture was stirred under argon at 100 °C for 24 h. After that the reaction mixture was allowed cooling to room temperature and solvent (toluene) was removed by a rotary evaporator. The solid residue was dissolved in chloroform-methanol mixture (5 mL) and the product was precipitated by adding of diethyl ether to solution (ca 10 mL). This precipitation gave a yellow solid product which was filtered off and washed with hexane, methanol and ether. The final product was dried in vacuum and weighted. Yield: 0.45 g, 65%. ^{1}H NMR (300 MHz, $CDCl_3$+CD_3OD, ppm) δ 8.19 (s, 4H-pyH), 7.6 (s, 2H-Th), 4.43 (t, 8H-CH_2N), 3.98 (t, 8H-CH_2O). ^{13}C NMR (400 MHz, $CDCl_3$+CD_3OD, ppm) δ 163.97, 147.71, 142.81, 141.96, 128.56, 121.74, 68.91, 54.95. Anal calculated for $C_{26}H_{22}N_6O_4S$ (*M*W 514.56 g.mol^{-1}), C, 60.69; H, 4.31; N, 16.33; O, 12.44; S, 6.23, found: C, 59.27; H, 4.41; N, 15.82; S, 6.02.

5,5'-bis(2,6-bis(4,5-dihydrooxazol-2-yl)pyridin-4-yl)-2,2'-bithiophene (**P-Bt**)

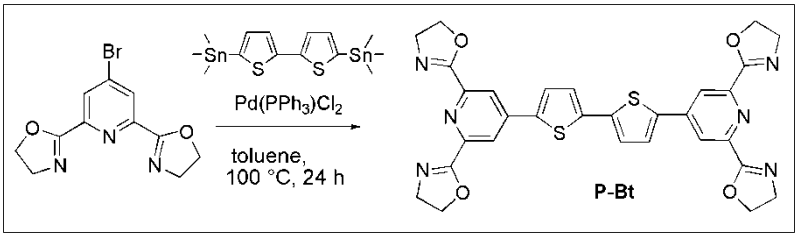

The **P-Bt** unimer was prepared applying the same procedure described for **P-Th** using $Pd(PPh_3)_2Cl_2$ (0.017 g, 0.025 mmol), 5,5'-bis(trimethylstannyl)-2,2'-bithiophene (0.22 g, 0.44 mmol) and ***pybox*-Br** (0.3 g, 1 mmol) in dry toluene (10 mL). Yield: 0.4 g, 66%. ^{1}H NMR (300 MHz, $CDCl_3$+CD_3OD, ppm) δ 8.07 (s, 4H-pyH), 7.43 (d, 2H-Th), 7.12 (d, 2H-Th), 4.36 (t, 8H-CH_2N), 3.9 (t, 8H-CH_2O). ^{13}C NMR (400 MHz, $CDCl_3$+CD_3OD, ppm) δ 164.02, 147.48, 142.78, 139.67, 138.96, 127.99, 126.08, 121.4, 68.84, 54.91. Anal. calculated for $C_{30}H_{24}N_6O_4S_2$ (*M*W 596.68 g.mol^{-1}), C, 60.39; H, 4.05; N, 14.08; O, 10.73; S, 10.75, found: C, 59.29; H, 4.04; N, 13.99; S, 10.74.

2,5-bis(2,6-bis(4,5-dihydrooxazol-2-yl)pyridin-4-yl)thieno[3,2-b]thiophene (**P-Te**)

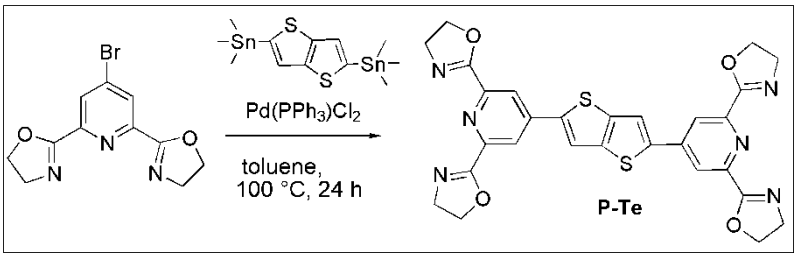

The **P-Te** unimer was prepared according to the procedure for **P-Th** and **P-Bt** using $Pd(PPh_3)_2Cl_2$ (0.017 g, 0.025 mmol), 2,5-bis(trimethylstannyl)-thieno[3,2-b]thiophene (0.21 g, 0.46 mmol) and ***pybox*-Br** (0.3 g, 1 mmol) in dry toluene (10 mL). Yield: 0.34 g, 59%. ^{1}H NMR (300 MHz, $CDCl_3$+CD_3OD, ppm) δ 8.15 (s, 4H-pyH), 7.75 (s, 2H-Te), 4.4 (t, 8H-CH_2N), 3.94 (t, 8H-CH_2O). ^{13}C NMR (400 MHz, $CDCl_3$+CD_3OD, ppm) δ 164.16, 147.43, 143.52, 142.86, 141.76, 121.49, 119.52, 68.72, 54.59. Anal. calculated for $C_{28}H_{22}N_6O_4S_2$ (*M*W 570.64 g.mol^{-1}), C, 58.94; H, 3.89; N, 14.73; O, 11.21; S, 11.24, found: C,58.17; H, 3.96; N, 13.98; S, 10.76.

5.3.3 Synthesis of the intermediate compounds leading to the poly[3-(6-bromohexyl)thiophene-2,5-diyl]s (**PHT-Br**) polymer precursors

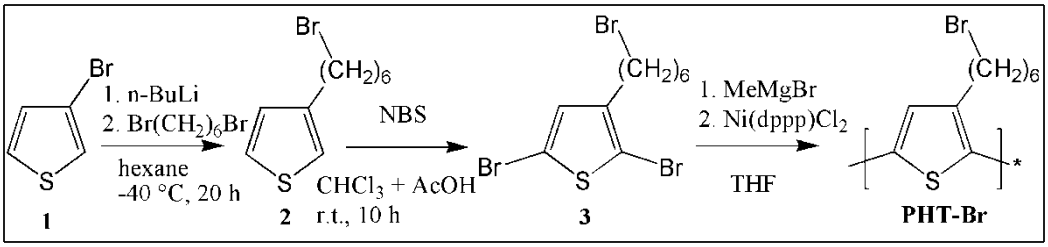

3-bromohexylthiophene (**2**)

A solution of 3-bromothiophene (40 g, 240 mmol) in dry hexane (250 mL) was cooled down to -50 °C. After that the solution of BuLi (116 mL, 290 mmol) was dropwise added and the resulting mixture was stirred for 10 min at -50 °C. Subsequently the reaction mixture was diluted with THF (30 mL) and allowed to warm to -10 °C within one hour. Then 1,6-dibromohexane (80 g, 320 mmol) was added under argon atmosphere and the mixture was warmed to room temperature and stirred within two hours. The resulting mixture was poured into water (500 mL) and separated product was extracted with hexane. Collected organic phase was washed with water (3x50 mL) and the crude product obtained after evaporation of hexane was purified by vacuum distillation. Isolated yield: 28 g, 47%. Purity of product **2** was controlled by the GC and NMR analysis. ^{1}H NMR (300 MHz, $CDCl_3$, ppm) δ 7.24 (1H, t), 6.92 (2H, m), 3.41 (2H, t), 2.64 (2H, t), 1.87 (2H, m), 1.65 (2H, m), 1.48 (4H, m).

2,5-dibromo-3-bromohexylthiophene (**3**)

N-bromosuccinimide (NBS) (5 g, 28 mmol) was divided into several portions and added to the solution of 3-bromohexylthiophene (**2)** (3.2 g, 13 mmol) in chloroform/acetic acid (1/1 by vol., 200 mL). The resulting mixture was stirred at room temperature for 24 h and poured into water. Separated organic phase was washed with water (5x100 mL) and $NaHCO_3$ (aq) (3x50 mL), dried with Na_2SO_4 and the product isolated by the solvent evaporation; isolated yield 81%. Purity of **3** was controlled by the GC and NMR analysis. ^{1}H NMR (300 MHz, $CDCl_3$, ppm) δ 6.77 (1H, s), 3.41 (2H, t), 2.52 (2H, t), 1.86 (2H, m), 1.56 (6H, m).

The synthetic procedure of the **PHT-Br** polymer precursors with various MW and H-T regioregularity was described above in Results and discussion.

5.3.4 Synthesis of the **PHT-EtP$^+$** and **PHT-PhP$^+$** cationic conjugated polyelectrolytes

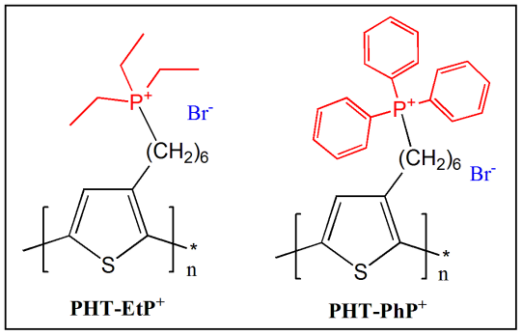

Poly{3-[6-(triethylphosphonium)hexyl]-thiophene-2,5-diyl bromide} (**PHT-EtP$^+$**)

A solution of triethylphosphine (8 mmol, i.e., 8 mL of 1 M solution in THF) was added to the solutions of **PHT-Br** with various MW and H-T (0.2 g, 0.8 mmol with respect to polymer repeating units) in toluene (10 mL). The resulting mixture was stirred under reflux for 24 hours. The excluded polyelectrolytes were twice precipitated from methanol/diethyl ether, washed by diethyl ether and dried to the constant weight in vacuum. The polyelectrolytes prepared with triethylphosphonium ionic side groups were denoted as **PL-EtP$^+$**, **PM-EtP$^+$** and **PH-EtP$^+$** according to the polymer precursor used. The yields and NMR spectra of the synthesized cationic conjugated polyelectrolytes containing triethylphosphonium groups with different MW and H-T *rr* are collected below.

PL-EtP$^+$. Yield: 0.18 g, 78%. ^{1}H NMR (300 MHz, CD_3OD, ppm) δ 7.12 (1H, s), 2.87 (2H, m), 2.28 (15H, m), 1.57 (6H, m), 1.20 (4H, m).

PM-EtP$^+$. Yield: 0.19 g, 82%. ^{1}H NMR (300 MHz, CD_3OD, ppm) δ 7.13 (1H, s), 2.86 (2H, m), 2.25 (15H, m), 1.56 (6H, m), 1.18 (4H, m).

PH-EtP$^+$. Yield: 0.21 g, 91%. ^{1}H NMR (300 MHz, CD_3OD, ppm) δ 7.13 (1H, s), 2.90 (2H, m), 2.26 (15H, m), 1.57 (6H, m), 1.19 (4H, m). ^{31}P NMR (300 MHz, CD_3OD, ppm) δ 38.48.

Poly{3-[6-(triphenylphosphonium)hexyl]-thiophene-2,5-diyl bromide} (**PHT-PhP$^+$**)

Triphenylphosphine (8 mmol, 2.1 g) was added to a solution of **PL-Br**, or **PM-Br**, or **PH-Br** (0.2 g, 0.8 mmol with respect to polymer repeating units) in toluene (10 mL) and stirred under reflux for 24 hours under argon atmosphere. The isolated polyelectrolytes were twice precipitated from methanol/diethyl ether, washed by diethyl ether and dried to the constant weight in vacuum. The synthesized polyelectrolytes bearing triphenylphosphonium pendant groups were coded as **PL-PhP$^+$**, **PM-PhP$^+$** and **PH-PhP$^+$** according to the polymer precursor

used. NMR spectra of the prepared cationic CPEs with triphenylphosphonium moieties are summarized below. Synthetic routes to conjugated polyelectrolytes both **PHT-EtP$^+$** and **PHT-PhP$^+$** are shown in **Scheme 9**.

PL-PhP$^+$. Yield: 0.22 g, 64%. ^{1}H NMR (300 MHz, CD_3OD, ppm) δ 7.75 (15H, m), 7.03 (1H, s), 3.43 (2H, m), 2.77 (2H, m), 1.63 (8H, m).

PM-PhP$^+$. Yield: 0.2 g, 58%. ^{1}H NMR (300 MHz, CD_3OD, ppm) δ 7.74 (15H, m), 7.0 (1H, s), 3.41 (2H, m), 2.76 (2H, m), 1.63 (8H, m).

PH-PhP$^+$. Yield: 0.25 g, 77%. ^{1}H NMR (300 MHz, CD_3OD, ppm) δ 7.77 (15H, m), 7.0 (1H, s), 3.42 (2H, m), 2.74 (2H, m), 1.63 (8H, m). ^{31}P NMR (300 MHz, CD_3OD, ppm) δ 23.65.

5.3.5 General procedure of the preparation of metallo-supramolecular polymers

The solutions of the prepared unimers (1 eq.) in the mixed solvent chloroform/methanol (1/1 by volume) or pure DMSO at concentration 2×10^{-4} M were mixed with the solutions of metal ions (1 eq.) such as Fe^{2+}, Zn^{2+}, Ni^{2+}, Cu^{2+} perchlorate hydrates in the same solvent system at concentration 2×10^{-2} M. After solvent evaporation or precipitation by less polar solvent with following filtration and drying, metallo-supramolecular polymers were obtained.

6 CONCLUSIONS

The aim of this work was development of novel conjugated polymers with tunable photophysical properties and improved processability from solutions. In particular, this work was focused on the development of *(i)* new linear unimers with chelate end-groups derived from the benzimidazole and oxazoline derivatives of pyridine that can be prepared from cheap chelidamic acid, which are able to undergo the self-assembly process with metal ions leading to the formation of MSPs, and *(ii)* polythiophene polyelectrolytes with phosphonium pendants that are soluble in aqueous mediums. The project solution required:

- Preparation of novel monotopic chelate ligands based on bis(benzimidazole)- and bis(oxazole)pyridyl moieties.
- Investigation of the complexation of synthesized ligands with metal ions and characterization of formed complexes in solution.
- Synthesis and characterization of conjugated ditopic unimers with the above chelate end-groups and oligothiophene central blocks.
- Preparation of metallo-supramolecular polymers by self-assembly process of synthesized unimers with metal ions. Analysis of prepared supramolecular assemblies by different spectroscopic methods.
- Detailed investigation of the self-assembly process.
- Synthesis of precursor polymers: poly[3-(6-bromohexyl)thiophene]s of different regioregularity using the GRIM polymerization method.
- Transformation of the precursor polymers into cationic conjugated polyelectrolytes by their modification with trialkyl(aryl)phosphates and characterization of the prepared CPEs.

The synthesis routes to new monotopic ligands and corresponding ditopic unimers have been developed, which use a quite cheap and easily available chelidamic (4-hydroxypyridine-2,5-dicarboxylic) acid as the starting material. Various mono- and ditopic compounds with two different tridentate chelate groups (ion selectors): 2,5-bis(benzimidazol-2-yl)pyridine-4-yl (*bzimpy*) and 2,5-bis(4,5-dihydrooxazol-2-yl)pyridine-4-yl (*pybox*) have been prepared, characterized and assembled with various metal ions (Zn^{2+}, Fe^{2+}, Ni^{2+}, Cu^{2+} and Eu^{3+} or Tb^{3+}). Monotopic ligands have been exploited for a detailed study of the process of coordination to

metal ions and also as intermediates at the syntheses of linear unimers. Thiophene-2,5-diyl, bithiophene-2,5´-diyl, thienothiophene-2,5-diyland terthiophene-2,5´´-diyl units have been used as the central blocks of newly prepared unimers. Studies on the properties of *bzimpy*-based unimers and MSPs were limited because these compounds have shown relatively low solubility in organic solvents.

A detailed study on the coordination mode of monotopic pybox ligands proved that these ligands easily form $[MtL_2]^{2+}$species which are in a dynamic equilibrium with species $[MtL]^{2+}$ and free ions, same as the ligands of terpyridine family. The *pybox* unimers also showed a good ability to coordinate to the above metal ions giving corresponding metallo-supramolecular polymers. The detailed study of the MSP assembly revealed three stages of this process, same as observed for bis(*tpy*) unimers: formation of "butterfly" dimers U-Mt^{z+}-U (U stands for a unimer species) at the Mt^{z+}/U mole ratios *r* up to ca 0.5, formation of longer MSP chains for *r* from above 0.5 to ca 1, and end-capping of MSP chains and their equilibrium depolymerization at *r* values above 1. The latter proves the constitutional-dynamic nature of the novel MSPs, which is the fastest for Zn-dynamers and the slowest for Fe-dynamers. The dynamic nature of MSP chains has been also examined through the reaction of MSPs with monotopic ligands leading to the chains end-capped with these ligands.

The incorporation of different metal ions into MSP chains has been shown to result in significant differences in optical properties of the MSPs formed. The highest bathochromic shift of absorption maximum as compared to the free unimer was observed for Cu^{2+}-dynamers while the lowest shift for Fe^{2+}-dynamer for all *pybox*-based unimers. On the other hand, all Fe^{2+}-dynamers showed a new absorption band attributed to the metal to ligand charge transfer process (MLCT). Among all prepared MSPs, only Zn^{2+}-dynamers exhibited fluorescence while the other ones showed only fluorescence quenching. A good solubility of the *pybox*-based MSPs in organic solvents allowed preparation of thin solid films.

The second newly developed materials: cationic conjugated polythiophene polyelectrolytes have been prepared using the well established polymer modification approach. First poly[3-(6-bromohexyl)thiophene-2,5-diyl]s of different chain regioregularity were prepared by the Grignard metathesis polymerizations. The chain regioregularity has been tuned by varying the temperature regime of the polymerization process. So prepared precursor polymers were characterized and then transformed into cationic conjugated polyelectrolytes by

simple quaternization reaction with triethylphosphine or triphenylphosphine. High solubility of these polyelectrolytes in water and water miscible solvents achieved thanks to the presence of phosphonium bromide pendant groups in their structure. Basic photophysical properties of these cationic conjugated polyelectrolytes were studied in water, methanol and DMSO solvents. These studies revealed solvatochromism of prepared polyelectrolytes and possibility of tuning their luminescence through the solvent polarity. The luminescence quenching by $K_4[Fe(CN)_6]$ and $K_3[Fe(CN)_6]$ has been also studied and quantitatively described by Stern-Volmer constant. All experiments performed pointed to the principle influence of the main-chain regioregularity on the polymer properties except for its solubility in polar solvents.

7 REFERENCES

[1] J.-M. Lehn, *Supramolecular Chemistry Concepts and Perspectives*; VCH: New York, **1995**.

[2] D. Philp, J. F. Stoddart, *Angew. Chem. Int. Ed. Engl*., **1996**, *35*, 1154-1196.

[3] G. M. Whitesides, J. P. Mathias, C. T. Seto, *Science*, **1991**, *254*, 1312-1319.

[4] J. S. Lindsey, *New J. Chem*., **1991**, *15*, 153-180.

[5] S. R. Batten, R. Robson, *Angew. Chem. Int. Ed*., **1998**, *37*, 1460-1494.

[6] J. D. Watson, F. H. C. Crick, *Nature*, **1953**, *171*, 737-738.

[7] P. M. Proulx-Curry, N. D. Chasteen, *Coord. Chem. Rev*., **1995**, *144*, 347-368.

[8] T. Emrick, J. M. J. Fréchet, *Curr. Opin. Colloid Interface Sci*., **1999**, *4*, 15-23.

[9] C. J. Janiak, *Chem. Soc. Dalton Trans*., **2000**, 3885-3896.

[10] V. C. Pierre, J. T. Kaiser, J. K. Barton, *Proc. Natl. Acad. Sci. USA*., **2007**, *104*, 429-434.

[11] G. F. Swiegers, T. J. Malefetse, *Coord. Chem. Rev*., **2002**, *225*, 91-121.

[12] J. L. Boyer, M. L. Kuhlman, T. B. Rauchfuss, *Acc. Chem. Res*., **2007**, *40*, 233-242.

[13] M. Ruben, J. Rojo, F. J. Romero-Salguero, L. H. Uppadine, J. Lehn, *Angew.Chem. Int. Ed*., **2004**, *43*, 3644-3662.

[14] M. D. Ward, J. A. McCleverty, J. C. Jeffery, *Coord. Chem. Rev*., **2001**, *222*, 251-272.

[15] D. Tranchemontagne, Z. Ni, M. O'Keeffe, O. Yaghi, *Angew. Chem. Int*. Ed., **2008**, *47*, 5136-5147.

[16] O. K. Farha, J. T. Hupp, *Acc. Chem. Res*., **2010**, *43*, 1166-1175.

[17] J.-M. Lehn, *Prog. Polym. Sci*., **2005**, *30*, 814–831.

[18] A. Ciferri, A. Ciferri, *Supramolecular Polymers*, CRC Press, 2nd edn, **2005**.

[19] M. Chiper, R. Hoogenboom and U. S. Schubert, *Macromol. Rapid Commun*., **2009**, *30*, 565–578.

[20] V. A. Friese and D. G. Kurth, *Coord. Chem. Rev*., **2008**, *252*, 199–211.

[21] C. Hu, T. Sato and J. Zhang, *ACS Appl. Mater. Interfaces*, **2014**, *6*, 9118–9125.

[22] G. Schwarz, I. Haslauer and D. G. Kurth, *Adv. Colloid Interface Sci*., **2014**, *207*, 107–120.

[23] A. T. ten Cate, R. P. Sijbesma, *Macromol Rapid Commun*., **2002**, *23*, 1094–1112.

[24] A. N. Khlobystov, A. J. Blake, N. R. Champness, D. A. Lemenkovskii, A. G. Majouga, N. V. Zyk, M. Schroder, *Coord Chem Rev*., **2001**, *222*, 155–192.

[25] U. S. Schubert, C. Eschbaumer, *Angew. Chem. Int Ed*., **2002**, *41*, 2892–2926.

[26] E. C. Constable, A. Thompson, *J. Chem. Soc. Dalton Trans*., **1992**, 3467-3475.

[27] M. Kimura, M. Sano, T. Muto, K. Hanabusa, H. Shirai, *Macromolecules*, **1999**, *32*, 7951-7953.

[28] R. Hogg, R. G. Wilkins, *J. Chem. Soc*., **1962**, 341-350.

[29] F. Vögtle, M. Plevoets, M. Nieger, G.C. Azzellini, A. Credi, L. De Cola, V. De Marchis, M. Venturi, V. Balzani, *J. Am. Chem. Soc*., **1999**, *121*, 6290-6298.

[30] E. C. Constable, P. Harverson, M. Oberholzer, *J. Chem. Soc, Chem. Commun*., **1996**, 1821-1822.

[31] H.-F. Chow, I. V.-K. Chan, C. C. Mak, *Tetrahedron Lett*., **1995**, *36*, 8633-8636.

[32] R. L. C. Lau, T. W. D. Chan, I. Y. K. Chan, H. F. Chow, *Europ. Mass Spec*., **1995**, *1*, 371-380.

[33] J.-C. G. Bunzli, C. Piguet, *Chem. Soc. Rev*., **2005**, *34*, 1048–1077.

[34] M. Martínez-Calvo, O. Kotova, M. E. Mobius, A. P. Bell, T. McCabe, J. J. Boland and T. Gunnlaugsson, *J. Am. Chem. Soc*., **2015**, *137*, 1983–1992.

[35] Y. Hasegawa, T. Nakanishi, *RSC Adv*., **2015**, *5*, 338–353.

[36] K. Wang, M. A. Haga, H. Monjushiro, M. Akiba, Y. Sasaki, *Inorg. Chem*., **2000**, *39*, 4022-4028.

[37] L. J. Grove, J. M. Rennekamp, H. Jude, W. B. Connick, *J. Am. Chem. Soc*., **2004**, *126*, 1594-1595.

[38] E. J. Rivera, C. Figueroa, J. L. Colon, L. Grove, W. B. Connick, *Inorg. Chem*., **2007**, *46*, 8569–8576.

[39] S. C. Yu, S. Hou, W. K. Chan, *Marcomolecules*, **1999**, *32*, 5251–5256.

[40] M. A. Haga, H. G. Hong, Y. Shiozawa, Y. Kawata, H. Monjushiro, T. Fukuo, R. Arakawa, *Inorg. Chem*., **2000**, *39*, 4566–4573.

[41] C. Piguet, B. Bocquet, E. MWller, A. F. Williams, *Helv. Chim. Acta*, **1989**, *72*, 323 –337.

[42] A. W. Addison, S. Burman, C. G. Wahlgren, *J. Chem. Soc. Dalton Trans*., **1987**, 2621–2630.

[43] S. Obara, M. Itabashi, F. Okuda, S. Tamaki, Y. Tanabe, Y. Ishii, K. Nozaki, M. A. Haga, *Inorg. Chem*., **2006**, *45*, 8907 –8921.

[44] V. G. Vaidyanathan, B. U. Nair, *Eur. J. Inorg. Chem*., **2005**, 3756 – 3759.

[45] M. Boča, R.,F. Jameson, W. Linert, *Coord. Chem. Rev*., **2011**, *255*, 290-317.

[46] D. Mishra, S. Naskar, S.,K. Chattopadhyay, M. Maji, P. Sengupta, R. Dinda, S. Ghosh, T.C.W. Mak, *Transit. Met. Chem*., **2005**, *30*, 352-356.

[47] W. Linert, M. Konecny, F. Renz, *J. Chem. Soc. Dalton Trans*., **1994**, 1523-1531.

[48] S. J. Rowan, Beck, J. B. *Faraday Discuss*., **2005**, *128*, 43-53.

[49] C. Piguet, J.-C. G. Bunzli, *Eur. J. Solid State Inorg. Chem*., **1996**, *33*, 165-174.

[50] J. B. Beck, S. J. Rowan, *J. Am. Chem. Soc*., **2003**, *125*, 13922-13923.

[51] D. Knapton, P. K. Iyer, S. J. Rowan, C. Weder, *Macromolecules*, **2006**, *39*, 4069-4075.

[52] W. Weng, J. B. Beck, A. M. Jamieson, S. J. Rowan, *J. Am. Chem. Soc*., **2006**, *128*, 11663-11672.

[53] Z. Derikvand, N. Dorosti, F. Hassanzadeh, A. Shokrollahi, Z. Mohammadpour, A. Azadbakht, *Polyhedron*, **2012**, *43*, 140-152.

[54] F. S. Richardson, *Chem. Re*v., **1982**, *82*, 541-552.

[55] J. P. Riehl, F. S. Richardson, *Chem. Re*v., **1986**, *86*, 1-16.

[56] P. A. Brayshaw, J.-C. G. Bunzli, P. Froidevaux, J. M. Harrowfield, Y. Kim, A. N. Sobolev, *Inorg. Chem*., **1995**, *34*, 2068-2076.

[57] H. Nishiyama, H. Sakaguchi, T. Nakamura, M. Horihata, M. Kondo, K. Itoh, *Organometallics,* **1989**, *8*, 846-848.

[58] J. Jankowska, J. Paradowska, B. Rakiel, J. Mlynarski, *J. Org. Chem*., **2007**, 72, 2228-2231.

[59] J. Jankowska, J. Paradowska, J. Mlynarski, *Tetrahedron Lett*., **2006**, *47*, 5281-5284.

[60] J. D. Nobbs, A. K. Tomov, R. Cariou, V. C. Gibson, A. J. P. White, G. J. P. Britovsek, *Dalton Trans*., **2012**, *41*, 5949-5964.

[61] K. Nomura, W. Sidokmai, Y. Imanishi, *Bull. Chem. Soc. Jpn*., **2000**, *73*, 599-605.

[62] M. Kawatsura, K. Kajita, S. Hayase, T. Itoh, *Synlett*, **2010**, 1243-1246.

[63] A. J. Davenport, D. L. Davies, J. Fawcett, S. A. Garratt, L. Lad, D. R. Russell, *Chem. Commun*., **1997**, *33*, 2347–2348.

[64] H. C. Aspinall, J. L. M. Dwyer, N. Greeves, P. M. Smith, *J. Alloys Compds*., **2000**, *303*, 173-177.

[65] H. C. Aspinall, N. Greeves, *J. Organomet. Chem*., **2002**, *647*, 151-157.

[66] H. C. Aspinall, J. F. Bickley, N. Greeves, R. V. Kelly, P. M. Smith, *Organometallics*, **2005**, *24*, 3458-3467.

[67] A. de Bettencourt-Dias, S. Viswanathan, A. Rollett, *J. Am. Chem. Soc*., **2007**, *129*, 15436-15437.

[68] G. Desimoni, G. Faita, S. Filippone, M. Mella, M. G. Zampori, M. Zema, *Tetrahedron*, **2001**, *57*, 10203-10212.

[69] G. Desimoni, G. Faita, P. Quadrelli, *Chem. Re*v., **2003**, *103*, 3119-3154.

[70] C.-L. Ho, W.-Y. Wong, *Coord. Chem. Rev*., **2011**, *255*, 2469-2502.

[71] U. S. Schubert, O. Hien, C. Eschbaumer, *Macromol. Rapid. Commun*., **2000**, *21*, 1156-1161.

[72] S. Schmatloch, A. M. J. van den Berg, A. S. Alexeev, H. Hofmeier, U. S. Schubert, *Macromolecules*, **2003**, *36*, 9943-9949.

[73] U. Mansfeld, A. Winter, M. D. Hager, W. Gьnther, E. Altuntas, U. S. Schubert, *J. Polym. Sci. Part A: Polym. Chem*., **2013**, *51*, 2006-2015.

[74] J. K. Stille, *Angew. Chem. Int. Ed. Engl*., **1986**, *25*, 508-524.

[75] N. Miyaura, A. Suzuki, *Chem. Rev*., **1995**, *95*, 2457-2483.

[76] K. Sonogashira, *J. Organomet. Chem*., **2002**, *653*, 46–49.

[77] K. Tamao, K. Sumitani, M. Kumada, *J. Am. Chem. Soc*., **1972**, *94*, 4374–4376.

[78] MacDiarmid, A. G. *Angew. Chem. Int. Ed*., **2001**, *40*, 2581-2590.

[79] A. Kraft, A. C. Grimsdale, A. B. Holmes, *Angew. Chem. Int. Ed*., **1998**, *37*, 402-428.

[80] A. J. Heeger, *Angew. Chem. Int. Ed*., **2001**, *40*, 2591-2611.

[81] N. Koumura, Z.-S. Wang, S. Mori, M. Miyashita, E. Suzuki, K. Hara, *J. Am. Chem. Soc*., **2006**, *128*, 14256-14257.

[82] Z.-S. Wang, N. Koumura, Y. Cui, M. Takahashi, H. Sekiguchi, A. Mori, T. Kubo, A. Furube, K. Hara, *Chem. Mater*., **2008**, *20*, 3993-4003.

[83] A. Mishra, M. K. R. Fischer, P. Bäuerle, *Angew. Chem. Int. Ed*., **2009**, *48*, 2474-2499.

[84] M.-H. Yoon, A. Facchetti, C. E. Stern, T. J. Marks, *J. Am. Chem. Soc*., **2006**, *128*, 5792-5801.

[85] S. Allard, M. Forster, B. Souharce, H. Thiem, U. Scherf, *Angew. Chem. Int. Ed*., **2008**, *47*, 4070-4098.

[86] J. A. Letizia, J. Rivnay, A. Facchetti, M. A. Ratner, T. J. Marks, *Adv. Funct. Mater*., **2010**, *20*, 50-58.

[87] Y. Kim, S. Cook, S. M. Tuladhar, S. A. Choulis, J. Nelson, J. R. Durrant, D. D. C. Bradley, M. Giles, I. McCulloch, C.-S. Ha, M. Ree, *Nat. Mater*., **2006**, *5*, 197-203.

[88] J-M. Lehn, M. Mascal, A. DeCian, J. Fischer, *J. Chem. Soc. Perkin Trans*., **1992**, *2*, 461–467.

[89] H. Yang, Q. Ma, Y. Tan, *J. Polym Res*., **2013**, *20*, 100–106.

[90] H. Hofmeier, R. Hoogenboom, M. E. L. Wouters, U. S. Schubert, *J. Am. Chem. Soc*., **2005**, *127*, 2913–2921.

[91] W. M. Huang, Y. Zhao, C. C. Wang, Z. Ding, H. Purnawali, C. Tang, J. L. Zhang, *J. Polym. Res*., **2012**, *19*, 9952–9985.

[92] T. F. A. D. Greef, M. M. J. Smulders, M. Wolffs, A. P. H. J. Schenning, R. P. Sijbesma, E. W. Meijer, *Chem. Rev*., **2009**, *109*, 5687-5754.

[93] G. R. Whittell, M. D. Hager, U. S. Schubert, I. Manners, *Nat. Mater*., **2011**, *10*, 176-188.

[94] E. A. Appel, J. Del Barrio, X. J. Loh, O. A. Scherman, *Chem. Soc. Rev*., **2012**, *41*, 6195-6214.

[95] X. Yan, F. Wang, B. Zheng, F. Huang, *Chem. Soc. Rev*., **2012**, *41*, 6042-6065.

[96] F. S. Han, M. Higuchi, D. G. Kurth, *J. Am. Chem. Soc*., **2008**, *130*, 2073-2081.

[97] A. Winter, C. Friebe, M. Chiper, M. D. Hager, U. S. Schubert, *J. Polym. Sci. Part A: Polym. Chem*., **2009**, *47*, 4083-4098.

[98] R. R. Pal, M. Higuchi, Y. Negishi, T. Tsukuda, D. G. Kurth, *Polym. J*., **2010**, *42*, 336-341.

[99] F. Han, M. Higuchi, D. G. Kurth, *Tetrahedron*, **2008**, *64*, 9108-9116.

[100] M. Burnworth, L. M. Tang, J. R. Kumpfer, A. J. Duncan, F. L. Beyer, G. L. Fiore, S. J. Rowan, C. Weder, *Nature*, **2011**, *472*, 334-337.

[101] M. Sun, H. Zhang, B. Liu, Y. Liu, *Macromolecules*, **2013**, *46*, 4268-4275.

[102] R. Dong, Y. Su, S. Yu, Y. Zhou, Y. Lu, X. Zhu, *Chem. Commun.,* **2013**, *49*, 9845-9847.

[103] P. Thordarson, *Chem. Soc. Rev*., **2011**, *40*, 1305-1323.

[104] C.-L. Ho, W.-Y. Wong, *Coord. Chem. Rev*., **2011**, *255*, 2469-2502.

[105] J. M. J. Paulusse, J. P. J. Huijbers, R. P. Sijbesma, *Chem. – Eur. J*., **2006**, *12*, 4928-4934.

[106] J. M. J. Paulusse, R. P. Sijbesma, *Angew. Chem. Int. Ed*., **2004**, *43*, 4460-4462.

[107] P. Štenclová, K. Šichová, I. Šloufová, J. Zedník, J. Vohlídal and J. Svoboda, *Dalton Trans*., **2016**, *45*, 1208-1224.

[108] A. Winter, C. Friebe,M.Chiper, M. D. Hager, U. S. Schubert, *J. Polym. Sci. Part A: Polym. Chem*., **2009**, *47*, 4083-4098.

[109] A. Wild, C. Friebe, A. Winter, M. D. Hager, U.-W. Grummt, U. S. Schubert, *Eur. J. Org. Chem*., **2010**, 1859-1868.

[110] C. Friebe, A. Wild, J. Perelaer and U. S. Schubert, *Macromol. Rapid Commun*., **2012**, *33*, 503-509.

[111] R. Siebert, Y. Tian, R. Camacho, A. Winter, A. Wild, A. Krieg, U. S. Schubert, J. Popp, I. G. Scheblykin and B. Dietzek, *J. Mater. Chem*., **2012**, *22*, 16041-16050.

[112] A. Winter, C. Friebe, M. D. Hager, U. S. Schubert, *Macromol. Rapid Commun*., **2008**, *29*, 1679-1686.

[113] Y.-Y. Chen, Y.-T. Tao and H.-C. Lin, *Macromolecules*, **2006**, *39*, 8559-8566.

[114] P. D. Vellis, J. A. Mikroyannidis, C.-N. Lo and C.-S. Hsu, *J. Polym. Sci. Part A: Polym. Chem*., **2008**, *46*, 7702-7712.

[115] Y.-Y. Chen and H.-C. Lin, *Polymer*, **2007**, *48*, 5268-5278.

[116] A. El-ghayoury, A. P. H. J. Schenning and E. W. Meijer, *J. Polym. Sci. Part A: Polym. Chem*., **2002**, *40*, 4020-4023.

[117] P. K. Iyer, J. B. Beck, C. Weder, S. J. Rowan, *Chem. Commun*., **2005**, 319-321.

[118] J. Braun, K. Renggli, J. Razumovitch, C. Vebert, *Supramol. Chem., John Wiley & Sons*, **2012**, 411.

[119] J.-F. Gohy, *Coord. Chem. Rev*., **2009**, *253*, 2214-2225.

[120] Y.-T. Chan, S. Li, C. N. Moorefield, P. Wang, C. D. Shreiner, G. R. Newkome, *Chem. Eur. J*., **2010**, *16*, 4164-4168.

[121] M. Kudera, C. Eschbaumer, H. E. Gaub and U. S. Schubert, *Adv. Funct. Mater*., **2003**, *13*, 615-620.

[122] S. Kelch, M. Rehahn, *Macromolecules,* **1999**, *32*, 5818–5828.

[123] W. Y. Ng, X. Gong, W. K. Chan, *Chem. Mater*., **1999**, *11*, 1165–1170.

[124] G. D. Storrier, S. B. Colbran, D. C. Craig, *J. Chem. Soc. Dalton. Trans*., **1997**, 3011–3028.

[125] U. Michelsen, C. A. Hunter, *Angew. Chem. Int. Ed*., **2000**, *39*, 764-767.

[126] C.-L. Ho and W.-Y. Wong, *Coord. Chem. Rev*., **2011**, *255*, 2469-2502.

[127] H. Naarmann, N. Theophilou, *Synth. Met*., **1987**, *22*, 1–8.

[128] I. D. Parker, *J. Appl. Phys*., **1994**, *75*, 1656-1666.

[129] P. C. Rodrigues, B. D. Fontes, B. B. M. Torres, W. S. Sousa, G. C. Faria, D. T. Balogh, R. M. Faria, L. Akcelrud, *J. Appl. Polym. Sci*., **2015**, *132*, 42579–42587.

[130] A. G. MacDiarmid, J. C. Chiang, A. F. Richter, A. J. Epstein, *Synth. Met*., **1987**, *18*, 285–290.

[131] L.-Z. Fan, Y.-S. Hu, J. Maier, P. Adelhelm, B. Smarsly and M. Antonietti, *Adv. Funct. Mater*., **2007**, *17*, 3083–3087.

[132] R. D. McCullough, *Adv. Mater*., **1998**, *10*, 93–116.

[133] B. S. Ong, Y. Wu, P. Liu, S. Gardner, *J. Am. Chem. Soc*., **2004**, *126*, 3378–3379.

[134] K. Kaneto, S. Ura, K. Yoshino, Y. Inuishi, *Jpn. J. Appl. Phys*., **1984**, *23*, 189–191.

[135] M. T. Bernius, M. Inbasekaran, J. O'Brien, W. Wu, *Adv. Mater*., **2000**, *12*, 1737–1750.

[136] Z. Li, J. Ding, J. Lefebvre, P. R. L. Malenfant, *Org. Electron*., **2015**, *26*, 15–19.

[137] L. Akcelrud, *Prog. Polym. Sci*., **2003**, *28*, 875–962.

[138] A. Kraft, A. C. Grimsdale, A. B. Holmes, *Angew. Chem. Int. Ed*., **1998**, *37*, 402–428.

[139] G. Horowitz, *Adv. Mater.*, **1998**, *10*, 365-377.

[140] H. Sirringhaus, *Adv. Mater*., **2005**, *17*, 2411–2425.

[141] S. Günes, H. Neugebauer, N. S. Sariciftci, *Chem Re*v., **2007**, *107*, 1324-1338.

[142] H. Shirakawa, E. J. Louis, A. G. MacDiarmid, C. K. Chiang, A. J. Heeger, *J. Chem. Soc. Chem. Commun*., **1977**, 578-580.

[143] H. Shirakawa, *Angew. Chem. Int. Ed*., **2001**, *40*, 2574-2580.

[144] A. G. MacDiarmid, *Angew. Chem. Int. Ed*., **2001**, *40*, 2581-2590.

[145] Y. Liang, Y. Wu, D. Feng, S. T. Tsai, H. J. Son, G. Li, L. Yu, *J. Am. Chem. Soc*., **2009**, 131, 56-57.

[146] E. Zhou, J. Cong, K. Tajima, C. Yang, K. Hashimoto, *J. Phys. Chem. C*, **2012**, *116*, 2608-2614.

[147] C. Chen, P. Dagneau, E. J. J. Grabowski, R. Oballa, P. O'Shea, P. Prasit, J. Robichaud, R. Tillyer, X. Wang, *J. Org. Chem*., **2003**, *68*, 2633-2638.

[148] F. C. Krebs, *Sol. Energ. Mat. Sol. C*, **2006**, *90*, 3633-3643.

[149] J. Y. Kim, S. H. Kim, H. H. Lee, K. Lee, W. Ma, X. Gong, A. J. Heeger, *Adv. Mater*., **2006**, *18*, 572–576.

[150] T. Yamamoto, K. Sanechika, A. Yamamoto, *J. Polym. Sci. Polym. Lett. Ed*., **1980**, *18*, 9-12.

[151] J. W. P. Lin, L. P. Dudek, *J. Polym. Sci. Polym. Chem. Ed*., **1980**, *18*, 2869-2873.

[152] R. D. McCullough, *Adv. Mater*., **1998**, *10*, 93-116.

[153] P. Bláhová, J. Zedník, I. Šloufová, J. Vohlídal, J. Svoboda, *Soft Mater*., **2014**, *12*, 214-229.

[154] H. Sirringhaus, P. J. Brown, R. H. Friend, M. M. Nielsen, K. Bechgaard, B. M. W. Langeveld-Voss, A. J. H. Spiering, R. A. J. Janssen, E. W. Meijer, P. Herwig, D. M. De Leeuw, *Nature*, **1999**, *401*, 685-688.

[155] Z. Bao, A. Dodabalapur, A. J. Lovinger, *Appl. Phys. Lett*., **1996**, *69*, 4108-4110.

[156] R. D. McCullough, S. Tristramnagle, S. P. Williams, R. D. Lowe, M. Jayaraman, *J. Am. Chem. Soc*., **1993**, *115*, 4910-4911.

[157] D. Bondarev, J. Zedník, I. Šloufová, A. Sharf, M. Procházka, J. Pfleger and J. Vohlídal, *J. Polym. Sci. Part A: Polym. Chem*., **2010**, *48*, 3073–3081.

[158] G. Hostnik, V. Vlachy, D. Bondarev, J. Vohlídal, J. Cerar, Phys. Chem. Chem. Phys., **2015**, *17*, 2475-2483.

[159] M. Hess, R. G. Jones, J. Kahovec, T. Kitayama, P. Kratochvíl, P. Kubisa, W. Mormann, R. F. T. Stepto, D. Tabak, J. Vohlídal, E. S. Wilks, *Pure Appl. Chem*. **2006**, *78*, 2067−2074.

[160] E. G. Tennyson, R. C. Smith, *Inorg Chem*., **2009**, *48*, 11483–11485.

[161] X. Zhao, H. Jiang, K. S. Schanze, *Macromolecules*, **2008**, *41*, 3422–3428.

[162] A. Satrijo, T. M. Swager, *J. Am. Chem. Soc*., **2007**, *129*, 16020–16028.

[163] S. Durben, Y. Dienes, T. Baumgartner, *Org. Lett*., **2006**, *8*, 5893–5896.

[164] J. H. Ortony, R. Yang, J. Z. Brzezinski, L. Edman, T-Q. Nguyen, G. C. Bazan, *Adv. Mater*., **2008**, *20*, 298–302.

[165] B. Liu, W. L. Yu, Y. H. Lai, W. Huang, *Chem. Commun*., **2000**, 551-552.

[166] C. Tan, M. R. Pinto, K. S. Schanze, *Chem. Commun*., **2002**, 446-447.

[167] A. Fujii, T. Sonoda, K. Yoshino, *Jpn. J. Appl. Phys*., **2000**, *39*, 249-252.

[168] C. Duan, L. Wang, K. Zhang, X. Guan, F. Huang, *Adv. Mater*., **2011**, *23*, 1665−1669.

[169] Z. Fang, A. A. Eshbaugh, K. S. Schanze, *J. Am. Chem. Soc*., **2011**, *133*, 3063−3069.

[170] A. O. Patil, Y. Ikenoue, F. Wudl, A. J. Heeger, *J. Am. Chem. Soc*., **1987**, *109*, 1858-1859.

[171] S. Shi, F. Wudl, *Macromolecules*, **1990**, *23*, 2119-2124.

[172] B. Liu, W. L. Yu, Y. H. Lai, W. Huang, *Macromolecules*, **2002**, *35*, 4975-4982.

[173] J. N. Wilson, Y. Q. Wang, J. J. Lavigne, U. H. F. Bunz, *Chem. Commun*., **2003**, 1626-1627.

[174] M. Liu, P. Kaur, D. H. Waldeck, C. H. Xue, H. Y. Liu, *Langmuir*, **2005**, *21*, 1687-1690.

[175] S. Y. Okada, R. Jelinek, D. Charych, *Angew. Chem. Int. Ed*., **1999**, *38*, 655-659.

[176] M. R. Pinto, K. S. Schanze, *Proc. Natl. Acad. Sci. USA*, **2004**, *101*, 7505-7510.

[177] K. E. Achyuthan, T. S. Bergstedt, L. Chen, R. M. Jones, S. Kumaraswamy, S. A. Kushon, K. D. Ley, L. Lu, D. McBranch, H. Mukundan, F. Rininsland, X. Shi, W. Xia, D. G. Whitten, *J. Mater. Chem*., **2005**, *15*, 2648-2656.

[178] S. A. Kushon, K. D. Ley, K. Bradford, R. M. Jones, D. McBranch, D. Whitten, *Langmuir*, **2002**, *18*, 7245-7249.

[179] B. S. Gaylord, A. J. Heeger, G. C. Bazan, *J. Am. Chem. Soc*., **2003**, *125*, 896-900.

[180] B. S. Gaylord, A. J. Heeger, G. C. Bazan, *Proc. Natl. Acad. Sci. USA*, **2002**, *99*, 10954-10957.

[181] Q. Zhou, T. M. Swager, *J. Am. Chem. Soc*., **1995**, *117*, 7017−7018.

[182] X. Song, H. l. Wang, J. Shi, J. W. Park, B. I. Swanson, *Chem. Mater*., **2002**, *14*, 2342-2347.

[183] C. G. Cassity, A. Mirjafari, N. Mobarrez, K. J. Strickland, R. A. O'Brien and J. H. Davis, *Chem. Commun*., **2013**, *49*, 7590–7592.

[184] S. Gu, R. Cai, T. Luo, Z. Chen, M. Sun, Y. Liu, G. He, Y. Yan, *Angew. Chem. Int*. Ed., **2009**, *48*, 6499–6502.

[185] E. G. Tennyson, S. He, N. C. Osti, D. Perahia, R. C. Smith, *J. Mater. Chem*., **2010**, *20*, 7984–7989.

[186] A. Kanazawa, T. Ikeda, T. Endo, *J. Polym. Sci. Part A: Polym. Chem*., **1993**, *31*, 335–343.

[187] P. Štenclová-Bláhová, J. Svoboda, I. Šloufová and J. Vohlídal, *Phys. Chem. Chem. Phys*., **2015**, *17*, 13743-13756.

[188] T. Vitvarova, J. Zednik, M. Blaha, J. Vohlidal, J. Svoboda, *Eur. J. Inorg. Chem*., **2012**, *2012*, 3866–3874.

[189] X. M. Xiao, M. Haga, M. I. Takeko, *J. Chem. Soc. Dalton Trans*., **1993**, 2477–2484.

[190] J. Wang , L. Shuai, X. Xiao, Y. Zeng, Z. Li, T. Matsumura-Inoue, *J. of Inorg. Biochem*., **2005**, *99*, 883–885.

[191] J. Zhang, C.-Y. Hsu, M. Higuchi, *J. Photopolym. Sci. Technol*., **2014**, *27*, 297-300.

[192] N. B. Shustova, A. F. Cozzolino, S. Reineke, M. Baldo, M. Dincă, *J. Am. Chem. Soc*., **2013**, *135*, 13326-13329.

[193] S. Singh, J. Chaturvedi, S. Bhattacharya, *Dalton Trans*., **2012**, *41*, 424-431.

[194] T. Vitvarová, J. Svoboda, M. Hissler, J. Vohlídal, Organometallics, **2017**, *36*, 777–786.

[195] D. Rais, M. Menšík, P. Štenclová-Bláhová, J. Svoboda, J. Vohlídal, J. Pfleger, *J. Phys. Chem. A*, **2015**, *24*, 6203–6214.

[196] A. De Bettencourt-Dias, S. Viswanathan, A. Rollett, J. *Am. Chem. Soc*., **2007**, *129*, 15436-15437.

[197] S. Inal, J. D. Kölsch, L. Chiappisi, M. Kraft, A. Gutacker, D. Janietz, U. Scherf, M. Gradzielski, A. Laschewsky, D. Neher, *Macromol. Chem. Phys*., **2013**, *214*, 435–445.

[198] H. A. Al Attar, A. P. Monkman, *J. Phys. Chem. B*, **2007**, *111*, 12418–12426.

[199] M. L. Davies, P. Douglas, H. D. Burrows, M. G. Miguel, A. Douglas, *Port. Electrochim. Acta*, **2009**, *27*, 525–531.

[200] S. Hladysh, D. Bondarev, J. Svoboda, J. Vohlídal, D. Vrbata, J. Zedník, *Eur. Polym. J.*, **2016**, *83*, 367–376.

[201] P. Urbánek, A. di Martino, S. Gladyš, I. Kuřitka, A. Minařík, E. Pavlova, D. Bondarev, *Synthetic Metals*, **2015**, *202*, 16-24.

8 LIST OF PUBLICATIONS

1) S. Hladysh, D. Václavková, D. Vrbata, D. Bondarev, D. Havlíček, J. Svoboda, J. Zedník, J. Vohlídal, Synthesis and characterization of metallo-supramolecular polymers from thiophene-based unimers bearing pybox ligands, *RSC Adv*., **2017**, *7*, 10718–10728.
2) S. Hladysh, D. Bondarev, J. Svoboda, J. Vohlídal, D. Vrbata, J. Zedník, Novel conjugated polyelectrolytes based on polythiophene bearing phosphonium side groups, *Eur. Polym. J*., **2016**, *83*, 367–376.
3) O. Trhlíková, S. Hladysh, J. Sedláček, D. Bondarev, SEC-DAD - effective method for the characterization of π-conjugated polymers, *Materials Science Forum*, **2016**, *851*, 167-172.
4) P. Urbánek, A. di Martino, S. Hladysh, I. Kuřitka, A. Minařík, E. Pavlova, D. Bondarev, Polythiophene-based conjugated polyelectrolyte: Optical properties and association behavior in solution, *Synthetic Metals*, **2015**, *202*, 16-24.

9 ATTACHMENTS

A. S. Hladysh, D. Václavková, D. Vrbata, D. Bondarev, D. Havlíček, J. Svoboda, J. Zedník, J. Vohlídal, Synthesis and characterization of metallo-supramolecular polymers from thiophene-based unimers bearing pybox ligands, *RSC Adv*., **2017**, *7*, 10718–10728.

B. S. Hladysh, D. Bondarev, J. Svoboda, J. Vohlídal, D. Vrbata, J. Zedník, Novel conjugated polyelectrolytes based on polythiophene bearing phosphonium side groups, *Eur. Polym. J*., **2016**, *83*, 367–376.

C. O. Trhlíková, S. Hladysh, J. Sedláček, D. Bondarev, SEC-DAD - effective method for the characterization of π-conjugated polymers, *Materials Science Forum*, **2016**, *851*, 167-172.

D. P. Urbánek, A. di Martino, S. Hladysh, I. Kuřitka, A. Minařík, E. Pavlova, D. Bondarev, Polythiophene-based conjugated polyelectrolyte: Optical properties and association behavior in solution, *Synthetic Metals*, **2015**, *202*, 16-24.